A STUDY TO DETERMINE THE FEASIBILITY OF A LOW SONIC BOOM SUPERSONIC TRANSPORT

by Edward J. Kane

1. Report No. NASA CR-2332	2. Government Accession No.	3. Recipient's Catalog No.
4. Title and Subtitle A Study to Determine the Feasibility of a Low Sonic Boom Supersonic Transport		5. Report Date December 1973
		6. Performing Organization Code
7. Author(s) Edward J. Kane		8. Performing Organization Report No. D6-41177
		10. Work Unit No.
9. Performing Organization Name and Address The Boeing Commercial Airplane Company P. O. Box 3707 Seattle, Washington 98124		
		11. Contract or Grant No. NAS1-11877
12. Sponsoring Agency Name and Address National Aeronautics and Space Administration Washington, D.C.		13. Type of Report and Period Covered Contractor Report November 1972-July 1973
		14. Sponsoring Agency Code

15. Supplementary Notes

This is a final report.

16. Abstract

A study was made to determine the feasibility of supersonic transport configurations designed to produce a goal sonic boom signature with low overpressure. The results indicate that, in principle, such a concept represents a potentially realistic design approach assuming technology of the 1985 time period. Two sonic boom goals were selected which included: A high speed design that would produce shock waves no stronger than 48 N/m^2 (1.0 psf); and an intermediate Mach number (mid-Mach) design that would produce shock waves no stronger than 24 N/m^2. The high speed airplane design was a Mach 2.7 blended arrow wing configuration which was capable of carrying 183 passengers a distance of 7000 km (3780 nmi) while meeting the signature goal. The mid-Mach airplane design was a Mach 1.5 low arrow wing configuration with a horizontal tail which could carry 180 passengers a distance of 5960 km (3220 nmi). This configuration did not quite meet the signature goal because the tail shock wave was approximately 36 N/m^2 (0.75 psf). At their current stage of development both airplanes exhibited some rather serious design deficiencies. These included: Requirement of a fail-safe canard actuator design for subsonic operation (High Speed Design); Ground instability during loading (Mid-Mach Design); and Marginal takeoff performance and community noise (both designs).

17. Key Words (Suggested by Author(s)) Aerodynamics, airplane, flight controls, noise, pressure, propulsion, sonic boom, structures, supersonic transport, weights	18. Distribution Statement Unclassified - unlimited		
19. Security Classif. (of this report) Unclassified	20. Security Classif. (of this page) Unclassified	21. No. of Pages 128	22. Price Domestic, $4.50 Foreign, $7.00

CONTENTS

A STUDY TO DETERMINE THE
FEASIBILITY OF A LOW SONIC
BOOM SUPERSONIC TRANSPORT

Edward J. Kane

The Boeing Commercial Airplane Company

SUMMARY

Conceptually, airplane shapes can be defined that will produce almost any shape of sonic boom signature. The objective of this study was to determine if an airplane designed to produce a sonic boom signature with low overpressure represented a feasible supersonic transport configuration. It has been found that, in principle, sonic boom designed configurations represent a potentially realistic concept assuming the technology of the 1985 time period.

The primary design goal was to achieve values of overpressure and impulse during cruise which were significantly below those produced by current SST designs. Specifically, the following two goals were chosen: An overpressure of 48 N/m^2 (1.0 psf), or less for a cruise Mach number of 2.7 and an altitude of approximately 16.8 km (55,000 ft); and an overpressure of 24 N/m^2 (0.5 psf) for a cruise Mach number of 1.5 and an altitude of approximately 13.7 km (45,000 ft). The following technology assumptions were made for purposes of the analysis: 1985 technology with a 1990 design go-ahead; advanced turbojet engines incorporating increased turbine temperatures, pressure ratios and improved materials; high temperature, advanced composite structural materials; use of a stability augmentation system for flutter damping; and use of a hardened stability augmentation system plus an alpha limiter for airplane control.

The initial design criterion was to meet the sonic boom goal while relaxing other normal design and operational requirements as necessary. Hence, the principal effort was to develop the cruise configuration while accepting workable compromises elsewhere in the flight profile. Due to the limited scope of this study, only preliminary answers were obtained.

The high speed design goal was achieved with a blended arrow wing configuration. For cruise at the design altitude this airplane has the potential of carrying 183 passengers a distance of 7000 km (3780 nmi). The mid-Mach number design was a low arrow wing configuration with a horizontal tail. This airplane did not quite achieve the design goal because the tail shock during cruise was about 36 N/m^2 (0.75 psf). For cruise at the design altitude this airplane has the potential of carrying 180 passengers a distance of 5960 km (3220 nmi).

Both airplanes exhibited some rather serious design deficiencies. For the High Speed Design these included: Requirement of a fail-safe canard actuator design for subsonic operation; and marginal take-off performance and community noise. The Mid-Mach Design deficiencies included: Inability to meet the sonic boom design goal because of the extreme aft body contouring required to reduce the strength of the tail shock wave; Ground instability requiring external supports during loading; and marginal take-off performance and community noise.

INTRODUCTION

Prohibition of overland sonic boom for supersonic transport airplanes limit the operational versatility of this mode of transportation. Current designs for this class of airplanes are expected to produce sonic boom overpressures on the order of 100 N/m^2 (2.0 psf) or greater during cruise. Recognition of the limitations imposed by such boom levels has led to a number of studies directed toward defining aerodynamic designs which would produce lower overpressures during cruise. Notable among these was the pioneering work of F. E. McLean (Reference 1) which revealed the possibility of large airplane designs which would produce pressure signatures that were non-asymptotic (not simple "N" waves). These principles were further exploited by Ferri (References 2 and 3) and by Carlson, Barger and Mack (Reference 4), in establishing aerodynamic designs with an overpressure of approximately 50 N/m^2 during cruise. The latter study contained preliminary considerations of airplane weight, balance and performance. In addition, a number of theoretical studies were conducted by Miller and Carlson (Reference 5), Seebass and George (Reference 6) and Jones (Reference 7) to determine other methods of minimization and sonic boom lower bounds. The influence of practical design considerations on the sonic boom produced by large conventional supersonic airplanes was investigated by Howell, Sigalla, and Kane (Reference 8).

In principle, an airplane shape can be defined to produce almost any sonic boom signature. The objective of the current work was to select 2 sonic boom signature goals and determine the feasibility of SST's designed to produce these signatures. The current state-of-the-art did not permit precise definition of psychoacoustically acceptable sonic boom signatures. It was generally agreed that the magnitude of the pressure jump across each shock wave in the signature and the impulse of the signature is closely associated with annoyance. Hence, the design goals were to achieve values of overpressure and impulse during cruise which were significantly below those produced by current SST configurations.

Mathematical expressions can be derived which relate the shape of a sonic boom pressure signature to the shape of an equivalent area distribution. Through these relationships it is possible to calculate airplane configuration characteristics such as weight and length as a function of the desired overpressure or signature shape. This procedure is discussed in more detail in Reference 9.

Preliminary calculations indicated that reasonable size and weight airplanes could be designed to produce overpressures in the range from 24 to 48 N/m^2 (0.5 to 1 psf). The magnitude of the overpressure is related to the airplane Mach number, altitude, weight and length. The higher overpressure values are associated with higher Mach numbers and altitudes. To obtain a maximum amount of information from the study two design conditions were selected: one at a high altitude and Mach number and the other at a lower altitude and Mach number.

The high speed design goal was an overpressure of 48 N/m^2 (1.0 psf) or less for a cruise Mach number and altitude of approximately 2.7 and 18.3 km (60,000 ft). This airplane would be representative of high Mach number technology including titanium structural material, internal compression inlets and advanced turbojet engines. The intermediate speed (mid-Mach) design goal was an overpressure of 24 N/m^2 (0.5 psf) or less for a cruise Mach number and altitude of approximately 1.5 and 15.2 km (50,000 ft). This airplane concept would be representative of more conventional technology represented by an aluminum structure, external compression inlets and advanced turbojet or moderate bypass ratio engines.

Both designs were to be evaluated on the basis of advanced technology typical of that available in the 1985 time period. This would be consistent with selection of a design go-ahead in 1990. Specific ground rules and assumptions are noted in the next where they apply and their impact upon the design is discussed.

This report consists of a separate discussion of each
design concept. The following section contains the detailed
design and configuration data for the High Speed Design while
the one following contains the same for the Mid-Mach Design.
Each of these sections is subdivided into separate discussions of
the individual technology evaluations. The final sub-section
for each airplane contains specific suggestions for additional
work that should be done to remedy the design problems revealed
by study of that particular configuration concept. The study
conclusions and recommendations for future work directed toward
exploiting these design concepts are given in the last section.

SYMBOLS

This section defines the symbols used in this document.

<u>Symbol</u>

AR	Wing aspect ratio (b^2/s)
b	Wing span
BL	Buttock line measured laterally from airplane centerline
BS	Body station measured longitudinally from 5.08m (200 in) ahead of nose
$\bar{c}$	Mean aerodynamic chord (MAC)
C_D	Coefficient of drag (D/qs)
C_{Do}	Coefficient of drag at zero lift
C_{DSYM}	Symmetric drag coefficient (friction + wave + excrescences)
cg	Center of gravity
C_L	Coefficient of lift (L/qs)
C_{Lp}	Lift at which induced drag equals $C_L^2/\pi\,AR$
C_{l_β}	Coefficient of rolling moment due to sideslip
C_{n_β}	Coefficient of yawing moment due to sideslip
C_{y_β}	Coefficient of side force due to sideslip
D	Airplane drag
GW	Airplane gross weight
K	Leading edge suction parameter
K_E	Shape factor for envelope drag polar ($C_D = K_E C_L^2$)
K_R	Sonic boom ground reflection coefficient
L	Airplane lift
M	Mach number
MLW	Maximum landing weight
MTW	Maximum taxi weight
n	Airplane lift load factor
OEW	Operational empty weight
ΔP	Sonic boom overpressure
q	Dynamic pressure
S_{REF}	Reference wing area
$S(X)$	Airplane cross-sectional area

ΔS_{LE}	Planform area increment for extended leading edge devices
V_{APP}	Approach speed
V_{BC}	Geometry limiting contact speed
$V_{MC\,a}$	Minimum control speed in air
$V_{MC\,g}$	Minimum control speed on ground
V_{MO}	Maximum operational speed in climb (structural placard)
V_{MU}	Minimum unstick speed
V_{NLO}	Nose wheel lift-off speed
X	Longitudinal distance measured from airplane nose
Y	Lateral distance measured from body centerline
ZFW	Zero fuel weight (OEW + payload)
$\propto$	Airplane angle of attack referred to a body waterline
$\propto_o$	Angle of attack for zero lift
δ	Control surface or flap deflection angle
Θ	Airfoil twist angle relaitve to body waterline
$\Delta\ddot{\Theta}$	Incremental pitch acceleration

HIGH SPEED DESIGN

The goal for the high speed design was an airplane that would cruise at a Mach number of 2.7 and produce a sonic boom signature with shock waves no stronger than 48 N/m^2 (1.0 psf) with a ground reflection factor, K_R, of 1.9. Generalized design data were calculated using relationships between sonic boom overpressure and airplane design characteristics such as Mach number, cruise altitude, airplane weight and length. As noted in the previous section, it is possible to relate sonic boom signature shape to an effective area distribution representing an airplane. A family of effective area distributions yielding desirable signatures was chosen and maximum allowable weights were computed as a function of airplane altitude. A typical example of such design data is shown in Figure 1. A design point which represented a reasonable weight and length was selected was selected from data similar to these. The initial values were taken as: Cruise Mach number of 2.7; Mid-Cruise weight of 250,000 kg (550,000 lb); Overall length of 93.6 m (307 ft); Cruise altitude of 16,800 m (55,000 ft); and Overall area distribution envelope proportional to (running length)$^{3/2}$.

Configuration Design

An overall area distribution envelope was computed based on the design point data. Definition of configuration components were made and initial layouts were drawn so that the airplane could be reviewed by the design team. This initial layout revealed a difficult balance situation which required that the fuselage be moved aft relative the wing. In addition, the total of all the component areas (including lift) exceeded that of the desired 3/2 power area envelope. The nose of the area envelope was made somewhat blunter to reduce the amount of fuselage ahead of the wing. This increased the amount of area available for the configuration components and presented the rate of area growth required to maintain the sonic boom signature within the design goal.

8

The resultant design mid-cruise area distribution is shown in Figure 2. The contribution of each component including lift is individually shown. This area distribution was obtained by passing Mach cutting planes through each component at the angle appropriate for Mach 2.7 and a point of observation directly beneath the flight path. For this flight condition the nose of the fuselage is at an angle of attack of about 4°. The fuselage equivalent area due to lift allowed some reduction in the nose bluntness. The remainder of the fuselage was contoured to fill the differences between the envelope and the other components. This figure also contains a definition of the wing planform.

A two-view drawing of the airplane is shown in Figure 3. This configuration is a blended mid-wing airplane with pod mounted advanced technology dry turbojet engines on the wing trailing edge. The wing was designed with dihedral to reduce the length and weight of the main landing gear required for takeoff rotation and landing flare. Dihedral increases the virtural length of the lift distribution which is desireable for sonic boom minimization but it also reduces lateral-directional stability. The amount required for significant overpressure reduction is generally too much from the control viewpoint (see "Lateral and Directional" page 19). The folding canard was used to improve the low speed balance requirement by moving the forward aerodynamic limit forward and to improve the lift-drag ratio during low speed operation. The leading edge surfaces are full span simple hinged leading edge flaps and the trailing edge surfaces are elevons. Two vertical tails and two ventral fins are mounted on the wing tips outboard of the engines. The main landing gear folds into a well in the wing and has a spash deflector to reduce the possibility of foreign object ingestion.

Internally the wing structural box passes through the body behind the passenger compartment. The wing forward of the box is attached to the body through frames around the passenger cabin. The cabin has

skylights rather than conventional windows because of the midwing
location. The seating would consist of 151 seats arranged in 5-6
abreast rows at 0.86 m (34 in) pitch which is the same as the 707
comfort level. Passenger services are equivalent to those for the
proposed U.S. SST design (B2707-300). Two type A loading doors which
are compatible with current airline ground-support equipment are
located forward of the passenger compartment. Space is available
adjacent to the entry doors for storing "carry-on baggage". Cargo
containers are located in the bay aft of the passenger compartment and
would be loaded from the bottom of the airplane. Pilot forward
visibility for takeoff and landing would be provided through optical
systems supplemented with side windows. Four passenger exits are
located in the lower wing surface which contain inflatible slides for
emergency evacuation. In addition, overhead hatches with stairs
have been provided for evacuation after ditching at sea or in the case
of a wheels-up landing.

Aerodynamics

High Speed - Climb, Cruise, Descent

The wing planform shown in Figure 2 was selected considering both
the longitudinal development of lift which influences the boom and
wing drag which affects the airplane performance. Camber and twist
for a design lift coefficient of .0725 were determined using a 3-term
optimization (Reference 10) restraining the design for a) sufficient
positive C_{Mo} to avoid large trim drag, and b) smoothing rapid twist
changes at planform leading edge breaks. The resulting twist distribu-
tion is shown in Figure 4. The wing thickness distribution was
selected by considering wave drag, weight and landing gear stowage
requirements.

The fuselage area distribution was specified after the other
components had been designed so that it could be used to obtain the
desired equivalent area envelope (see Figure 2). This envelope shape
was required to meet the design goal sonic boom signature at mid-
cruise. As a result the fuselage does not represent an optimum shape
for minimum wing-body wave drag. The wing-body wave drag for this

airplane is about 15% higher than it would be if the fuselage were optimized for wave drag holding the length and minimum cross-section in the passenger cabin fixed. This penalty is directly attributable to the sonic boom design constraint.

Aerodynamic lift and drag characteristics were calculated at several Mach numbers. Skin friction drags were computed for each individual component using the method of Sommer and Short (Reference 11). Zero lift wave drags were estimated using the method described in Reference 12. Drag due to lift and lift curves were calculated using the method developed by Middleton and Carlson in Reference 13.

Wetted areas and friction drags of the various components are listed in Table 1 for the airplane as shown in Figure 3. A summary of the airplane zero lift drag is contained in Table 2 for several Mach numbers and altitudes. Airplane drag polars and lift curves for Mach 2.7 and Mach 1.5 are shown in Figures 5 and 6 respectively. The polar shape and lift curve slope for the wing and nacelles were calculated using the method of Reference 13 and slender body theory was used to account for the effect of the forebody. The symmetric drag is indicated on both figures. The estimated polar shape is compared with that for a flat plate wing and the theoretical optimum wing in Figure 5. The envelope polar shape factor is less than that for the flat wing by about 60% of the difference between the flat and optimum wings which is quite reasonable. The lift curve is referenced to the fuselage (body waterline) angle of attack.

For purposes of computing airplane performance these data were recast into a more convenient form which allows interpolation as a function of Mach number. The drag polars such as those shown in Figures 5 and 6 were separated into zero lift drag (wave and friction) and drag due to lift. An envelope polar shape factor was used for calculating the drag due to lift. In general, these envelope curves match the actual polars at lift coefficients corresponding to the nominal flight profile. These data are shown in Figure 7 as a function of Mach number. The envelope polar shape factor at Mach 0.8 was estimated using wind tunnel data for similar planforms.

Low Speed - Takeoff, Landing

Low speed aerodynamic characteristics were estimated using unpublished NASA data for the SCAT 15F as the basis for leading and trailing edge flap lift effectiveness. Drag characteristics were assumed to be in the form,

$$C_D = C_{Do} + (1-K) C_L \tan (\alpha - \alpha_o) + \frac{K C_L^2}{\pi AR}$$

where K is a leading edge suction parameter. Values for this parameter were extracted from the above mentioned data as a function of $(C_L - C_{LP})$. These were considered to be somewhat optimistic because the leading edge area ($\Delta S_{LE}/S_{WING}$) deflected on the airplane is not as large as that on the model. However, further detailed consideration of the flap system was not considered warranted at this stage in the development of the configuration.

The estimated lift and drag characteristics at takeoff and landing for this airplane are shown in Figures 8 and 9 for cg locations of 0.53 $\bar{c}$ and 0.465 $\bar{c}$ respectively. The former cg location is representative of the takeoff configuration while the latter is the forward limit for landing. Both the canard and TE up elevon are required for landing at the forward cg location. No credit was taken in these data for the lift generated by the canard. The effects of ground proximity were estimated using a simplified theoretical method. The height parameter, h, was taken as the distance from 0.25 $\bar{c}$ to the ground with the oleos extended at the geometry limited attitude.

Weights

Weight and Balance Summary

A weight and balance summary of the Operational Empty Weight (OEW) and Zero Fuel Weight (ZFW) are presented in Table 3. The weight data shown are representative of the following configuration definition:

1. Configuration geometry per Figure 3.

2. Structural and systems design concept definitions per References 14 and 17 except for the fixed geometry nose (optical system provided for pilot visibility).

3. Engine airflow per engine (GE4/J6H2)
   1975 Technology - 230 kg/sec (507 lb/sec)
   1985 Technology - 195.5 kg/sec (431 lb/sec)

4. Operational and design criteria from Reference 16 (2707-300 PPD U.S. SST) except for canard requirements as discussed in the following sub-section.

5. Center of gravity tolerance of ±0.25 m (±10 in) to provide for customer variations and cg indication system.

Methods of analysis used to derive the weights were based upon the 2707-300 PPD and 969-336C configuration and weight definitions (References 14-17). These consisted of the following:
   o Body Structure and Contents - 2707-300 extrapolated cantilever beam
   o Wing Structure and Contents - Reference 17 (969-336C) unit weights, modified for geometry differences and updated for 2707-300 structural development experience.
   o Vertical Tail Structure and Contents - 2707-300 unit weights
   o Propulsion Pod - GE4/J6H2 base engine airflow 408 kg/sec (900 lb/sec) scaled for airflow requirement at cruise.
   o Landing Gears - 2707-300 extrapolated length.
   o Canard - 969-336C unit weight

The weight increments for advanced design concepts are representative of 1985 technology with a 1990 design go-ahead. These increments are consistent with the AST Task II program weight data.

Center of Gravity Management

Loadability and fuel management for this airplane is shown in Figure 10 for the nominal cg location (see "Tolerance" item 5 above). This chart shows the location of the airplane cg through the mission from taxi at 340,000 kg, through cruise as fuel is burned (295,000 kg to 190,000 kg) to landing and disembarking of baggage and passengers at 140,000 kg. Aerodynamic limits are shown for subsonic (canard in and out) and supersonic portions of the mission. The passenger cg location is shown as an envelope which includes all combinations of seating. The cg management schedules are presented in Tables 4 and 5, for two alternatives for handling the descent and landing fuel. These data are based on the fuel tank definitions of Figures 11 and 12.

The OEW and ZFW cg are outside of the aerodynamic forward limit without the canard because the payload is located a significant distance ahead of the OEW cg. To move the OEW and ZFW cg aft of .519 $\bar{c}$ would require major configuration revisions which would result in exceeding the sonic boom design goal. Rather than reconfiguate, operational flexibility was extended by including the folding canard which moved the aerodynamic limit forward.

Cruise to an alternate airport at gross weights less than the maximum landing weight (MLW) requires that the canard be extended for the use of Alternative I fuel management. To achieve the subsonic operational capability with the canard in at the MLW, cruise range must be sacrificed because the cg for zero trim drag cannot be achieved below a gross weight of 225,000 kg. In addition, the airplane would have to be landed at the MLW because, with the canard folded, control could not be achieved at lower weights. The canard actuation would have to be "fail safe" because it is highly unlikely that operation without it could be certified.

The cruise segments between 225,000 kg (.449 $\bar{c}$) and 283,000 kg (.473 $\bar{c}$) are managed by outboard wing fuel (Tank 6A and 7A) in combination with forward tanks. Due to the requirement for the large moment change between MLW and 225,000 kg this segment is the latest during the mission profile at which outboard wing fuel (Tanks 6A and 7A) can be held.

14

Between 283,000 kg and takeoff a departure from the zero trim
drag cg is required to achieve the canard in forward limit at climb
gross weights. The airplane's cg can be managed more easily at
high gross weight because the fuel capacity is 39% greater than the
mission requirement which provides greater flexibility.

Alternative II Management offers longer cruise range by sacri-
ficing the capability of canard in (folded) subsonic flight at gross
weights less than MLW. The zero trim drag cg can be achieved at
204,000 kg (versus 225,000 kg for Alternative I).

Between 204,000 kg and 283,000 kg the cg is managed with outboard
wing fuel, in combination with tanks different from those used for
Alternative I. Above 283,000 kg management is identical to the
schedule for Alternative I.

Flight Controls

Aerodynamic data for this design were generated from previous
Boeing estimates of the SCAT 15 configuration characteristics and
NASA wind tunnel tests. Certain aerodynamic comparisons, particularly
for the canard and elevons are only approximate and must be judged
accordingly. Aeroelastic effects, which can be very significant for
slender configurations, were obtained from previous Boeing analyses
of SCAT 15 configurations and applied uncorrected since no structural
analysis was undertaken.

Stability and control areas of concern in this design are:
o high angle of attack stability and control for recovery
o canard lift and pitching moment effects with wing body interference
o control effectiveness of elevons, particularly with aeroelastic
      degradation and with ground effects at takeoff
o large wing dihedral effect on lateral/directional dynamics and
      handling qualities, including crosswing landing
o engine failure controlability

Control System Description

Longitudinal. The three view drawing of the high speed configuration in Figure 3 shows the location of the pitch controls on the wing trailing edge and the folding canard trim surface ahead of the wing. The canard surface is a high lift flapped trim surface with no control operation other than the extend and retract functions which induce a nose up pitching moment on the airplane. The wing trailing edge control surfaces are simple hinged with deflections +25° for pitch control.

Referring to Figure 3, the trailing edge pitch controls are:

Panel	Location	Function	Sec. Function
1	Between body and inboard nacelle	All speed elevator	Drooped, canard out
2	Between nacelles	All speed elevon	Drooped, canard out
3	Outboard of outboard nacelle	Low speed elevon	Drooped, canard out

Lateral. The two view drawing, Figure 3, shows the location of the lateral control surfaces integrated with the wing trailing edge pitch controls. The spoiler surfaces are activated when the low speed elevon panel 3 is locked out for high speed flight.

Referring to Figure 3, the lateral controls are:

Panel	Location	Function	Sec. Function
4	Wing T.E. outboard	Low speed aileron	None
3	Outboard of outer nacelle	Low speed elevon	Drooped, canard out
Spoilers	Ahead of panel 3	High speed lateral control	Speed brakes

Directional. Figure 3 shows the configuration with twin vertical tails each carrying large full span rudders. Each rudder is divided into two spanwise panels; the lower panel operates at all speeds and has good aeroelastic properties. The top rudder panel operates at low speeds only because of low aeroelastic effectiveness at high speeds.

No analyses have been made on lockout schedules for the flight controls on the high speed design.

Auxiliary Systems. The longitudinal flight control system incorporates a hardened stability augmentation system (HSAS) to allow the airplane to fly with the cg up to 6% aft of the unaugmented maneuver point. This system would be designed from Boeing SST experience which showed the feasibility and extent to which negative stability margins could be safely controlled.

Previous Boeing analyses of SCAT 15 configurations identified low speed pitch up instability which was partially remedied with control functions on the inboard leading edge flaps. The low sonic boom High Speed Design has not been analyzed with regard to high angle of attack pitch up but the problem has been recognized by incorporating an angle of attack limiter in the design. The limiter will prevent angles of attack beyond 21°. A warning system will trigger the angle of attack limiter at angles of attack less than 21° by applying nose down elevator control in order to prevent dynamic overshoot beyond 21°. The alpha limiter may also operate the wing leading edge flap surfaces, as envisioned on the Boeing SCAT 15 studies, to improve the pitch recovery.

The lateral-directional axes will include a stability augmentation system to provide dutch roll damping, improve the roll mode time constant and to provide automatic directional control for asymmetric conditions such as engine failures.

It is probable that, like the Boeing SST, the directional axis control to the rudder at high speed only will be performed by the lateral SAS and trim systems with the pilot input via the rudder pedals locked out.

Airplane Characteristics

Longitudinal. The airplane balance as shown in Figure 13 is limited by longitudinal control effectiveness, which is provided by the trailing edge wing controls. The use of a hardened stability augmentation system allows the cg to be up to 6% aft of the unaugmented maneuver point. This removes the stability restriction for aft cg at most flight conditions. The permissible cg limits move aft abruptly at low speed when the canard is retracted. For this reason, it would be difficult to make this a practical configuration without further analysis and wind tunnel test data. These tests would be required to investigate the possible solutions which include the use of intermediate canard positions to allow the fuel management system to change airplane cg before complete retraction or extension takes place. At higher speeds the canard and forward body will have the possibility of divergent aeroelastic characteristics. Hence, the need does exist to have retraction take place early after takeoff, and extension just before terminal area speeds are reached.

The low speed cg limits, canard out, are shown in Figures 14 and 15 to be a function of lift coefficient, C_L, and hence speed. The speeds in Figure 14 are quoted for an approach weight of 204,000 kg (450,000 lbs). The forward limit is a landing flare control requirement at α_{limit}, (see "Criteria" on page 20). At speeds and C_L's corresponding to $\alpha_{limit} = 21°$ the forward cg limit is a trim requirement. The limit of 21° is an absolute limit that the system will not allow the airplane to exceed irrespective of pitch rate. The alpha limit system will incorporate a pitch rate signal that will give alpha

warning at angles of attack less than 21° to prevent dynamic over-
shoot beyond 21°.

The high speed center of gravity limits are represented by the
Mach 2.7 pitching moment plot, Figure 16. The forward cg limit
(.420 $\bar{c}$) is defined by a trim requirements (with stable pitch slope)
for maximum positive pitch control ($\delta_{elevators}$ $E_1 = E_2 = -25°$)
at a load factor (n) of 2.

The aft cg limit (.548 $\bar{c}$) is determined by a pitch down control
requirement for an unstable condition where the control limit is taken
to n = 2.5 + $\Delta\alpha$ = 5° (see "Criteria".) The $\Delta\alpha$ = 5° is an allowance:
a) to provide a small margin of ΔCm at the limit of n = 2.5; and b) to
provide a small margin for possible pitch overshoot beyond n = 2.5.

The Mach 2.7 case chosen in Figure 16 is start of cruise at
16.8 km (55,000 ft). A more detailed study of all possible altitude
conditions covering the range from minimum operating speeds to dive
speeds is required to establish the cg limits more accurately.

Takeoff rotation capability is shown in Figure 17 as the speed
at which full control can raise the nose gear off the ground. The
case shown is at maximum takeoff weight. At the forward cg limit of
.465 $\bar{c}$ the nose lift off speed, V_{NLO}, is high; fortunately the
practical loading cg at 340,000 kg (750,000 lbs) is at .53 $\bar{c}$ where
the V_{NLO} is satisfactory. Intermediate takeoff weights could occur
with forward cg positions and high nose lift off speeds. These
conditions have not been investigated.

Lateral and Directional. The basic stability characteristics are
based on Boeing analysis of SCAT 15 wind tunnel data. Figures 18
and 19 show values of C_{n_β}, C_{ℓ_β} and C_{y_β} at low speed and high speed
respectively. Of note in the data is the dihedral effect, C_{ℓ_β},
which is high because of the large geometric dihedral of the wing
compared with the SCAT 15 (969-336C) airplane. Configuration changes
would be required to improve the lateral-directional characteristics
for disturbances such as engine failures. Increased directional

stability could be obtained by increasing the vertical tail size and the adverse dihedral effect can be reduced by decreasing the geometric dihedral or by using compound dihedral inboard and anhedral outboard (as on the U.S. SST).

Figure 20 shows the rudder capability to control and trim an outboard engine failure at takeoff as a function of thrust and speed. V_{MCg} is the minimum control speed on the ground with no nose wheel force or moment available to steer the airplane. Criteria listed on page 20 are expected to be met, depending on takeoff performance.

Engine failures at cruise speed are shown in Figures 21 and 22 and mainly because of the large geometric dihedral the upset rolling moments are uncontrollable for the engine failures designated on the figures. These failures are not extremely remote and must be designed for. To avoid using the undesireable system of sympathetic unstarts for opposite engines the wing and tail could be modified in the manner mentioned above. Such changes were beyond the study scope.

Geometric dihedral also adversely affects the crosswind landing capability, Figure 23. High approach speeds are required with strong crosswinds because of the lateral control trim limitation which may necessitate incorporation of a crosswind gear on the design. The rudder requirement for crosswind, Figure 24, is not critical.

No lateral control estimates for roll response requirements have been made although Boeing SCAT 15 estimates have been used for assessing the engine failure upset at Mach 2.7.

No assessment of the capability of the lateral control surfaces as drawn (except for crosswind landing) has been made.

Flight Control Criteria

The following flight control criteria were used in evaluating and analyzing both low sonic boom airplane configurations.

1.0 Longitudinal

1.1 Stability Margins

The aft cg can be up to 6% aft of the unaugmented maneuver point using "Hard Stability Augmentation System" (HSAS)

HSAS is designed as an integral part of its flight control system having a failure rate of extremely remote.

1.2 Control

a. Longitudinal control shall be adequate to meet design maneuver requirements for the configuration -- usually $n = 2.5$ to 0 for transport airplanes.

b. At approach and landing, which is usually critical for longitudinal control sizing at the forward cg limit, the criteria for (L/W) versus $\Delta\ddot{\Theta}$ must be satisfied as shown in Figure 25.

c. Longitudinal control at aft cg shall provide a stable nose down pitching moment at any attainable attitude within the airplane flight envelope. (Use $C_{L_{control\ at\ aft\ cg}} = C_{L_{max\ dem}} + 5°$ where $C_{L_{max\ dem}} = 1.5\ C_{L_{approach}}$)

d. Longitudinal control at forward cg shall be adequate for nose wheel liftoff (rotation) at takeoff. The nose wheel liftoff speed shall not compromise the takeoff field length.

Experience shows $V_{NLO} = V_{BC} - 15$ (kts)

$$V_{NLO} = .96\ V_{MU} - 15 (kts)$$

V_{NLO} = nose wheel liftoff speed

V_{BC} = geometry limiting contact speed

V_{MU} = minimum unstick speed

2.0 Lateral and Directional
   2.1 Stability
      a. The vertical tail size must be adequate to provide a
         positive restoring moment at all attainable angles-of-
         attack and angles of sideslip within the flight
         envelope.
      b. The vertical tail in combination with the other geometry
         variables such as wing dihedral must provide a level of
         Dutch roll undamped frequency at the most critical
         condition (usually minimum operational speeds) such that
         $\omega_N \geq .3$ rad/sec.

   2.2 Control
      a. Vertical tail/rudder size must provide directional
         control for asymmetric flight conditions. The usual
         critical sizing condition is at takeoff with a critical
         engine failure. The FAR 25 regulations apply:

$$V_{MC_g} \leq V_1$$

$$V_{MC_a} \leq V_R/1.05$$

$$\leq V_{2_{Min}}/1.10$$

      B. Lateral Control
         No criteria or control sizing are made in the initial
         design stage as the influence of lateral control on the
         preliminary weight, balance and performance estimates
         is minimal.

Propulsion

Engine Characteristics

The engine for the Mach 2.7 low sonic boom airplane is based upon
a scaled and modified version of the GE4/J6 study H2 engine (Referen-
ces 18 and 19). The GE4/J6H2 engine is a dry turbojet with a
retractable jet noise suppressor and was the final engine submittal

by General Electric for a production SST airplane prior to the termination of the previous SST contracts in 1971.. In anticipation of additional improvements in technology which could be achieved before the development of the low sonic boom airplane is complete it is assumed that the performance of the GE4/J6H2 engine could be attained with an engine whose airflow and weight was reduced 15% from the engine of Reference 18. These improvements would be accomplished by increasing the turbine temperature combined with an increased engine pressure ratio and some improvement in materials and structural technology.

By sizing the engine for supersonic cruise an engine with an airflow size of 195.5 kg/sec was chosen. The dimensions for this engine pod are shown in Figure 26.

The engine intake is an axisymmetric translating centerbody intake with variable throat doors, variable bypass doors, and blow-in takeoff doors. The intake is essentially the same as that developed for the U.S. SST prototype which is described in Reference 20. The intake recovery and excess air drag are given at various conditions in Table 6. Also given in Table 6 at the same conditions are nozzle thrust coefficients, installed engine thrust and specific fuel consumption.

The engine noise suppressor is a retractable 32 chute design which reduces jet noise by 8 EPNdB for a 5% thrust loss at takeoff power.

Propulsion System Failures

The propulsion pod placement is such that a failure involving an intake unstart (above about Mach 2.0) on an inboard engine will also cause a mutual intake unstart on the adjacent outboard engine. Because of the aft stagger of the outboard nacelle an intake unstart on an outboard engine nacelle is not expected to result in a mutual

unstart of the adjacent inboard intake. Therefore the worse propulsion system failures will be an outboard engine seized rotor, or an inboard engine seized rotor combined with an outboard intake unstart. The transient axial loads (net thrust minus intake drag) during cruise for a seized rotor and following an intake unstart accompanied by a burner flameout is shown in Figure 27. Generally the burner is not expected to flameout as a result of an intake unstart, but the estimated probability is still high enough that it is included for purposes of failure analysis. Because wind tunnel data on the effect of intake excess air spillage on airplane yawing moment is not available, the intake spillage drag was included in the thrust transient curves and yawing moment can be calculated from the change in axial force.

The probability of a seized rotor is such that it should be considered during climb and cruise, but not during an upset dive or during a 2 g maneuver. During unusual conditions where the airplane stability is decreased such as during an upset dive or during 2 g maneuver, the most serious propulsion system failure with a probability greater than extremely remote is a locked-in compressor stall. The axial load transient for locked-in stall during cruise is also shown in Figure 27.

Advanced Fuels

The possibility of reducing fuel weight by using a fuel with higher heating value was not considered at this time. Much additional study would be required to determine if advantages are offered by using these fuels.

Structures

Structural Arrangement

The wing structure consists of spar and rib construction as shown in Figure 3. The spars are perpendicular to the airplane centerline in the center section and break and sweep aft at the Buttock Line (BL) 5.23 rib. Outboard of the break, the spars continue parallel. Forward of Body Station (BS) 70.14 the spars run perpendicular to the centerline out to the leading edge with no break. The spars at BS 62.97 and BS 70.30 form the front and rear walls of the wheel wells.

Each wing has five ribs. The ribs at BL 5.23 and 8.89 act as engine support ribs redistributing the engine loads into the wing box. The former rib reacts the kick loads due to the break in the spars. The rib at BL 14.61 supports the fin. The other two ribs closeout the root at the side of the body, and the wing tip. The side of body rib and the BL 5.23 rib form the sides of the wheel well. The wing covers are sandwich panels combining the benefits of high end load capability with good thermal insulation.

Experience indicates that the flexible airframe combined with the aft mounted engines tend to be critical for flutter. It is assumed that any flutter deficiencies will be corrected through the use of flutter SAS.

The fuselage is a blended wing-body arrangement which has frames that carry the wing loads around the passenger compartment. There are no conventional windows, but skylights are provided in the upper surface. Pivots are provided at BS 22.30 for the folding canard.

The fuselage skins are sandwich design in the highly loaded regions, and stiffened skin in the more lightly loaded regions. The portion of the fuselage between the radome and the flight deck is unused volume. Due to the very low loads, it would be constructed of high-temperature advanced composites to minimize the weight.

Structural Materials

The 450°F temperature associated with Mach 2.7 cruise conditions requires that the airframe be built of titanium and high temperature advanced composites. The weight estimates have allowed for a distributed weight saving of 7.5% of OEW to account for the use of the composite materials.

Airplane Performance

The 195.5 kg/sec (431 lb/sec) engine shown in Figure 3 was selected by considering only the thrust required during cruise and at Mach 1.2 during climb. (A complete engine airframe matching study was beyond the scope of the present study.) Initial performance calculations indicated that this engine lacked sufficient thrust margin at Mach 1.5 (before the inlet started) so that excessive time was spent at this inefficient flight condition until the weight was reduced enough to continue to cruise. It appeared that increased range could be obtained by increasing the engine size. In addition, it was noted that the constant cruise altitude used to select the design conditions had an adverse influence on airplane range.

These considerations suggested that the effect of parametric variations in engine size and cruise altitude be calculated. The purpose was to approximately determine a more suitable engine size and to study the influence of altitude on both range and sonic boom characteristics for the parametric variations noted.

26

Payload-Range Summary

This analysis was conducted using the same standard day, mission profile as was used for the U.S. SST program. Subsonic legs before and after cruise were not included. The quoted ranges presume still air and allow for reserves based upon "Production Technology Reserve Rules" for the 1990 time period. These rules were used for the SST also and result in fuel reserves of 27,200 kg (60,000 lb). The payload range capability of the High Speed Design is summarized in Figure 28.

This airplane can carry a 14,070 kg (31,000 lb) (151 passenger) in excess of 6850 km (3700 N.Mi.) on a standard day. To accomplish this requires engines which are 5% larger than shown in Figure 3 in order to begin cruise without exceeding maximum continuous thrust rating. The M = 2.7 cruise is conducted at 16.8 km (55,000 ft) pressure altitude.

Increased airflow allows an improved cruise match at 16.8 km (55,000 ft) and results in more range. The effect of increased engine size on airplane weight is shown in Figure 29. Larger engines do require forward counterweight to maintain balance. This can be either ballast or for this particular configuration, increased payload. Both cases have been computed. After the weight effects from the engines and ballast are included, an engine size increase of about 27% to an airflow of 247 kg/sec (545 lb/sec) improves the range to a maximum of 7060 km (3820 N.Mi.). When this increased engine size is balanced by increased payload the airplane will fly 7000 km (3780 N.Mi.) with 183 passengers or 17,050 kg (37600 lb) payload. A 42% increase in airflow will allow a balanced airplane with a payload of 201 passengers but at a reduced range (see Figure 28).

The effect of engine size increases on range and climb gradient capability is shown in Figure 30. The range values shown are for a

constant payload of 151 passengers. Increasing the payload rather
than using ballast will result in a slight decrease in the values
shown because more passenger weight is needed to keep the cg location
fixed. (The passenger moment arm is shorter than the ballast arm).
In addition this figure shows the effect of a climbing cruise rather
than one at the constant design altitude. Allowing the airplane to
cruise at the altitude for the best value of km/kg while also increas-
ing engine size by about 27% optimizes the cruise match throughout
and allows a standard day range of about 7950 km (4300 N.Mi.) with
the design payload of 151 passengers. Relative to the airplane with
27% more airflow cruising at a constant altitude the climbing cruise
would increase the range by 12%.

Noise and Low Speed Characteristics

     Low speed performance was estimated by usual means assuming a
STD +15°C day, at sea level. Two degrees of tail clearance at lift-
off and one degree on approach (3 degree glide slope) is assumed.
F.A.R. takeoff field lengths are based on generalized performance data
for current 4 engine airplanes. No assessment of stall margins or
rotation capabilities was attempted at this time. The low speed and
noise characteristics are summarized in Figure 31 as a function of
engine size.

     For the above conditions the airplane defined in Figure 3 requires
F.A.R. field lengths in excess of 6,100 m (20,000 ft). The climb
capability at 2nd segment is marginal even with all engines operating,
and it cannot accommodate an engine failure during takeoff. At .65 m
(.35 nmi) to the side of the runway centerline, per F.A.R. 36, the
maximum noise during takeoff is about 108 EPNdB. This is due to the
jet suppression included in the advanced engine and the power limit
(84% max) observed at takeoff. However, noise on the extended runway
centerline 64.8 km from brake release, per F.A.R. 36, will be much
louder since the altitude will be very low. A detailed analysis was

not conducted but noise levels well in excess of 120 EPNdB can be expected. Landing performance and approach noise were not computed in detail but are not expected to be as critical as takeoff. Approach speeds of 300 km/hr, EAS, (162 kts, EAS) are expected at mission landing weights. The range of engine size increases studied for determining the maximum cruise performance are not large enough for acceptable takeoff characteristics. As noted above, engine size increases beyond about 27% would result in some range loss.

Sonic Boom Characteristics

Sonic boom signatures were calculated for several of the above described parametric airplane variations. Specifically these were:

1. Baseline airplane (Figure 3) with 5% larger airflow at constant cruise altitude.

2. Baseline airplane with 27% airflow increase at constant cruise altitude.

3. Baseline airplane +27% airflow with a climbing cruise for best range.

The estimated sonic boom signatures are shown in Figures 32-34 respectively for Mach 1.5 in climb, beginning of cruise, mid-cruise, and end of cruise.

In all cases the Mach 1.5 signature exceeds the design goal by containing pressure jumps in excess of 48 N/m^2 (1.0 psf). During cruise at a constant altitude the signatures are very near the design objective. Increasing the altitude during cruise to increase the range (by about 12%) results in signatures which exceed 48 N/m^2 total pressure change. However, each shock wave in the signature is less than the design goal. More information is needed on psychoacoustic responses to determine the acceptability of such variations in signature shape, but the obvious performance benefits should provide suitable motivation.

Considerations For Continued Study

The fundamental constraint of this study was to define a high speed
airplane configuration that would produce a cruise sonic boom signa-
ture with shock waves no stronger than 48 N/m^2 (1.0 psf). In doing
so, many constraints such as takeoff field length, landing speeds,
community noise, minimum drags, etc. were relaxed. It has been
shown in the preceding material that such an airplane could be designed,
but it is marginal in many of these practical aspects. A number of
these could be corrected by continuing to cycle the design. Such
exercises would result in a more optimum airplane and would better
indicate its commercial viability. The following is a summary of the
problem areas along with the outline of methods that could be used to
obtain a solution. The probable effect of these solutions on the
primary design goal is also noted.

Airplane Balance

The most critical problem with this configuration is the balance
at subsonic speeds and low weights. At the lower weights the cg is
ahead of the aerodynamic forward limit with the canard folded. This
situation severely limits the operational flexibility and fail safe
canard actuation systems are required. These considerations were
discussed earlier. At higher gross weights the cg can be maintained
within the aerodynamic limits by proper distribution of fuel.

Probable solutions consist of the following:

1. Increase the engine size to move the ZFW cg aft.
2. Modify the wing planform to move the aerodynamic limit
    forward

The first alternative listed above may have beneficial effects
for low speed operation as well as improving the airplane balance
since it appears that the engines shown in Figure 3 are too small for
acceptable airport operation. However, such engine size growth would

require a reduction of aft body diameter to avoid exceeding the envelope area curve. In addition, the zero lift drag would change and the possibility of requiring wing flutter suppression would become more likely. Each of these would require study but it currently appears that the motivation for an engine size increase is quite strong.

The second alternative would likely be used in combination with the first. This would probably consist of increasing the trailing edge sweep (cutout) and the wing strake size. Such a revision would have two beneficial effects: A forward movement of the aerodynamic limit; and a reduction of the wing volume contribution in the aft body region. A more conventional aft body shape and closure drag would result.

Improvement of the airplane balance through a combination of the above two alternatives would result in an increase in the allowable payload. The passenger cabin shown in Figure 3 has room for about 210 passengers but this capacity can be used only if the OEW cg can be moved aft. The effect of these alternatives should be studied because it appears that these changes have numerous benefits.

Drag Improvement

The match between the airplane cruise condition and the conditions for maximum lift to drag ratio (L/D) is not as close as would be desired for maximum cruise range. This situation can be improved by:

1. Reducing the zero lift drag
2. Displacing the airplane polar so that $(L/D)_{max}$ will occur nearer the cruise lift coefficient

Significant zero lift drag improvement could be obtained by optimizing the fuselage shape for minimum wing body wave drag. This however, would change the shape of the sonic boom signature and might result in

an overpressure greater than the design goal. A systematic study of the effect of the fuselage shape on both drag and boom should be made to determine if such a change could improve the airplane performance without significantly affecting the sonic boom signature.

Addition of camber to the wing would displace the drag polar to improve the match between the cruise lift coefficient and that required for maximum lift-drag ratios. However, such changes would result in changes in the longitudinal load distribution and changes in the zero lift pitching moment. The former would necessitate some changes in body contouring to maintain the area envelope required for the sonic boom goal. The latter would require some changes in the cg management during cruise to avoid large trim drag. The influence of revised wing twist and camber should be investigated to determine its effect on improving the airplane cruise match.

Operations and Sizing

Several aspects of the airplane operational criteria have a significant effect on its design and overall mission performance. The configuration as shown in Figure 3 was designed without detailed consideration of these operational constraints. A redesign cycle around this basic configuration would indicate changes which could be made to meet these constraints, improve the performance and maintain the sonic boom design goals.

Normally such a cycle would vary both wing area and engine size. Because of the nature of a sonic boom designed airplane the wing area, mid-cruise weight, and cruise altitude generally can be varied only slightly. The remaining variables of interest are cruise flight profile and engine size and cycle.

Varying the flight altitude during cruise will lead to an improvement in cruise range because the airplane will operate closer to

$(L/D)_{max}$. Such operation will result in some change in sonic boom
signature shape at beginning and end of cruise. This effect should
systematically be studied. Engine size variation will result in
some additional configuration changes which were discussed above. A
complete sizing study should be conducted to select the proper engine
airflow for low speed (takeoff and landing) operation and acceptable
community noise. Once the engine size has been selected, the effect
on the remaining configuration characteristics should be assessed.
These two investigations should be conducted simultaneously with those
described above to obtain a recycled configuration that more closely
meets practical operating constraints.

MID-MACH DESIGN

An intermediate design Mach number was chosen because preliminary
data indicated that a reasonable size and weight airplane could be
designed to produce a cruise sonic boom signature with shock waves of
24 N/m^2 (0.5 psf) or less for K_R = 1.9. This is illustrated in Figure
35 which shows the variation of allowable weight as a function of
altitude for an overpressure of 24 N/m^2 and a configuration length of
106.7 m (350 ft). These data indicate that a quadratic area distri-
bution would result in an airplane with the highest allowable cruise
weight. Hence this form of the area variation was chosen as the
envelope shape for the configuration design. The design point values
were taken as: Cruise Mach number of 1.5; Mid-cruise weight of
284,000 kg (625,000 lb); Overall length of 102.4 m (335 ft); and
Cruise altitude of 13,700 m (45,000 ft).

Configuration Design

The design point area distribution for the airplane was quite
slender at the nose to maintain the front shock overpressure within
the design criteria. For instance, attempts to use a conventionally
shaped nose such as a 6:1 ogive resulted in bow shock overpressures
produced by the nose of about 62 N/m^2 (1.3 psf). The shape of the
equivalent area envelope was also very close to the longitudinal
development of lift for a delta wing planform. This consideration
dictated the use of an arrow wing planform and an up-loaded horizontal
tail for longitudinal balance and trim so that there would be
sufficient difference between the envelope and the lift contribution
to allow for the configuration volume.

The envelope area distribution and the area distribution for each
of the components for this configuration are shown in Figure 36.
This figure also contains a definition of the wing planform. The
data shown were obtained by passing Mach cutting planes through the

34

configuration at the appropriate angle for Mach 1.5 and a point of observation directly beneath the airplane. The nose of the fuselage was designed to be at zero degrees angle of attack at the midcruise condition. This was to minimize the aerodynamic loads so that it would be as light as possible. The remainder of the fuselage was contoured to fill the differences between the envelope curve and the total area of the other components.

A two view drawing of the airplane is shown in Figure 37. The airplane has a low mounted arrow wing with the main structural spars running under the floor. Due to the camber of the root airfoil the wing strake is above the floor line and is attached through frames at the body side. Four pod mounted advanced technology dry turbojet engines are mounted at the wing trailing edge and are supported by external beams attached to the rear spar. Low speed high lift devices consist of full span leading edge flaps and trailing edge flaps. Both are simple hinged surfaces. Longitudinal trim and control are achieved through a horizontal tail with a geared elevator. The main landing gear folds into the wing and has a splash deflector to reduce foreign object ingestion.

The passenger cabin is located in the middle one-third of the fuselage and consists of 180 seats arranged in 6 and 4 abreast configurations at 0.86 m (34 inch) pitch which is compatible with 707 seating comfort. Passenger services are equivalent to those for the U.S. SST design. The cabin has conventional type windows located on 40" centers and the floor height at the loading door is 5.64 m (18.5 ft) which is slightly higher than that for the 747. Two type A loading doors are located forward of the passenger compartment and are compatible with current airline ground support equipment. Pilot forward visibility is provided through the use of optical systems while side windows are available for use during ground maneuvering. Cargo containers are located below the passenger compartment floor and are loaded through a door on the starboard side. These

35

containers are the same size as were specified for the U.S. SST.
Four overwing emergency exits are located throughout the cabin.
Each would contain slides for evacuation.

Aerodynamics

High Speed - Climb, Cruise, Descent

As noted previously the shape of the design envelope equivalent
area distribution dictated the use of the arrow wing planform. The
planform shown in Figure 36 was selected on the basis of sonic boom
requirements for longitudinal lift distribution, reasonable drag
polar shape and low wave drag.

The methods used to design the wing twist and camber are the same
as described previously for the high speed airplane. However, signi-
ficant geometric modifications were made in the root region to
accomplish a) a reasonable wing-body fit without excessive body
camber and, b) a reasonable amount of wing incidence so that the low
speed characteristics would not be severely compromised. The result-
ing wing twist distribution is shown in Figure 38. The wing
thickness distribution was selected by considering weight, wave drag
and main gear stowage. Wing dihedral was used to increase the virtual
length of the lift distribution and to reduce the length of the main
landing gear required for engine clearance during takeoff and landing.

The fuselage shape was determined by taking the difference between
the envelope area and the total area for the remaining components.
Some wave drag penalty was incurred due to the requirements of meeting
a given sonic boom design goal. The penalty amounts to about 10% of
the wing-body wave drag when compared to a fuselage with the same
passenger capacity that had been optimized for minimum wave drag.

Lift and drag characteristics were calculated at several Mach numbers by the methods outlined in the previous section. Wetted areas and friction drags for the configuration as shown in Figure 37 are listed in Table 7 for two Mach numbers and altitudes. A summary of zero lift drags is contained in Table 8 for the same flight conditions. A complete high speed drag polar and lift curve is shown in Figure 39. This figure also contains the variation of trim drag with cg location and a comparison between the envelope polar shape and those for a flat wing and the theoretical optimum. The predicted polar shape appears to be reasonable.

Envelope polar shape factors and zero lift drags were extracted as described previously and were plotted as a function of Mach number for purposes of calculating airplane performance. These data are shown in Figure 40. The zero lift drag was separated into friction drag and wave drag contributions so that the former could be scaled with size or altitude. The value for the polar shape factor at Mach 0.8 was estimated from wind tunnel data for similar wing planforms.

Low Speed - Takeoff, Landing

Low speed lift and drag characteristics were estimated in the manner outlined in the previous section. The predictions are slightly optimistic because the leading edge flap area shown in Figure 37 is slightly less than that on the wind tunnel model which constituted the data base. Both the leading edge and trailing edge flaps are simple hinged surfaces.

The lift and drag characteristics predicted for this airplane are shown in Figures 41 and 42 for trailing edge flap settings of 0° and 30° respectively. The former flap setting was used for takeoff and the latter for landing. The aerodynamic forward limit of 0.50 $\bar{c}$ was taken for the cg location for takeoff and a value of 0.42 $\bar{c}$ was used for landing. Both free air and ground effect estimates are shown. The method of accounting for the influence of ground proximity was discussed in the previous section.

Weights

Weight and Balance Summary

A weight and balance summary of the OEW and ZFW are presented in Table 9. The weight data shown is representative of the following configuration definition:

1. Configuration geometry per Figure 37.

2. Structural and systems concept definitions per Reference 14 except for;
   a. Aluminum structural material
   b. Fixed geometry nose with pilot visibility provided by optical systems
   c. Fixed geometry pitot engine air intake (including takeoff doors).

3. Engine airflow per engine (GE4/J6H2)
   1975 Technology - 270.3 kg/sec (596 lb/sec)
   1985 Technology - 229.5 kg/sec (506 lb/sec)

4. 2707-300 PPD operational and design criteria (Reference 16) for Mach $<$ 1.5

5. Center of gravity tolerance of $\pm$0.25 m ($\pm$10 in) to provide for *customer variations and cg indication system*

Methods of analysis used to derive the weights were based upon the 2707-300 PPD configuration and weight definitions (References 14-16). Consistency has been maintained with the methods used in the High Transonic Speed Transport Aircraft Study Program (Contract NAS2-7031) for material, temperature and pressure differences. The basic methods used were:

o   Body Structure and Contents - 2707-300 extrapolated
    cantilever beam.

o   Wing Structure and Contents - adjustments for geometry
    and wing loading differences.

·o   Empennage Structure and Contents - 2707-300 unit weights.

o   Propulsion Pod - GE4/J6H2 base engine airflow (408 kg/sec.)
    scaled for airflow requirement at cruise. Adjustment made
    for fixed geometry pitot engine intake.

o   Landing Gears - 2707-300 extrapolated length.

Lead ballast was required to provide ground stability (OEW cg.
relative to the Main Landing Gear.)

The weight increments for advanced design concepts are representa-
tive of 1985 Technology with a 1990 design go-ahead. This increment
is consistent with the High Transonic Speed Transport Aircraft Study
Program weight data.

Center of Gravity Management

Loadability and fuel management for the airplane mission is shown in
Fig. 43 for the nominal cg location (see "tolerance" item 5 above).
The cg management schedule is presented in Table 10, based on the fuel
tank definition of Fig. 44.

Ground stability (a measure of the distance between the OEW cg
and Main Landing Gear) is not adequate. Since this distance is only
.025 m. (1 in.), an aft body support is required when the airplane
gross weight is OEW. This requirement could be eliminated by a trans-
ferrable ballast material such as water or fuel. (The forward move-
ment of the ZFW cg resulting from a more forward location of the OEW
cg would be outside of the forward cg limit without transferrable
ballast). Rather than define the loading procedure with transferrable
ballast, greater simplicity was achieved by defining lead (fixed)

ballast and requiring an aft body support. Ground stability could be improved and ballast eliminated by moving the Main Landing Gear aft with a revised configuration definition. Such modifications were beyond the scope of the present study.

The cg for minimum trim drag is behind the aft control limit for a stabilizer deflection of +5°. This location could be achieved for only 10-15% of the cruise duration, due to airplane volume limitations and large changes in cg required. Since moving this control limit aft from .57 to .60 $\bar{c}$ would require a significant weight penalty for larger tail hinge moments for an insignificant reduction of trim drag, the most aft cruise cg selected was .561 $\bar{c}$.

Outboard wing fuel (Tanks 9A and 10A) cannot be held any later during the mission than gross weights between 283,000 kg. (625,000 lb) and 249,000 kg. (549,700 lb). The lowest weight wing structure is obtainable by holding outboard fuel as long as possible, so the optimum use of outboard tanks would be for reserve fuel. Tanks 9A and 10A are too far aft to provide the versatility of flying zero payload (OEW + reserve fuel).

Flight Controls

Aerodynamic data for this design was generated from analyses and wind tunnel data of an early Boeing SST configuration, the 733-290. Comparisons for body size and wing sweep are only approximate although wing aspect ratio is well matched. Aeroelastic effects were based on the Boeing 733-290 configuration with approximate corrections to delete the influence of the wing pivot. No structural analysis, to obtain aeroelastic effects, was made.

Stability and control areas of concern in this design are:

o high angle of attack stability and control for recovery
o tail effectiveness due to tail and body aeroelastic effects
o large wing dihedral effect on lateral and directional
   dynamics and handling qualities, including crosswind
   landing
o engine failure controlability

Control System Description

Longitudinal. The stabilizer (Fig. 37) is a fully hydraulic powered all-flying surface and through its rotation capability it carries all pitch control, trim and SAS functions. The stabilizer carries a mechanically geared trailing edge flap constrained to follow motions of the stabilizer to increase camber and hence lift capability. This stabilizer/flap design was used on the Boeing SST airplane. Limit stabilizer/flap deflections are $+8.5^0/+17^0$ to $-5^0/-10^0$ at high speed, and $+8.5^0/+17^0$ to $-17^0/30^0$ at low speed.

Lateral. The drawing, Fig. 37, shows the location of the lateral control surfaces integrated with the wing trailing edge flap system as noted below:

Panel	Location	Function	Sec. Function
4	Wing T.E. outboard	Low speed aileron	None
3	Outboard of outer nacelle	Flap	None
2	Between nacelles	High speed aileron	Flap at low speed
Spoilers	Outboard of outer nacelle	All speed control	Speed brakes
Spoilers	Between nacelles	Low speed control	Speed brakes

<u>Directional</u>. Figure 37 shows the configuration with a single vertical tail carrying a large full span rudder split spanwise into two panels. The lower panel operates at all speeds and has good aeroelastic properties. The upper rudder panel operates at low speed only because of low aeroelastic effectiveness at high speeds.

<u>Auxiliary Systems</u>. The longitudinal flight control system incorporates a hardened stability augmentation system (HSAS) to allow the airplane to fly with the cg up to 6% aft of the unaugmented maneuver point.

The high angle of attack (pitch up) characteristics of this configuration are expected to be severe, hence an angle of attack limiting system is identified for the airplane but its characteristics are not defined at this stage.

The lateral-directional axes will include a stability augmentation system to provide Dutch roll damping, improvement in the roll mode time constant, and also provide automatic directional control for assymetric conditions such as engine failures.

Airplane Characteristics

<u>Longitudinal</u>. The airplane balance is shown in Fig. 45 and indicates that at the low and high speed conditions the center of gravity range is limited by the control capability of the horizontal tail and not by airplane stability. This situation is a direct result of incorporating a hardened stability augmentation in the design.

ɔ The low speed center of gravity limits are shown in Figs. 45 and 46 and are seen to be a function of trimmed lift coefficient and hence speed. The forward cg is limited by landing requirements (see "Criteria" pg. 20). The aft cg is limited by push control and since the pitching moment characteristic is an unstable one, Fig. 47, then the limit is taken at $C_{L_{max}} + \Delta \alpha = 5^0$ for pitch overshoot. The high

speed(Mach 1.5) cg limits are shown in Figures 45 and 48 and are seen
to be limited by the deflection capability of the horizontal tail.
The deflection limits chosen of i_H = +8.5° to -5° are chosen to provide
a useable cg range and are not thought to require excessive hinge
moment capabilities of the tail actuators. The forward cg (.456 $\bar{c}$)
is determined by a horizontal tail deflection limit of -5° and a load
factor of 2, a stable condition. The aft cg (.57 $\bar{c}$) is obtained
from the positive tail deflection limit and from a control limit taken
at n = 2.5 + $\Delta\alpha$ = 5° for pitch overshoot, resulting in unstable
pitching moment characteristics.

Takeoff rotation capability is shown in Figure 49 as the speed
at which full pitch control raises the nose gear. At forward cg the
minimum rotation speed is not expected to compromise takeoff
performance.

Lateral and Directional. The basic stability characteristics are
based on past Boeing wind tunnel data for highly swept wing SST
configurations corrected for the appropriate vertical tail size.
Figures 50 and 51 show the low speed and high speed values of C_{n_β} ,
C_{ℓ_β} , C_{y_β} respectively. Of note in the data is the dihedral effect.
C_{ℓ_β} , which is the high because of the high sweep and large geometric
wing dihedral.

Figure 52 shows the rudder capability to control and trim an
adverse (outboard) engine failure at takeoff. At maximum takeoff
thrust the minimum control speed V_{MCg} is sufficiently low to not
influence takeoff performance.

No analyses of high speed engine failure upsets have been made
but they are expected to be severe because of the large wing dihedral
effect causing the roll due to sideslip to be excessive. The engine/
inlet failures themselves are not expected to be severe since the
inlet is a simple pitot external compression type.

The large dihedral effect is evident in the crosswind landing situation shown in Fig. 53 where strong crosswinds require high approach speeds or a crosswind gear to prevent the lateral control trim requirement to be exceeded. The rudder requirement for cross-wind landing is not critical and is not shown.

The only lateral control estimates made are the requirements to provide a minimum roll response capability at landing approach as a comparison for the crosswind landing requirement shown in Fig. 53. No other assessment of the capability of the lateral control surfaces as drawn has been made.

Propulsion

The engine for the mid-Mach low sonic boom airplane is also based upon a scaled and modified version of the GE4/J6 study H2 engine of References 18 and 19. It incorporates the same retractable jet noise suppressor as specified for the High Speed Design and assumes a 15% red-uction in airflow and weight achieved from technology improvements.

An optimum cycle for a Mach 1.5 cruise SST has not been determined; however, previous studies indicate significantly improved fuel consumption for a higher pressure ratio turbojet as compared to the GE4/J6H2 dry turbojet which had a pressure ratio of 12.5. Therefore, it was assumed that the pressure ratio of the turbojet was increased to 15.5 for a Mach 1.5 cruise vehicle. This resulted in the following changes relative to the GE4/J6H2 engine:

a. At takeoff, subsonic cruise, and acceleration from takeoff
    to Mach .95: same thrust; SFC 4% lower.
b. At supersonic cruise at Mach 1.5 and acceleration from
    Mach .95 to Mach 1.5: Maximum thrust 2% less, and SFC
    3% less.
c. Nozzle performance and weight same as that of the trans-
    lating shroud plug nozzle of the GE4/J6H2 engine.

44

d. The intake is a pitot intake with takeoff doors rather
than a translating spike intake. The intake drag and
weight are reduced accordingly.

By sizing the engine for cruise at Mach 1.5 an airflow size of
229.5 kg/sec was chosen. The pod dimensions for this engine are shown
in Fig. 54.

Various intake, nozzle, and engine performance values are given
in Table 11 at selected operating conditions. The discussion on high
energy fuels applies to both the Mach 1.5 and Mach 2.7 airplanes.

STRUCTURES

Structural Arrangement

The wing structure consists of spar and rib construction as shown
in Fig. 37. The spars are perpendicular to the centerline inboard of
the Buttock Line (BL) 5.94 rib, and sweep aft outboard of that point.
All spars are parallel to the rear spar. The spars at Body Station
(BS) 71.63 and 78.23 form the front and rear walls of the wheel wells.

Each wing has four major ribs. The side-of-body rib and the
BL 5.94 rib form the boundaries of the wheel wells. The latter rib
also supports the inboard engine. The outboard engine is supported by
the rib at BL 9.91. The remaining rib closes out the wing tip. The
wing covers are bonded sandwich panels incorporating the most advanced
material developments available.

Experience indicates that the very flexible airframe combined
with aft mounted engines, tends to be flutter critical. It is assumed
for purposes of this study that any such deficiency will be corrected
through the use of flutter SAS.

The fuselage is a highly contoured envelope sitting on top of the wing. The circular frames transmit wing loads around the passenger compartment. Small windows are provided along the side of the body. The body skins over the more highly stressed regions will be sandwich construction, while the less heavily loaded areas will be stiffener stabilized sheet. The very long nose cone, being very lightly loaded is assumed to be constructed of advanced composite material taking maximum advantage of the specific strength and stiffness of that material.

The landing gear consists of two main gear posts mounted on the BS 78.23 spar. Each post has twelve wheels. The nose gear consists of a single post with double wheels mounted at BS 42.16.

Structural Materials

The moderate temperatures associated with cruise at Mach 1.5 permits the use of aluminum and advanced composite structures using organic adhesives and matrices. The weight estimates have allowed for a distributed weight saving of 10% of OEW to account for the use of these advanced materials.

Airplane Performance

The configuration shown in Fig.37 was designated the "baseline airplane". The 229.5 kg/sec (506 lb/sec) engines selected by considering only the cruise thrust requirements were found too small for take-off because of the high gross weight. It was also noted that cruising at the design altitude had an adverse effect on range.

Since a complete engine-airframe matching study was beyond the scope of this investigation, the effect of several parametric changes in engine airflow was calculated to approximately determine a more

46

suitable size. In addition, the effect of a varying cruise altitude on range and sonic boom characteristics was studied. The following material is a summary of the payload-range, take-off and landing, noise and sonic boom characteristics for the parametric variations noted.

Payload-Range Summary

The assumptions used in calculating the performance capability of this airplane were the same as those previously described for the High Speed Design. A summary of the payload range characteristics is shown in Fig. 55.

This airplane can carry a 16730 kg (36900 lb) payload (180 pass.) in excess of 5960 km, (3220 nmi). To accomplish this requires engines which are 10% larger than shown in Fig. 37 in order to begin cruise without exceeding maximum continuous thrust rating. The M = 1.5 cruise is conducted at 13.7 km (45,000 ft.) pressure altitude.

Increasing the engine size beyond 10% does not significantly improve the cruise match at 13.7 km (45,000 ft). This is because the larger engine requires the addition of forward ballast to maintain balance. The effect of increasing engine size on airplane weight is shown in Figure 56. When these effects are included the influence of larger engines is a reduction in range. The effect of engine size on range and climb gradient capability is shown in Fig. 57. This figure also shows the influence of allowing the airplane to cruise at the altitude for best value of km/kg which optimizes the cruise match throughout. The standard day range for this case is just in excess of 6070 km (3280 nmi) with the design payload of 180 passengers. This represents about 2% increase in range over the design constant altitude cruise case.

Noise and Low Speed Characteristics

The assumptions used in calculating the low speed performance and noise characteristics were the same as outlined for the High Speed Design. These characteristics are summarized in Fig. 58 as a function of engine size.

At sea level on a Standard +15°C day this configuration requires F.A.R. field lengths in excess of 5300 m (17,400 ft). Its takeoff climb capability at 2nd segment is marginal even with all engines operating and it cannot accommodate an engine failure during takeoff. At .65 km (.35 nmi) to the side of the runway centerline, per F.A.R. 36, the maximum noise during takeoff is about 108 EPNdB. This is due to the jet suppression included in the advanced engine and power limit (84% max) observed at takeoff. However, noise on the extended runway centerline 65 km (3.5 nmi) from brake release, per F.A.R. 36, will be much louder since the altitude will be very low. A detailed analysis was not conducted but noise levels well in excess of 120 EPNdB can be expected. Landing performance and approach noise were not computed in detail but are not expected to be as critical as takeoff. Approach speeds of 257 km/hr, EAS, (139 kts, EAS) are expected at mission landing weights. More acceptable takeoff performance could be achieved with larger engines but, as noted above, this would cause a decrease in airplane range or payload.

Sonic Boom Characteristics

Sonic boom signatures were calculated for two of the parametric cases discussed above. These were: The baseline airplane (Fig. 37) with 10% larger engines at a constant cruise altitude of 13.7 km (45,000 ft); and this same airplane with a climbing cruise for best range. The estimated sonic boom signatures in cruise are shown in Figs. 59 and 60, respectively, for beginning of cruise, mid-cruise, and end of cruise.

48

All of the signatures shown have a tail shock wave of about 36 N/m^2 (0.75 psf) which exceeds the design goal. This shock wave could not be reduced further without some extreme aft body contouring which would have resulted in unacceptable drags. The remainder of the signatures for both cases have shock waves which are each less, than the design goal. The total pressure change exceeds 24 N/m^2, but this is achieved through a series of smaller pressure jumps and isentropic pressure increases.

Considerations for Continued Study

The basic criteria for the design of this airplane was to meet a sonic boom goal of a cruise signature with shock waves no stronger than 24 N/m^2 (0.5 psf) while relaxing other constraints as necessary. These constraints consisted of items such as low speed operational restrictions, community and airport noise, cruise drag minimization, and passenger capacity. Due to the limited scope of this study only the most fundamental answers have been obtained and the influence of these constraints were not evaluated in depth. Additional work would be required to determine the full potential of this configuration and to formulate solutions to the problem areas that have been identified. The following material is a brief review of these areas along with an outline of the investigations that would be directed toward obtaining solutions. The probable impact on the sonic boom goal is also noted.

Drag Improvement

Analysis of this airplane has indicated a reasonably good match between the airplane design cruise condition and the flight condition for maximum ratio of lift and drag, $(L/D)_{max}$. Hence improvements in cruise drag could be obtained by reducing the zero lift drag and by

49

improving the shape of the drag polar. Further improvement in the high lift characteristics would also improve the overall capability of the airplane.

The largest contribution to high zero lift drag is the wing-body wave drag. The fuselage was shaped to fill the area envelope required for the sonic boom goal. As such it does not represent the shape for minimum wave drag. A systematic study of the influence of fuselage shaping on drag and boom should be made to determine the best compromise.

Some difficulty was encountered in mating the wing and body due to the wing camber and twist distribution. The fuselage was slightly cambered to achieve a compatible structural arrangement and to avoid reducing the low speed - high lift efficiency. It would be desirable to investigate the influence of camber and twist changes on the polar shape, low speed characteristics and structural arrangement. The effect of a more compatible design on the fuselage shape to achieve the sonic boom goal would be evaluated. Such a design cycle would be necessary to reduce the fuselage structural weight.

The effect of engine size on sonic boom characteristics, drag and airplane balance should also be studied since it appears that some adjustment should be made. The effect on meeting the design goal signature should be small because the aft body shape can be adjusted to maintain the area envelope shape. The effect on airplane balance and drag may be more significant. These influences should be studied in a systematic manner.

Operations

To obtain the maximum cruise range the airplane should be allowed to change altitude during cruise. Such changes will result in variations in the signature shape produced. A systematic study of these effects should be made to determine the relationship between

range increments and sonic boom characteristics during cruise.

Reduction of Tail Shock Strength

The tail shock wave currently exceeds the goal of 24 N/m^2. The strength of this shock wave is quite sensitive to the aft shape of the area envelope. Preliminary efforts to reduce the strength through aft body contouring resulted in unacceptable drags. Alternate methods should be studied. These include: variations in horizontal tail loading; changes in engine plume effects; small changes in aft body contouring; and use of secondary air exhausted from the aft body.

CONCLUSIONS AND RECOMMENDATIONS

The purpose of this study was to determine if an airplane designed to produce a sonic boom singature with low overpressure during cruise would represent a feasible commercial transport. Two configurations were designed and reviewed. These were a high speed Mach 2.7 airplane and an intermediate speed Mach 1.5 airplane.

The fundamental design criteria was to meet the sonic boom design goals relaxing other normal design and operational constraints as necessary. Due to the limited scope of the study only preliminary answers have been obtained. The work accomplished indicates that, in principle, a sonic boom designed SST appears to be a feasible concept. The airplanes as they are presently defined in this document have not been optimized and additional work will be necessary to formulate solutions to some fairly serious problems that have been identified. This work should be concentrated in the following areas:

o   Configuration design to improve cruise efficiency within the constraints imposed by the sonic boom goal.

o   Compliance with takeoff, landing and noise constraints.

o   Determination of acceptable sonic boom signature shapes for establishment of further guidelines.

Of the two airplanes investigated the High Speed Design concept seems to offer the greatest potential as an SST configuration. The results of the study indicate that the design objectives for this concept could be revised to obtain a more optimum overland airplane. The new objectives could consist of the following:

o   Sonic boom maximum overpressure less than 48 N/m^2
    (1.0 psf).

o   Transcontinental range for sonic boom design purposes
    with attendant reductions in takeoff and cruise
    weight.

o   Cruise Mach number less than 2.7 to allow associated
    reductions in goal sonic boom overpressure.

o   Design point conditions based on initial cruise con-
    ditions to assure conformance to the sonic boom goal
    throughout cruise.

An airplane with these design objectives should be more
nearly capable of meeting the low speed constraints because
of the reduced takeoff gross weight. Also such an airplane may
offer the potential of intercontinental range over water where
sonic boom level is not a restraint.

REFERENCES

1. McLean, F. E. "Some Nonasymptotic Effects on the Sonic Boom of Large Airplanes". NASA TND-2877, June 1965.

2. Ferri, A. "Airplane Configurations for Low Sonic Boom". NASA SP-225, pages 255-275, October 1970.

3. Ferri, A., Wang, H. C., and Sorensen, H. "Experimental Verification of Low Sonic Boom Configuration". NASA CR-2070, June 1972.

4. Carlson, H. W., Barger, R. L., and Mack, R. J. "Application of Sonic Boom Minimization Concepts in Supersonic Transport Design". NASA TND-7218, June 1973.

5. Miller, D. S. and Carlson, H. W. "A Study of the Application of Heat or Force Fields to the Sonic Boom Minimization Problem". NASA TND-5582, December 1969.

6. Seebass, A. R. and George, A. R., "Sonic Boom Minimization". Journal of Acoustical Society of America, Volume 51, No. 2 (Part 3), February 1972.

7. Jones, L. B. "Lower Bounds for Pressure Jumps of the Shock Waves of a Supersonic Transport of Given Length". Aeronautical Quarterly, Volume 23, February 1972.

8. Howell, C. S., Sigalla, A., and Kane, E. J., "Sonic Boom Considerations in Aircraft Design". AGARD Conf. Proc. No. 42, May 1969.

9. Kane, E. J., "A Review of Current Sonic Boom Studies". AIAA Journal of Aircraft, Vol. 10, No. 7, July 1973.

10. Carlson, H. W. and Middleton, W. D., "A Numerical Method for the Design of Camber Surfaces of Supersonic Wings with Arbitrary Planforms". NASA TND-2341, 1964.

11. Sommer, S. C. and Short, B. J., "Free-Flight Measurements of Turbulent Boundary Layer Skin Friction in the Presence of Severe Aerodynamic Heating at Mach Numbers from 2.8 to 7.0". NACA TN 3391, March 1955.

12. Harris, R. V., "An Analysis and Correlation of Aircraft Wave Drag". NASA TMX-947, 1964.

13. Middleton, W. D. and Carlson, H. W., "Numerical Method of Estimating and Optimizing Supersonic Aerodynamic Characteristics of Arbitrary Planform Wings". J. Aircraft, Vol. 2, No. 4, pages 261-265, July-August 1965.

14. "Design Data Manual - SST". Boeing Document D6-6725-1, May 1969.

15. "Weight and Balance Status Report". Boeing Document D6A-10552-1 June 1970.

16. "SST PPD Airplane Design Objectives, Requirements, Criteria". Boeing Document D6-6800, October 1968.

17. "Mach 2.7 Fixed Wing SST, Model 969-336C (SCAT 15F)". Boeing Document D6A-11666-1, August 7, 1969 (Contract FA-SS-67-3).

18. "Advanced Technology Turbojet Engine". General Electric Report, GE4/J6 Study H2, January 29, 1971.

19. "Instructions for the Use of the General Electric GE4/J6 Study
    H2 Dry Turbojet Engine Estimated Performance Data Deck".
    General Electric Report R70 AEG 332B, Feb. 1971. (Confidential)

20. Tjonneland, E., "The Design, Development and Testing of a
    Supersonic Transport Intake System". AGARD report AGARD-CP-91-71
    paper no. 18, 1971.

LSB/HS-3		Friction Drag S_{REF} = 721.8 m^2		
Component	Wetted Area m^2	M = 2.7 Alt = 16.8 km	M = 1.5 Alt=11.3 km	M = 0.8 Alt = 11.0 km
Wing	1551.9	.00258	.00331	.00428*
Body	809.3	.00111	.00139	.00176
Nacelles	157.8	.00031	.00039	.00048
Vert. Tail	163.5	.00033	.00042	.00051
Ventral	27.9	.00006	.00007	.00008
Total	2710.4	.00439	.00558	.00711

*Includes profile drag

TABLE 1   SUMMARY OF WETTED AREAS AND
FRICTION DRAG

LSB/HS-3	Drag S_{REF} = 721.8 m^2		
Item	M = 2.7 Alt = 16.8 km	M = 1.5 Alt = 11.3 km	M = 0.8 Alt = 11.0 km
Friction	.00439	.00558	.00711
Wave	.00280	.00330	-
Misc*	.00025	.00052	.00034
Total	.00744	.00940	.00745

*Includes roughness, protuberances and air conditioning

TABLE 2   SUMMARY OF ZERO LIFT DRAG

| ITEM | WEIGHT | | C.G. | | % |
| | kg. | lb. | BODY STATION | | MAC |
			m.	in.	
Nose to Wing Front Spar sta. 5.08(200) to 70.358(2770)	(38,692)	(85,300)	(44.145)	(1738)	
Body and Contents	36,605	80,700	45.187	1779	
Nose Landing Gear (up)	726	∘1,600	32.512	1280	
Canard (out)	1,361	3,000	22.301	878	
Wing Front Spar to Rear Spar sta. 70.358(2770) to 80.518(3170)	(112,808)	(248,700)	(75.844)	(2986)	
Body and Contents	13,336	29,400	75.438	2970	
Wing Structure	41,821	92,200	71.653	2821	
Wing Contents	12,610	27,800	69.596	2740	
Propulsion Pod	29,710	65,500	86.868	3420	
Main Landing Gear (up)	11,748	25,900	66.802	2630	
Vertical Tail and Contents	3,583	7,900	86.868	3420	
Aft Body sta. 80.518(3170) to 96.520(3800)	(1,814)	(4,000)	(85.090)	(3350)	
OEW (Gears up)-1975 Technology	[153,314]	[338,000]	[67.945]	[2675]	[50.9]
Advanced Technology Increments	(-12,700)	(-28,000)	(67.107)	(2642)	
Decrease engine airflow 15%	-3,402	-7,500	86.868	3420	
Design concepts on airplane less propulsion pod (~7.5%)	-9,298	-20,500	59.868	2357	
OEW (Gears up)-1985 Technology	[140,614]	[310,000]	[68.021]	[2678]	[51.1]
Payload	(14,040)	(30,955)	(51.765)	(2038)	
Passengers (151)	11,300	24,915	47.803	1882	
Baggage	2,740	6,040	68.072	2680	
Zero Fuel Weight (ZFW) - 1985 Technology	[154,654]	[340,955]	[66.548]	[2620]	[47.3]
C.G. Tolerance			-.254	-10	
Forward C.G. Limit (low speed)			66.29	2610	46.6

TABLE 3   WEIGHT AND BALANCE SUMMARY -
HIGH SPEED DESIGN

ITEM	TANK	WEIGHT		C.G.		
				BODY STATION		%
		kg.	lb.	m.	in.	MAC
OEW [2]		(140,614)	(310,000)	(68.021)	(2678)	(51.1)
Allow Payload (151 PAX)		14,041	30,955	51.765	2038	
Zero Fuel Weight (ZFW) [2]		(154,654)	(340,955)	(66.548)	(2620)	(47.3)
Reserve Fuel	1,2,3,4	34,040	75,045	77.90	3067	
Max. Landing Wt. (MLW)		(188,694)	(416,000)	(68.580)	(2700)	(52.6)
Aux. Fuel	10A,11A	36,287	80,000	50.267	1979	
SUB-TOTAL		(224,982)	(496,000)	(65.837)	(2584)	(44.9)
Aux. Fuel	6A,7A	13,154	29,000	81.255	3199	
	8A,9A	11,340	25,000	56.591	2228	
Mid-Cruise (MC)		(249,476)	(550,000)	(66.040)	(2600)	(45.9)
Aux. Fuel	6A,7A	13,834	30,500	81.255	3199	
	8A,9A	11,340	25,000	56.591	2228	
	3A,4A	8,845	19,500	71.501	2815	
SUB-TOTAL		(283,495)	(625,000)	(66.593)	(2621)	(47.3)
Aux. Fuel	1A,2A	11,340	25,000	74.016	2914	
Start of Cruise (SOC)		(294,835)	(650,000)	(66.85)	(2632)	(48.1)
Aux. Fuel	1A,2A	4,536	10,000	74.016	2914	
	5A	27,215	60,000	85.852	3380	
Canard-out-placard [1]		(326,586)	(720,000)	(68.580)	(2700)	(52.6)
Aux. Fuel	1A,2A	6,804	15,000	74.016	2914	
	3A,4A	6,804	15,000	71.501	2815	
Max. Design Taxi Wt. (MTW)		(340,194)	(750,000)	(68.605)	(2701)	(53.1)

[1] V_e = 180 m/s (350 knots)

[2] 1985 Technology

TABLE 4 C.G. MANAGEMENT SCHEDULE, ALTERNATIVE I - HIGH SPEED DESIGN

ITEM	TANK	WEIGHT		C.G.		
				BODY STATION		%
		kg.	lb.	m.	in.	MAC
OEW [2]		(140,614)	(310,000)	(68.021)	(2678)	(51.1)
Allow Payload (151 PAX)		14,041	30,955	51.765	2038	
Zero Fuel Weight (ZFW)		(154,654)	(340,955)	(66.548)	(2620)	(47.3)
Reserve Fuel	1,2, 3,4,	34,040	75,045	66.599	2622	
Max. Landing Wgt. (MLW)		(188,694)	(416,000)	(66.548)	(2620)	(47.3)
Aux. Fuel	8A,9A	15,604	34,400	50.267	1979	
SUB-TOTAL		(204,298)	(450,400)	(65.303)	(2571)	(44.0)
Aux. Fuel	3A,4A	11,158	24,600	71.501	2815	
	8A,9A	13,154	29,000	50.267	1979	
	6A,7A	20,865	46,000	81.255	3199	
Mid-Cruise (MC)		(249,476)	(550,000)	(66.040)	(2600)	(45.9)
	6A,7A	17,645	38,900	81.255	3199	
	8A,9A	9,979	22,000	50.267	1979	
	3A,4A	6,396	14,100	71.501	2815	
SUB-TOTAL		(283,495)	(625,000)	(66.573)	(2621)	(47.3)
Aux. Fuel	1A,2A	11,340	25,000	74.016	2914	
Start-of-Cruise (SOC)		(294,835)	(650,000)	(66.85)	(2632)	(48.1)
Aux. Fuel	1A,2A	4,536	10,000	74.016	2914	
	5A	27,215	60,000	85.852	3380	
Canard-out-placard [1]		(326,586)	(720,000)	(68,580)	(2700)	(52.6)
Aux. Fuel	1A,2A	6,804	15,000	74.016	2914	
	3A,4A	6,804	15,000	71.501	2815	
Max. Design Taxi Wt. (MTW)		(340,194)	(750,000)	(68.605)	(2701)	(53.1)

[1] V_e = 180 m/s (350 knots)

[2] 1985 Technology

TABLE 5   C. G. MANAGEMENT SCHEDULE, ALTERNATIVE II -
HIGH SPEED DESIGN

Condition	Mach	Alt. Std. Day m	Intake Recovery P_{t2}/P_{to}	Nozzle/After-body Thrust Coefficient, $\dfrac{F_{ga}-D_{ab}}{F_{g\ ideal}}$	Excess Air intake Drag. D_{int}/q m^2	Internal Installed Thrust F_{Ni}/q m^2	Installed Specific Fuel Consumption SFC* mg/s/N
Takeoff (Suppressed)	.34	0 (Std. +15°C)	.977	.919	.026	24.0	35.4
Climb	.8	6553	.972	.961	.033	5.79	35.6
"	1.5	12192	.915	.956	.139	3.02	38.7
"	2.7	16764	.905	.979	.077	1.93	41.3
Cruise	2.7	16764	.905	.980	.077	1.72	41.1
"	.9	11521	.972	.940	.066	3.28	33.3
Hold	.525	4572	.982	.945	.048	3.29	33.2

*Does not include effect of excess air intake drag

TABLE 6   SUMMARY OF ENGINE PERFORMANCE CHARACTERISTICS - HIGH SPEED DESIGN

LSB/MM-3		Friction Drag $S_{REF} = 751.2$ m^2	
Component	Wetted Area m^2	M = 1.5 Alt = 13.7 km	M = 0.8 Alt = 11.0 km
Wing	1379.6	.00305	.00376*
Body	853.1	.00149	.00161
Nacelles	179.7	.00044	.00052
Vert Tail	109.2	.00029	.00033
Horiz Tail	150.9	.00040	.00046
Total	2672.5	.00567	.00668

*Includes profile drag

TABLE 7   SUMMARY OF WETTED AREAS
AND FRICTION DRAG

LSB/MM-3	Drag $S_{REF} = 751.2$ m^2	
Item	M = 1.5 Alt = 13.7 km	M = 0.8 Alt = 11.0 km
Friction	.00567	.00668
Wave	.00372	-
Misc*	.00054	.00032
Total	.00993	.00700

*Includes roughness, protuberances and air conditioning

TABLE 8   SUMMARY OF ZERO LIFT DRAG

ITEM	WEIGHT		C.G.		
			BODY STATION		%
	kg.	lb.	m.	in.	MAC
Nose to Wing Front Spar Sta.5.08(200) to 71.63(2820)	(32,160)	(70,900)	(47.96)	(1888)	
Body and Contents	28,803	63,500	49.96	1967	
Chines	227	500	30.73	1210	
Nose Landing Gear (up)	1,134	2,500	39.37	1550	
Ballast (lead)	1,996	4,400	25.65	1010	
Wing Front Spar to Rear Spar Sta.71.63(2820) to 84.84(3340)	(124,375)	(274,200)	(83.34)	(3281)	
Body and Contents	11,884	26,200	78.84	3104	
Wing and Contents	67,993	149,900	82.70	3256	
Propulsion Pod	30,346	66,900	90.17	3550	
Main Landing Gear (up)	14,152	31,200	75.44	2970	
Aft Body Sta.84.84(3340) to 107.44(4230)	(16,783)	(37,000)	(95.68)	(3767)	
Body and Contents	11,294	24,900	92.91	3658	
Horizontal Tail & Contents	3,311	7,300	102.11	4020	
Vertical Tail & Contents	2,177	4,800	100.33	3950	
OEW (GEARS UP)-1975 Technology	[173,318]	[382,100]	[77.95]	[3069]	[50.7]
Advanced Technology Increments	(-18,144)	(-40,000)	(80.06)	(3152)	
Decrease engine airflow 15%	- 2,812	- 6,200	90.17	3550	
Flutter stiffness	+ 2,041	+ 4,500	82.70	3256	
Design concepts (-10%)	-17,373	-38,300	78.74	3100	
OEW (GEARS UP)-1985 Technology	[155,174]	[342,100]	[77.70]	[3059]	[49.8]
Payload	(16,738)	(36,900)	(60.91)	(2398)	
Passengers (180)	13,472	29,700	60.60	2386	
Baggage	3,266	7,200	62.10	2445	
Zero Fuel Weight (ZFW) 1985 Technology	[171,912]	[379,000]	[76.07]	[2996]	[44.1]
C.G. Tolerance			- .25	- 10	
Forward C.G. Limit (low speed) Req'd			75.82	2985	
Forward C.G. Limit (low speed) Prov'd			75.82	2985	43.3

TABLE 9 WEIGHT AND BALANCE SUMMARY -
MID-MACH DESIGN

ITEM	TANK ▷	WEIGHT		C.G.		
				BODY STATION		%
		kg.	lb.	m.	in.	MAC
OEW ▷		(155,174)	(342,100)	(77.70)	(3059)	(49.8)
Allow.Payload (180 Pax.)		16,738	36,900	60.91	2398	
Zero Fuel Weight (ZFW) ▷		(171,912)	(379,000)	(76.07)	(2995)	(44.1)
Reserve Fuel	1,2,3,4	35,153	77,500	80.52	3170	
Max. Landing Wt.(MLW)		(207,065)	(456,500)	(76.84)	(3025)	(46.8)
Aux. Fuel	11A	42,275	93,200	92.71	3650	
Sub Total		(249,340)	(549,700)	(79.53)	(3131)	(56.1)
Aux. Fuel	9A,10A	21,319	47,000	86.87	3420	
	7A,8A	12,837	28,300	67.31	2650	
Mid-Cruise (MC)		(283,495)	(625,000)	(79.53)	(3131)	(56.1)
Aux. Fuel	4A,5A	24,948	55,000	82.04	3230	
	2A,3A	24,948	55,000	75.44	2970	
Start-of-Cruise (SOC)		(333,390)	(735,000)	(79.40)	(3126)	(55.7)
Climb Fuel	1A	18,144	40,000	45.72	1800	
Max. Design Taxi Wt. (MTW)		(351,534)	(775,000)	(77.65)	(3057)	(49.6)

▷ 1985 Technology

▷ Approximate location - tank boundary definitions were not iterated after initial definition. Refer to Figure   .

TABLE 10   C. G. MANAGEMENT SCHEDULE -
MID-MACH DESIGN

Condition	Mach	Alt. Std. Day m	Intake Recovery P_{t2}/P_{to}	Nozzle/After-body Thrust Coefficient, $\dfrac{F_{ga}-D_{ab}}{F_{g\ ideal}}$	Excess Air intake Drag. D_{int}/q m²	Internal Installed Thrust F_{Ni}/q m²	Installed Specific Fuel Consumption SFC* mg/s/N
Takeoff (Suppressed)	.3	0 (Std. +15°C)	.977	.919	.008	27.7	34.0
Climb	.8	6553	.972	.961	.014	5.92	34.2
"	1.5	13720	.915	.956	.09	3.36	37.6
Cruise	1.5	13720	.915	.953	1.03	2.67	36.0
"	.9	11521	.972	.935	.03	3.09	32.4
Hold	.5	4572	.982	.940	.025	3.57	33.0

*Does not include effect of excess air intake drag.

TABLE 11   SUMMARY OF ENGINE PERFORMANCE CHARACTERISTICS - MID-MACH DESIGN
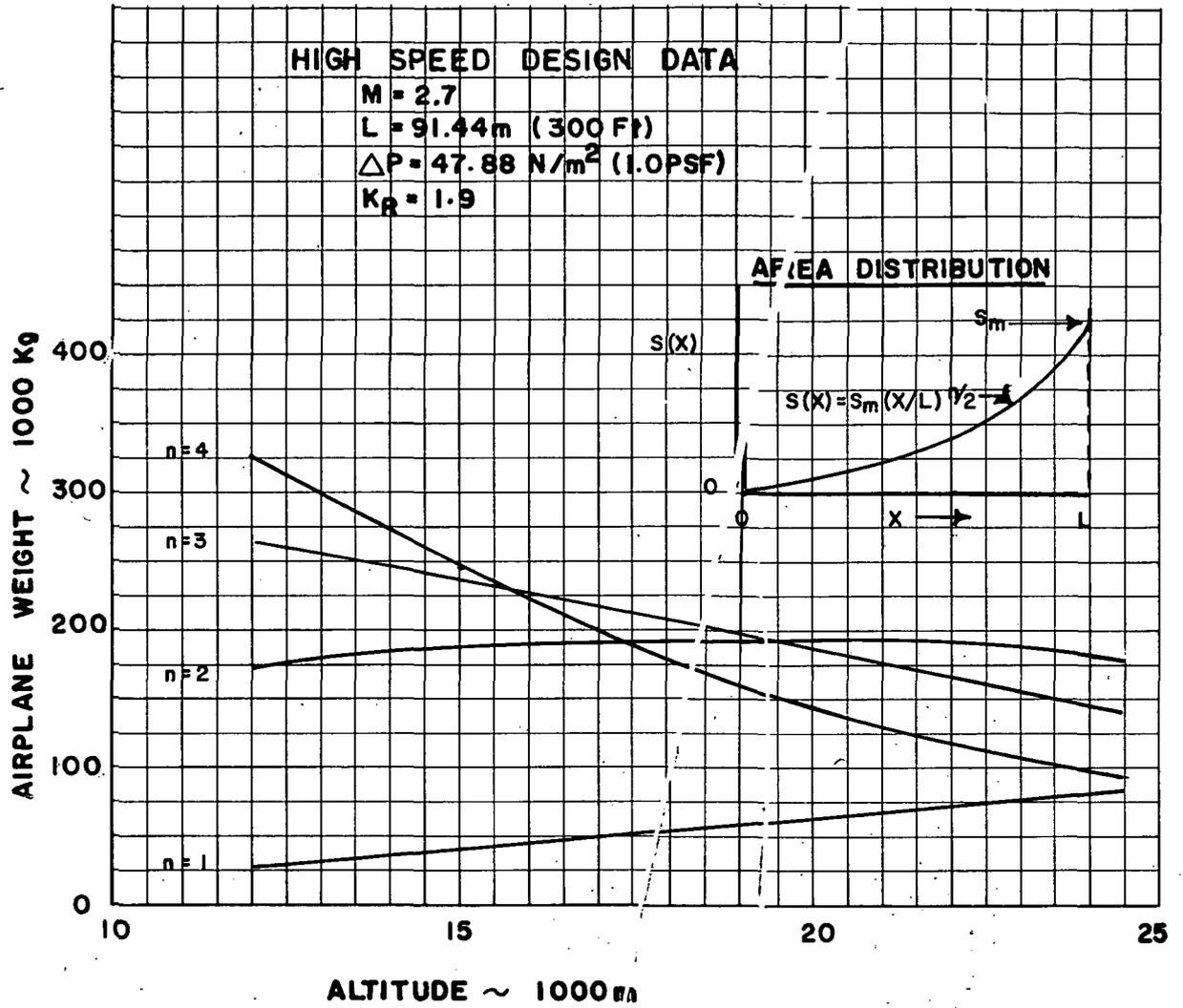
FIG. 1   HIGH SPEED DESIGN DATA

66
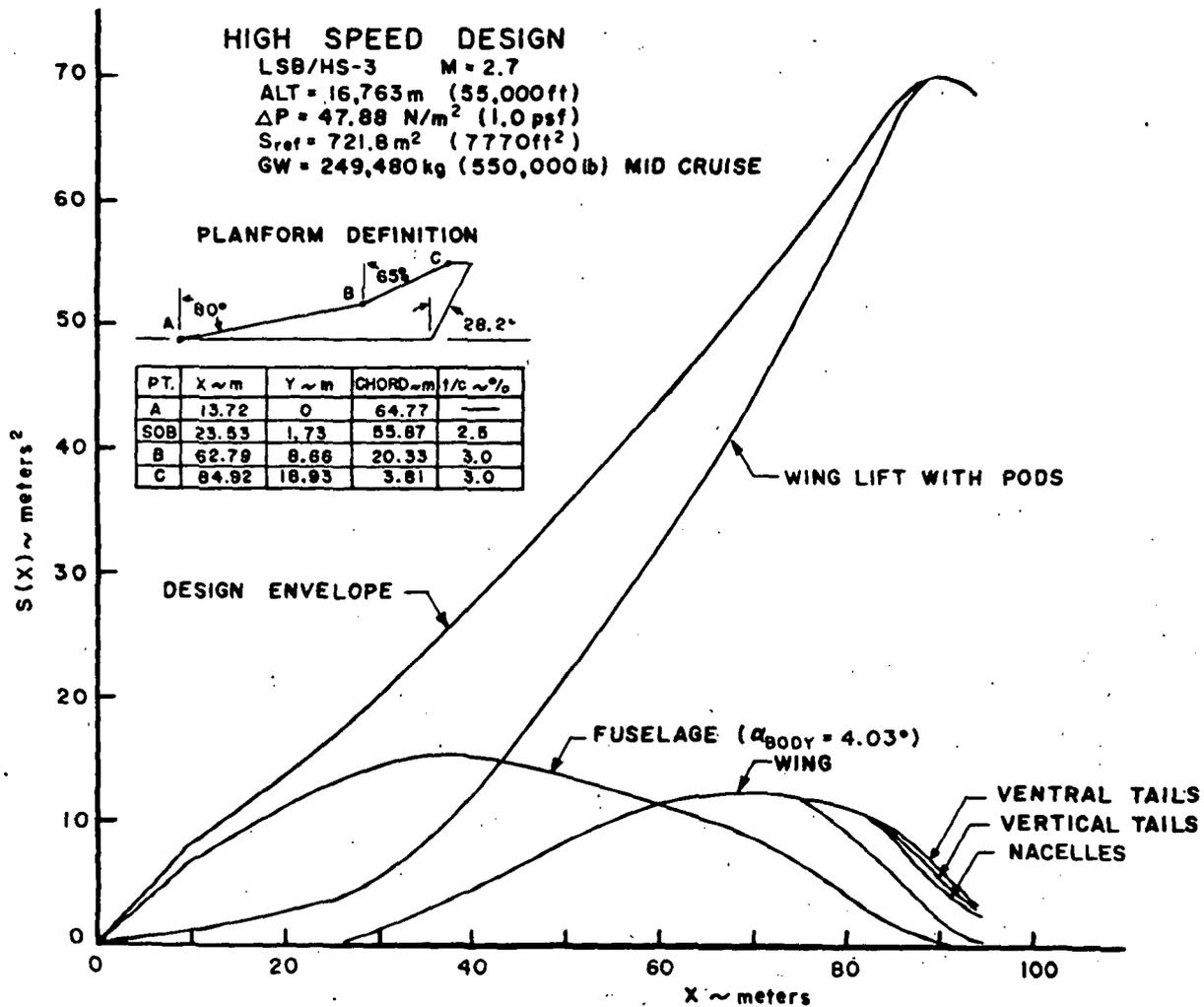
FIG. 2   DESIGN POINT AREA DISTRIBUTION ~ HIGH SPEED DESIGN
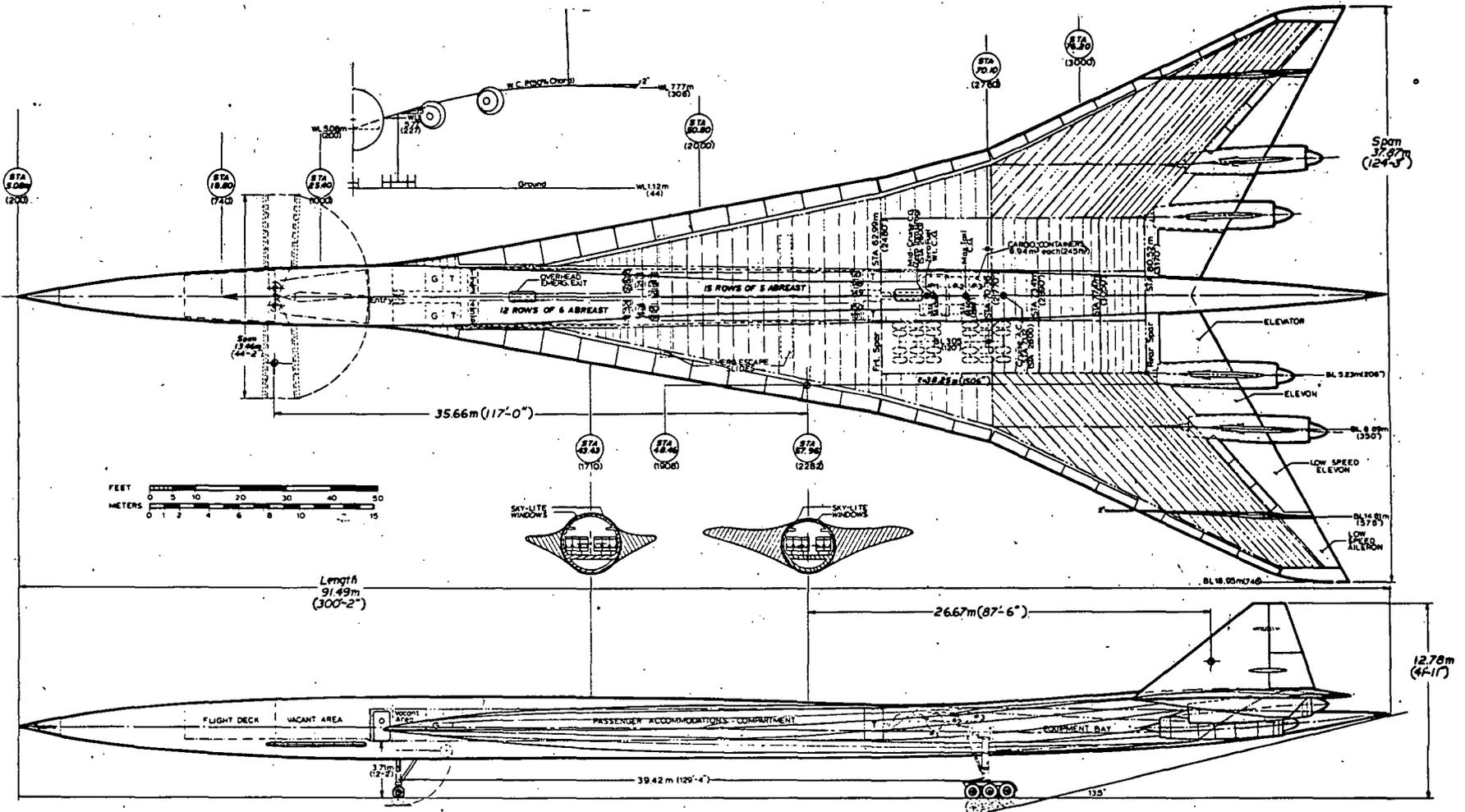
FIG. 3   HIGH SPEED DESIGN CONFIGURATION - LSB/HS-3

LSB/HS-3 Mach=2.7 CONFIGURATION DATA

GROSS WEIGHT 340,136 kg. (750,000 lbs.)		NOMINAL PAYLOAD 14,059 kg. (31,000 lbs.)		O. E. W. 140,590kg. (310,000 lbs.)
SURFACES	WING	HORIZONTAL	VERTICAL	CANARD
Area m² ft²	721.8* (7770)	———	40.88/Side ** (440/Side)	15.98 ▲ (172)
Aspect Ratio	2.0	———	.76	8.13
Taper Ratio	.056	———	.19	1.1
Thick. Ratio	2.5%/3.0%	———	3.0%	12.0%
Dihedral	15° / -2°	———	———	———
Incidence	0°	———	———	———
L.E. Sweep	80°/ 65°	———	50°	0°
BODY	Length	Max. Dia.	Seating	Baggage
	91.49m (300' 2")	4.06m (160")	151	3,583 kg. (7,900 lbs.)
POWERPLANT	No. Eng.	Type	Airflow	Inlet Dia.
	4	Adv. Tech. GE4/J6H2	195.5kg/sec (431 lb/sec)	1.3 m (51 in.)
LANDING GEAR	Nose	Main	Main Loc.	Pressure
	.86m x .38m (34"x15")	1.0m x .36m (40" x 14")	57% MAC	1.38×10^6 N/m² (200 psi)
FUEL CAPACITY kg. (lbs.)	Wing	Body	Total	C. G.
	231,292 (510,000)	27,211 (60,000)	258,503 (570,000)	STA 69.77m (Sta 2747")
C. G. LIMITS	Takeoff & Landing ◆		Mid-Cruise	
	STA 71.35--74.57 m (Sta 2809"—2936")		STA 69.59--74.65 m (Sta 2740"—2939")	
MATERIAL:	TITANIUM			

* REFERENCE AREA; ACTUAL AREA=994m²(10,700ft²).
** VENTRAL AREA=6.97m² (75ft²)PER SIDE.(L.E.SWEEP=80°)
*** ENGINE PERFORMANCE SHOULD BE CALCULATED FOR A 230.0 KG/SEC (407 LB/SEC) SIZE GE4/J6H2 ENGINE AND ENGINE WEIGHT AND DIMENSIONS TO BE BASED ON 195.5KG/SEC(431 LB/SEC).
▲ EXPOSED AREA.
◆ CANARD EXTENDED

(All dimensions are in International Standard Units [SI] with U. S. units shown in parenthesis.)

FIG. 3 (CONT.) HIGH SPEED DESIGN CONFIGURATION - LSB/HS-3

DESIGN WING TWIST DISTRIBUTION
LSB/HS-3
θ MEASURED RELATIVE TO BODY WL
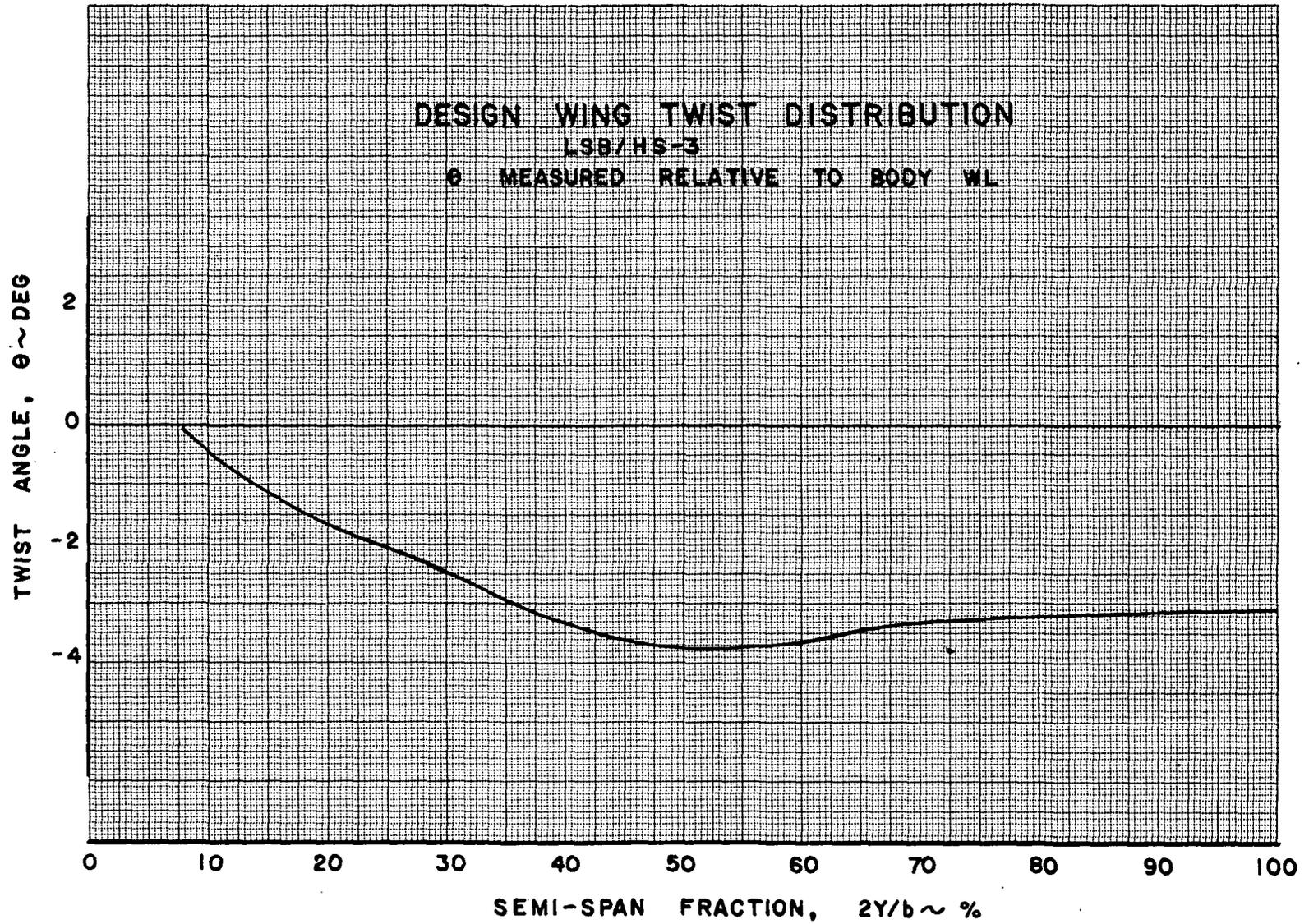
FIG. 4   WING TWIST DISTRIBUTION - HIGH SPEED DESIGN

FIG. 5   CRUISE LIFT - DRAG CHARACTERISTICS - HIGH SPEED DESIGN

HIGH SPEED DESIGN DRAG
M = 1.5
ALT = 11,290 m. (37,000 ft.)
LSB/HS-3 CONFIGURATION
S_{ref} = 721.8 m. (7770 ft.)
NO PROPULSION DRAG
NO THRUST EFFECTS
NO TRIM DRAG

LIFT CURVE

C_L

$\alpha_{body} \sim$ DEG

C_L

C_{Dsym}

C_D
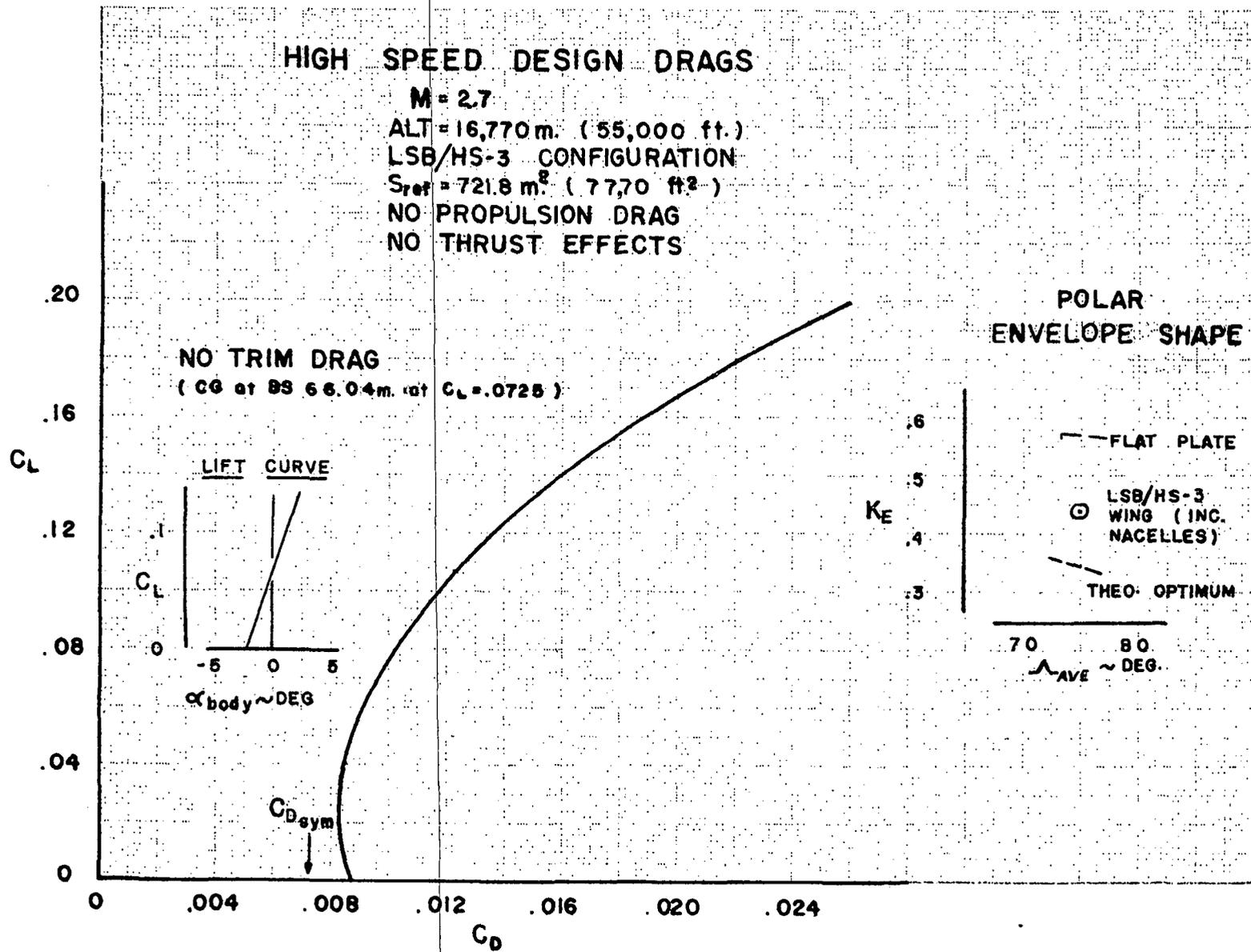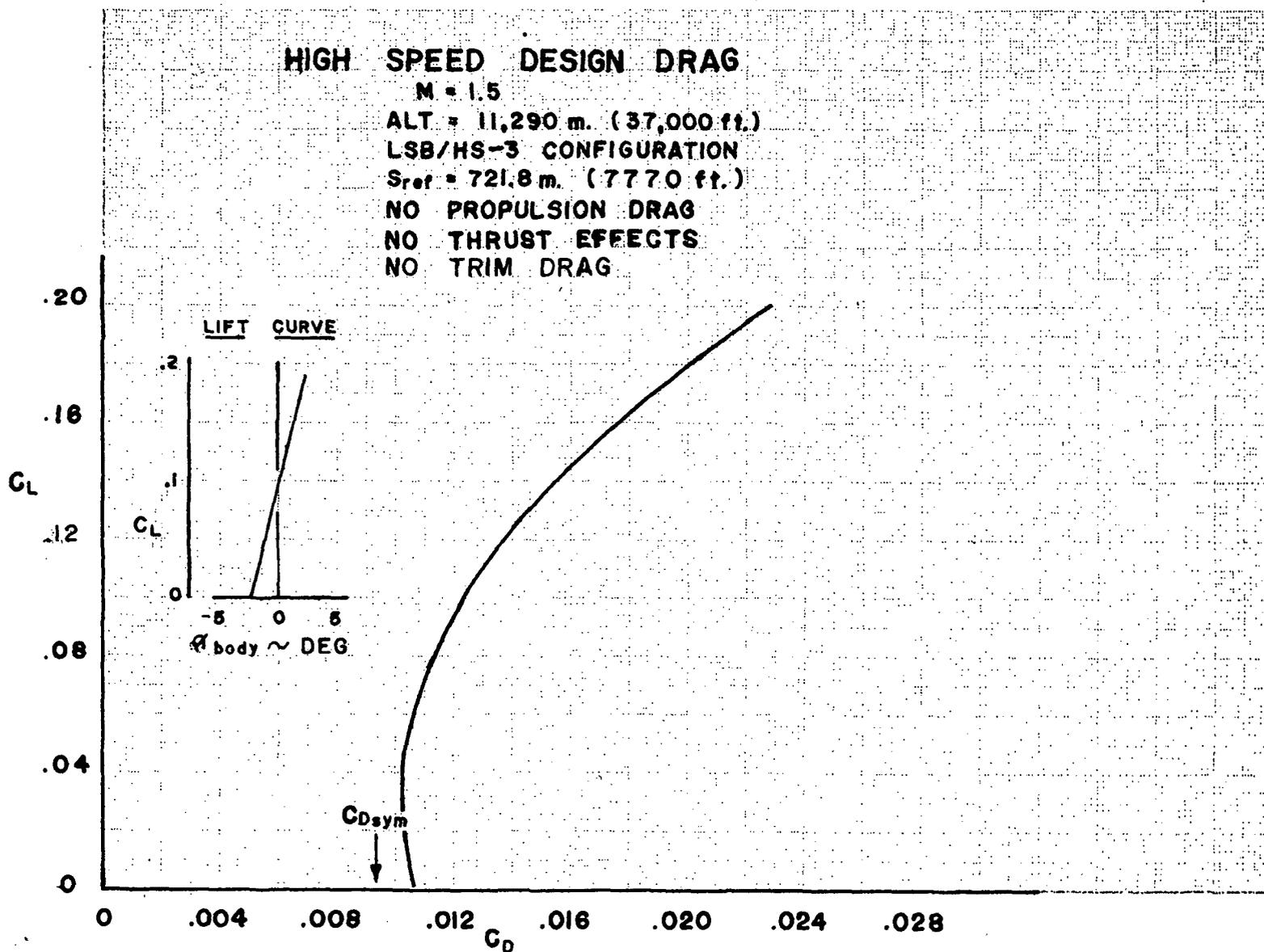
FIG. 6 CLIMB LIFT - DRAG CHARACTERISTICS - HIGH SPEED DESIGN
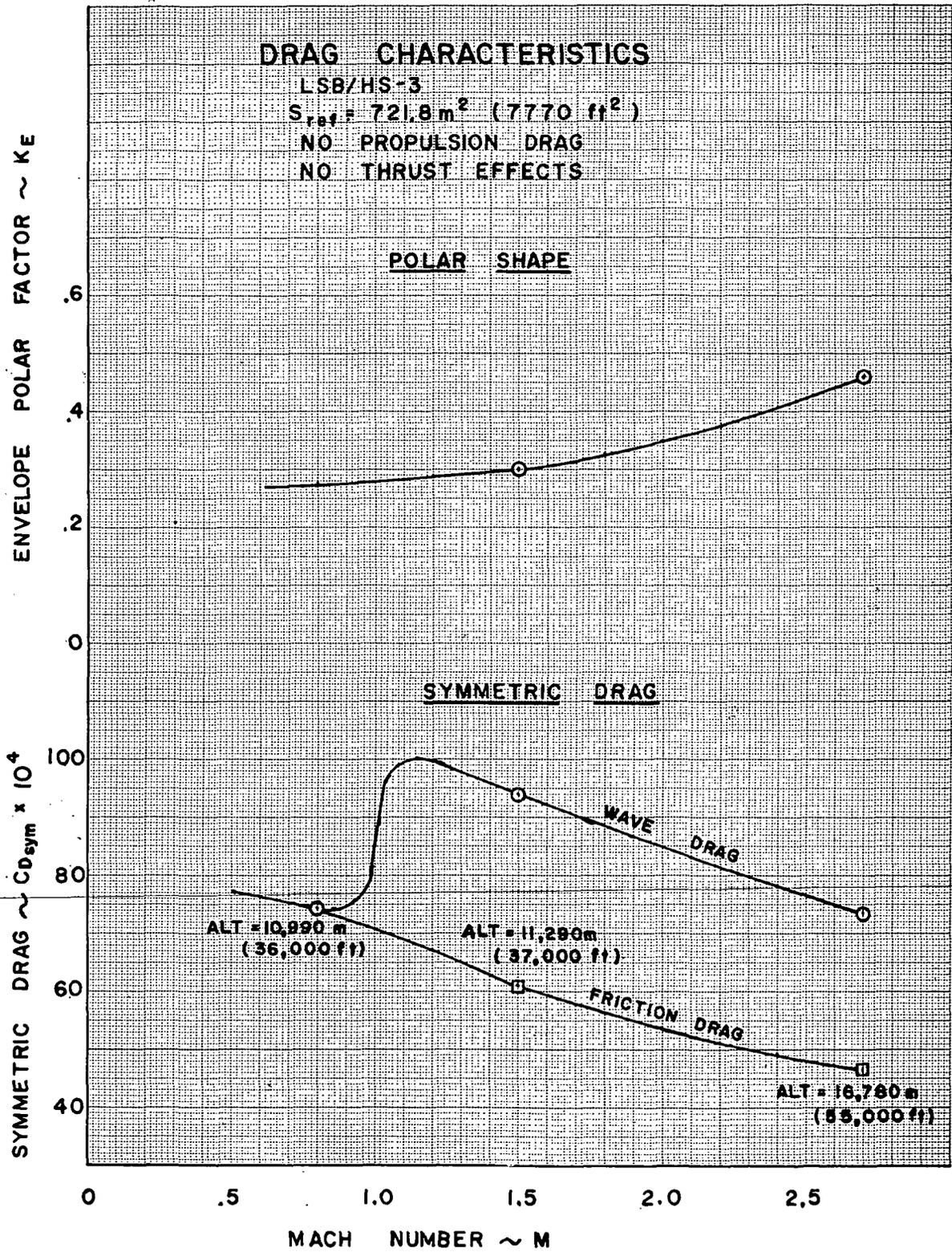
FIG. 7   ZERO LIFT DRAG AND POLAR SHAPE - HIGH SPEED DESIGN

73
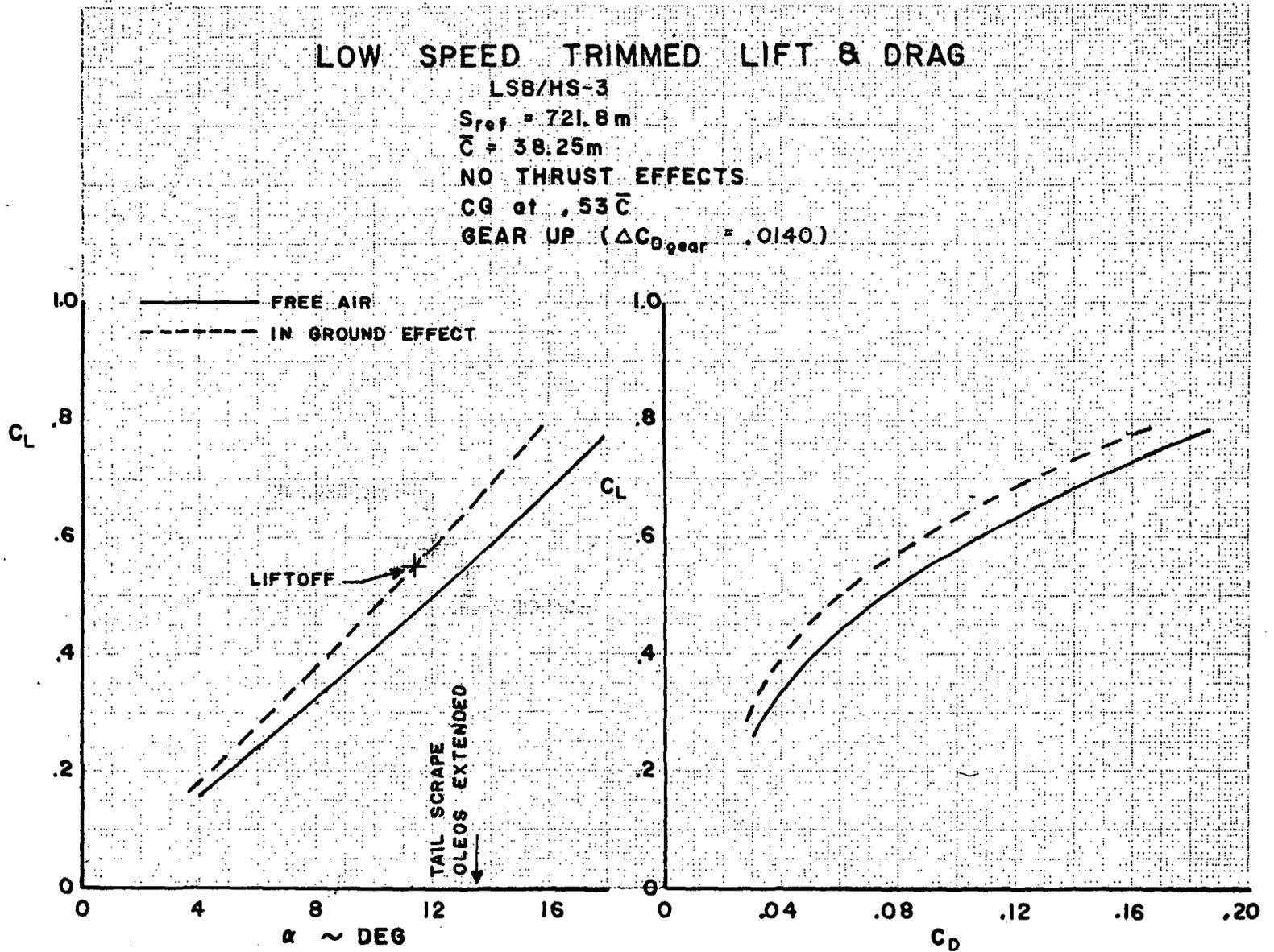
FIG. 8 TAKEOFF CHARACTERISTICS , CG = .53c̄ - HIGH SPEED DESIGN
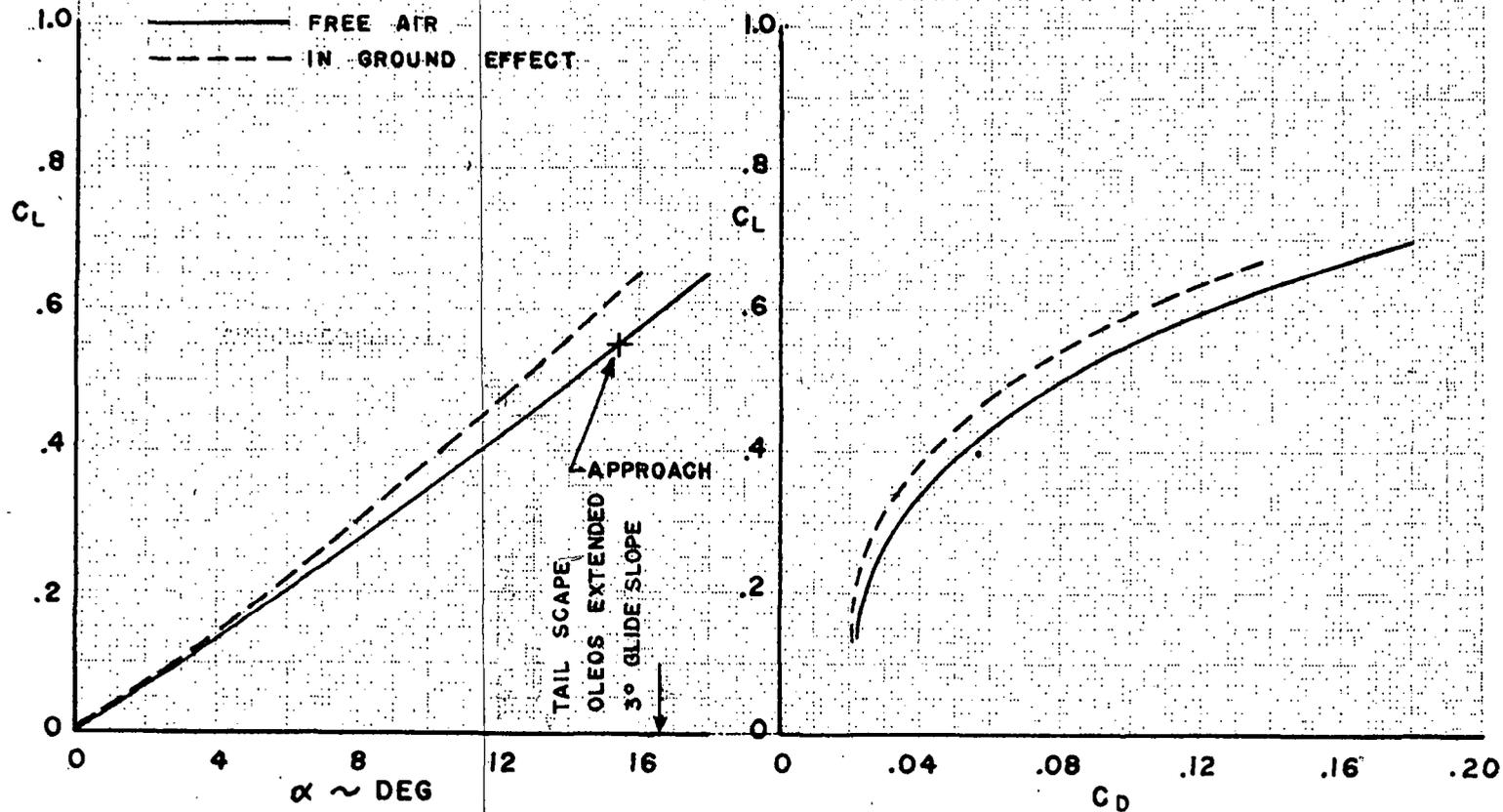
FIG. 9 LANDING CHARACTERISTICS, CG = .465c̄ - HIGH SPEED DESIGN

GROSS WEIGHT - THOUSANDS OF KILOGRAMS (POUNDS)

| 140 (308.6) | 160 (352.7) | 180 (396.8) | 200 (440.9) | 220 (485.0) | 240 (529.1) | 260 (573.2) | 280 (617.3) | 300 (661.4) | 320 (705.5) | 340 (749.6) |

1985 TECHNOLOGY
FUEL MANAGEMENT PER TABLE
MAC = 38.25 m. (1506 in.);   LEMAC = BODY STA. 48.46 m. (1908 in.)
MAX. V_e FOR CANARD OUT FLIGHT = 180 m./sec. (350 knots)
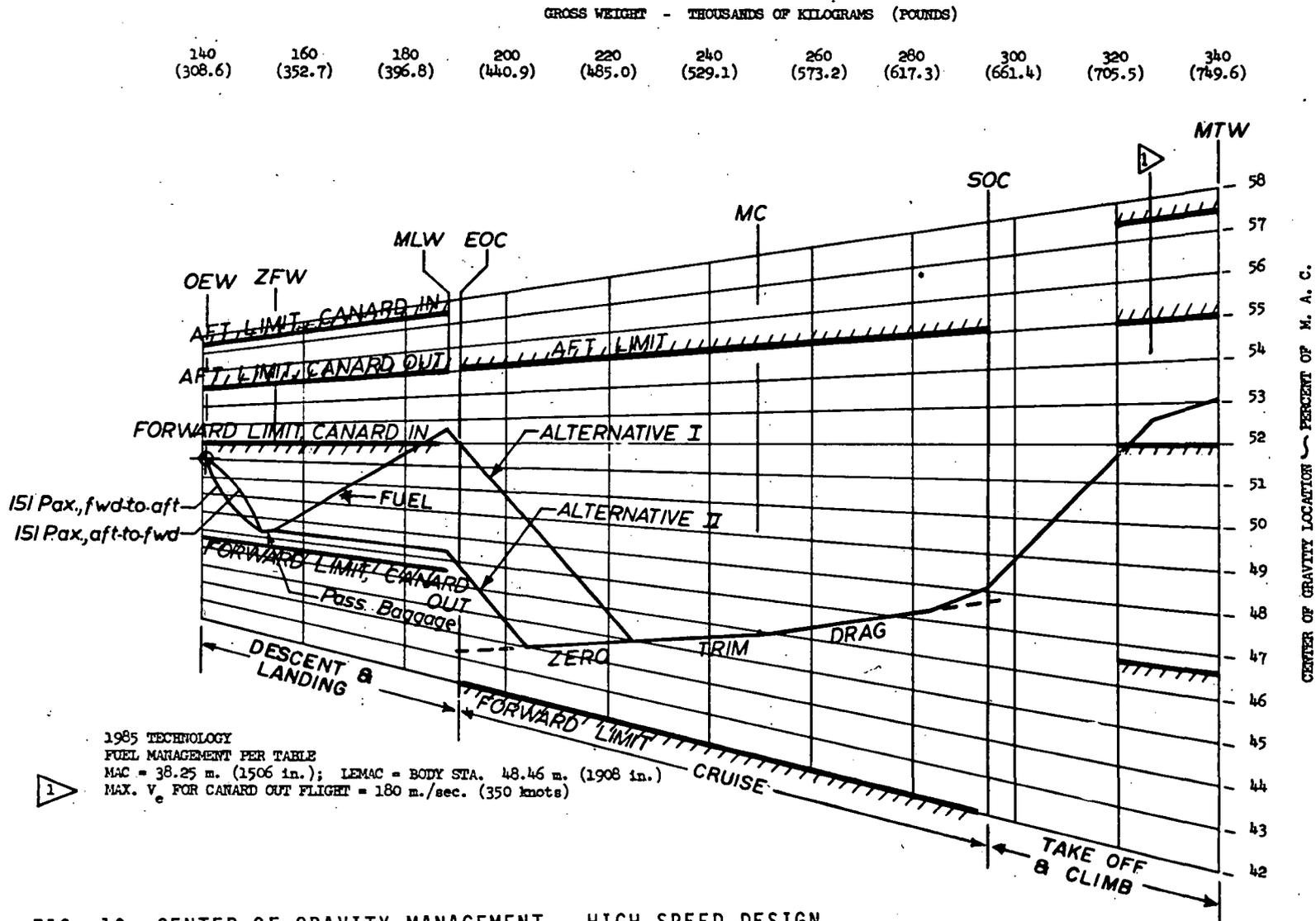
FIG. 10   CENTER OF GRAVITY MANAGEMENT - HIGH SPEED DESIGN
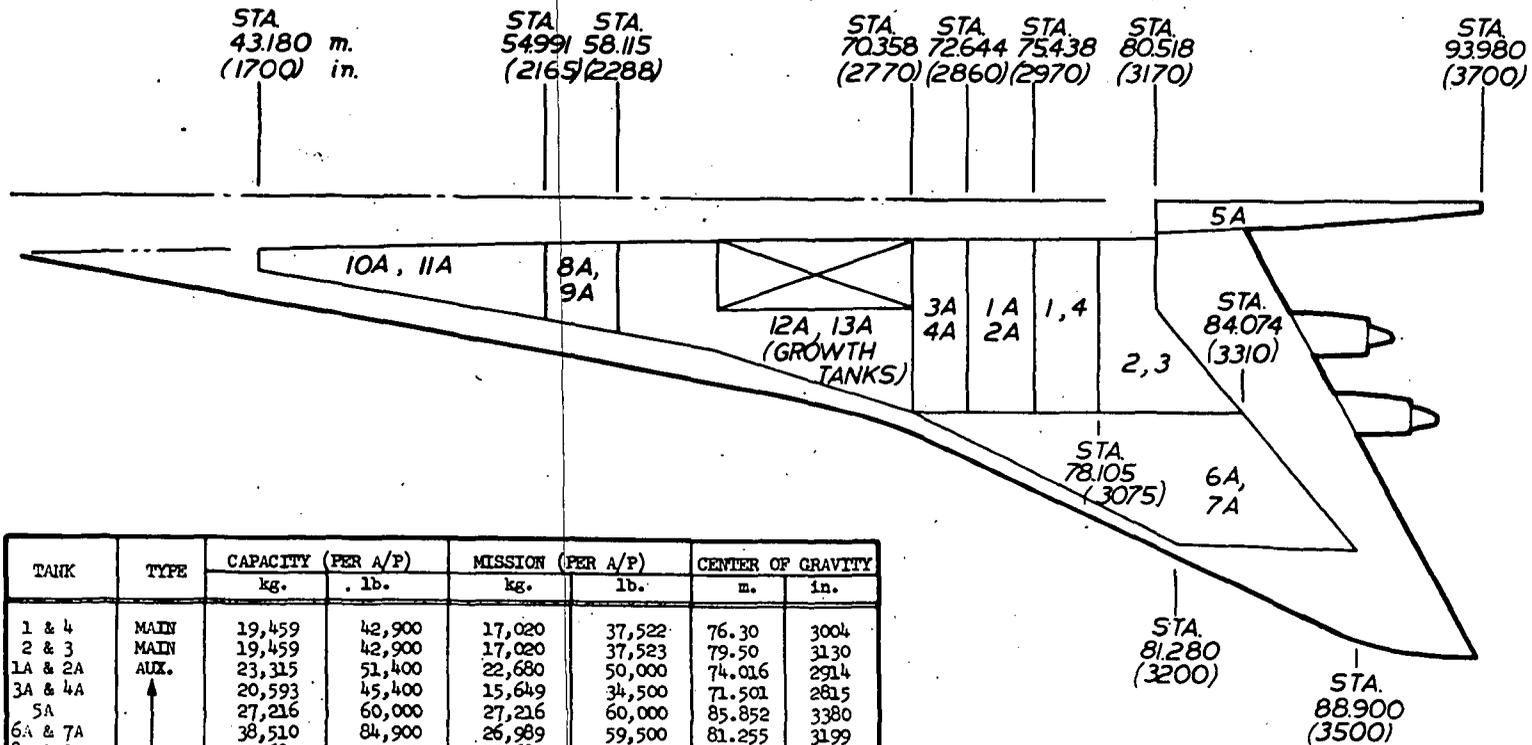
TANK	TYPE	CAPACITY (PER A/P)		MISSION (PER A/P)		CENTER OF GRAVITY	
		kg.	lb.	kg.	lb.	m.	in.
1 & 4	MAIN	19,459	42,900	17,020	37,522	76.30	3004
2 & 3	MAIN	19,459	42,900	17,020	37,523	79.50	3130
1A & 2A	AUX.	23,315	51,400	22,680	50,000	74.016	2914
3A & 4A		20,593	45,400	15,649	34,500	71.501	2815
5A		27,216	60,000	27,216	60,000	85.852	3380
6A & 7A		38,510	84,900	26,989	59,500	81.255	3199
8A & 9A		22,680	50,000	22,680	50,000	56.591	2228
10A & 11A		37,195	82,000	36,287	80,000	50.267	1979
12A & 13A	AUX.	55,565	110,500	0	0	63.627	2505
TOTAL		(258,547)	(570,000)	(185,540)	(409,045)		(2707) [1]

[1] Based on Capacity

FIG. 11 FUEL TANK DEFINITION, ALTERNATIVE I CG MANAGEMENT - HIGH SPEED DESIGN

77

STA. 43.180 m. (1700) in. STA. 54.991 (2165) STA. 62.230 (2450) STA. 67.056 (2640) STA. 70.358 (2770) STA. 72.644 (2860) STA. 75.438 (2970) STA. 80.518 (3170) STA. 93.980 (3700)

5A

8A, 9A

10A, 11A (GROWTH TANKS)

1,4 | 2,3 | 3A 4A | 1A 2A | 12A, 13A (GROWTH TANKS)

6A, 7A

STA. 84.074 (3310)

STA. 81.280 (3200)

STA. 88.900 (3500)

TANK	TYPE	CAPACITY (PER A/P)		MISSION (PER A/P)		CENTER OF GRAVITY	
		kg.	lb.	kg.	lb.	m.	in.
1 & 4	MAIN	17,020	37,522	17,020	37,522	64.62	2544
2 & 3	MAIN	17,020	37,523	17,020	37,523	68.55	2699
1A & 2A	AUX.	23,315	51,400	22,680	50,000	74.016	2914
3A & 4A		24,358	53,700	24,358	53,700	71.501	2815
5A		27,216	60,000	27,216	60,000	85.852	3380
6A & 7A		38,510	84,900	38,510	84,900	81.255	3199
8A & 9A		38,736	85,400	38,736	85,400	50.267	1979
10A & 11A		37,219	82,055	0	0	58.445	2301
12A & 13A	AUX.	35,153	77,500	0	0	78.334	3084
TOTAL		(258,547)	(570,000)	(185,540)	(409,045)		

FIG. 12   FUEL TANK DEFINITION - ALTERNATIVE II - CG MANAGEMENT - HIGH SPEED DESIGN
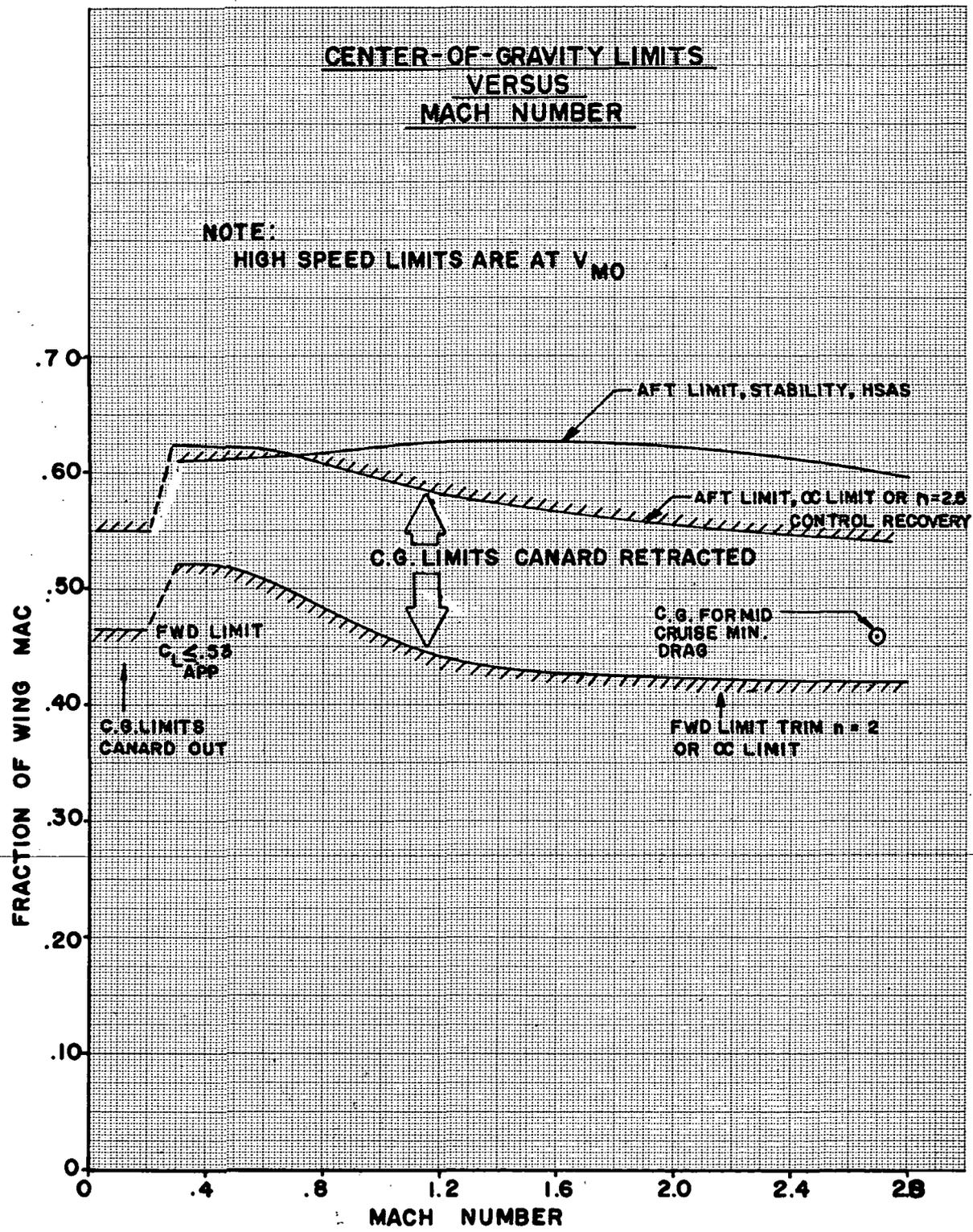
FIG. 13 LONGITUDINAL AERODYNAMIC LIMITS - HIGH SPEED DESIGN
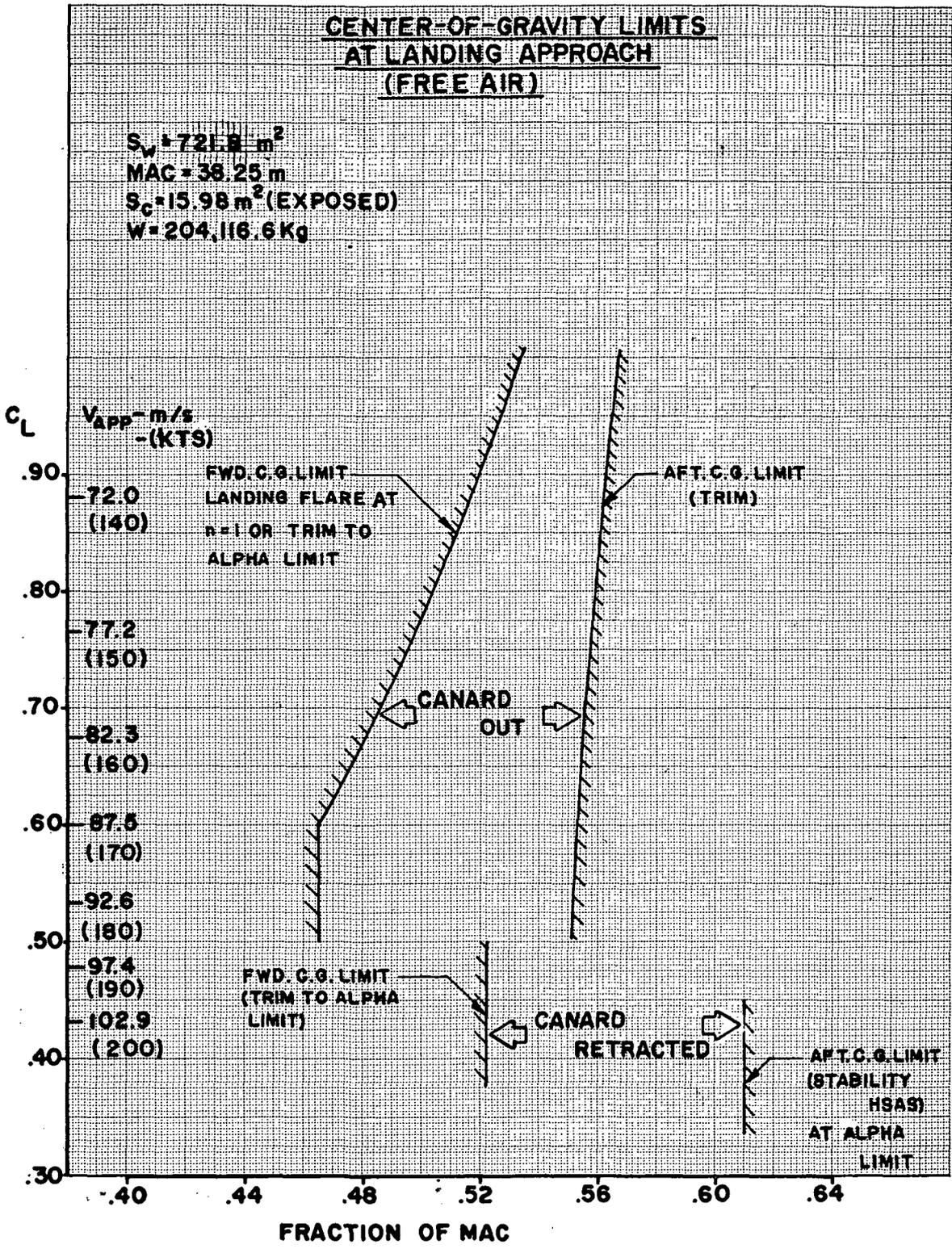
FIG. 14   LOW SPEED AERODYNAMIC LIMITS - HIGH SPEED DESIGN
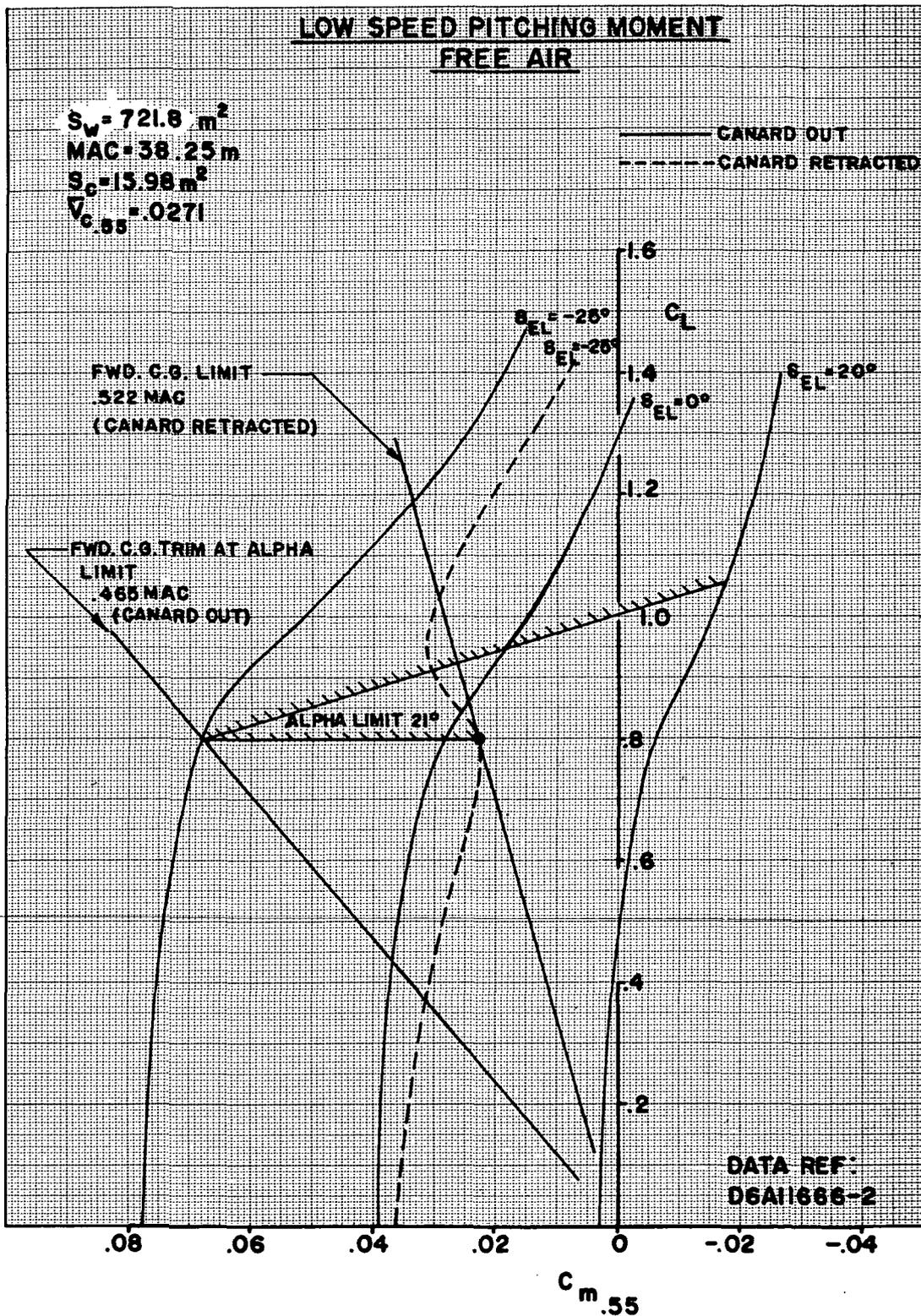
FIG. 15 LOW SPEED PITCHING MOMENT CURVES - HIGH SPEED DESIGN

81
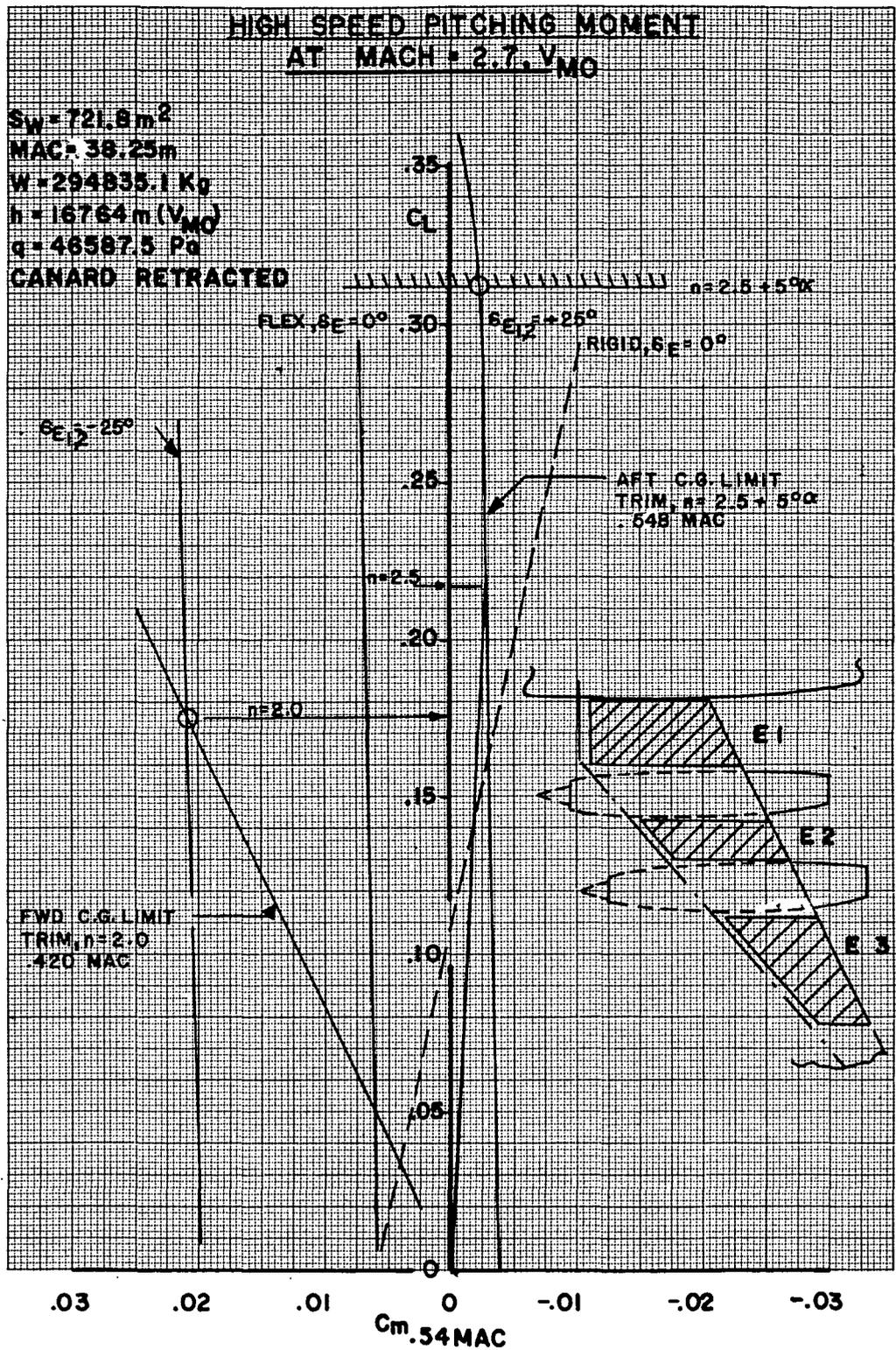
FIG. 16 CRUISE PITCHING MOMENT - HIGH SPEED DESIGN
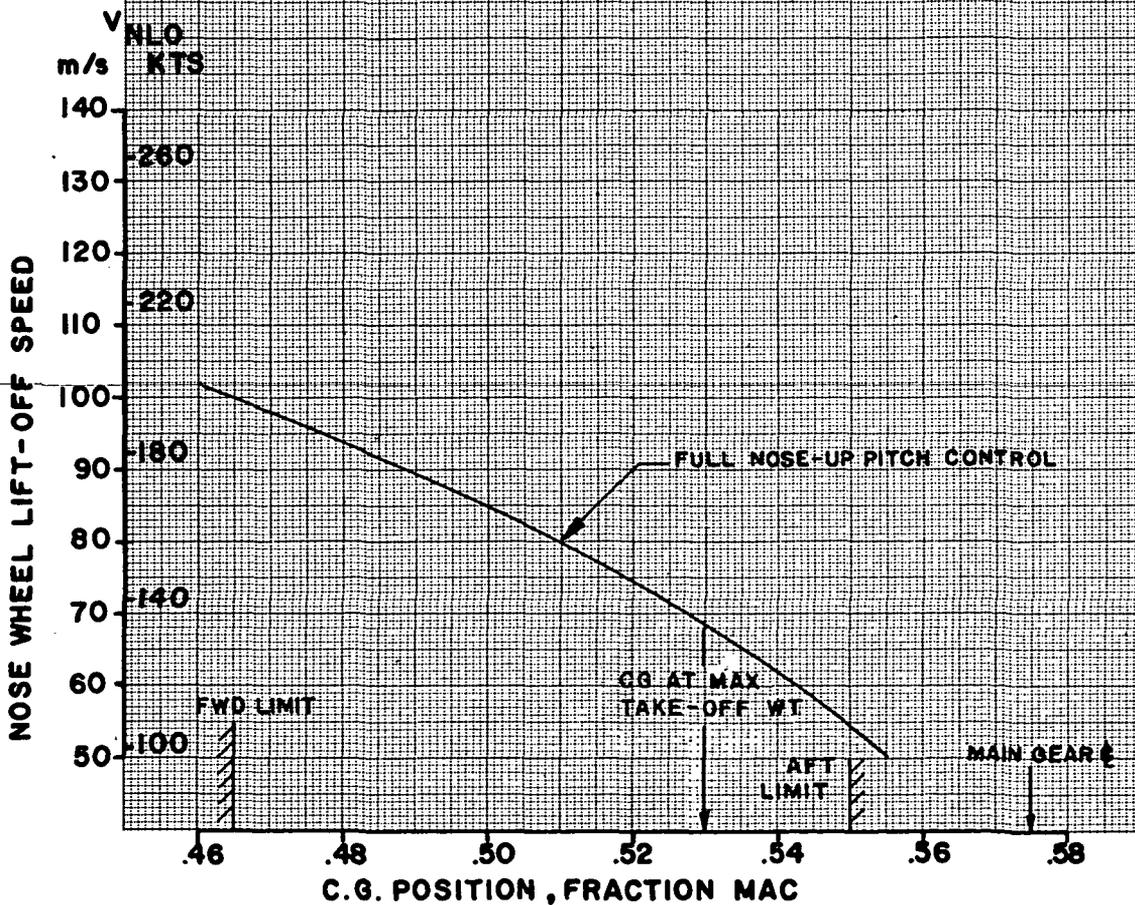
FIG. 17 TAKEOFF ROTATION CAPABILITY - HIGH SPEED DESIGN
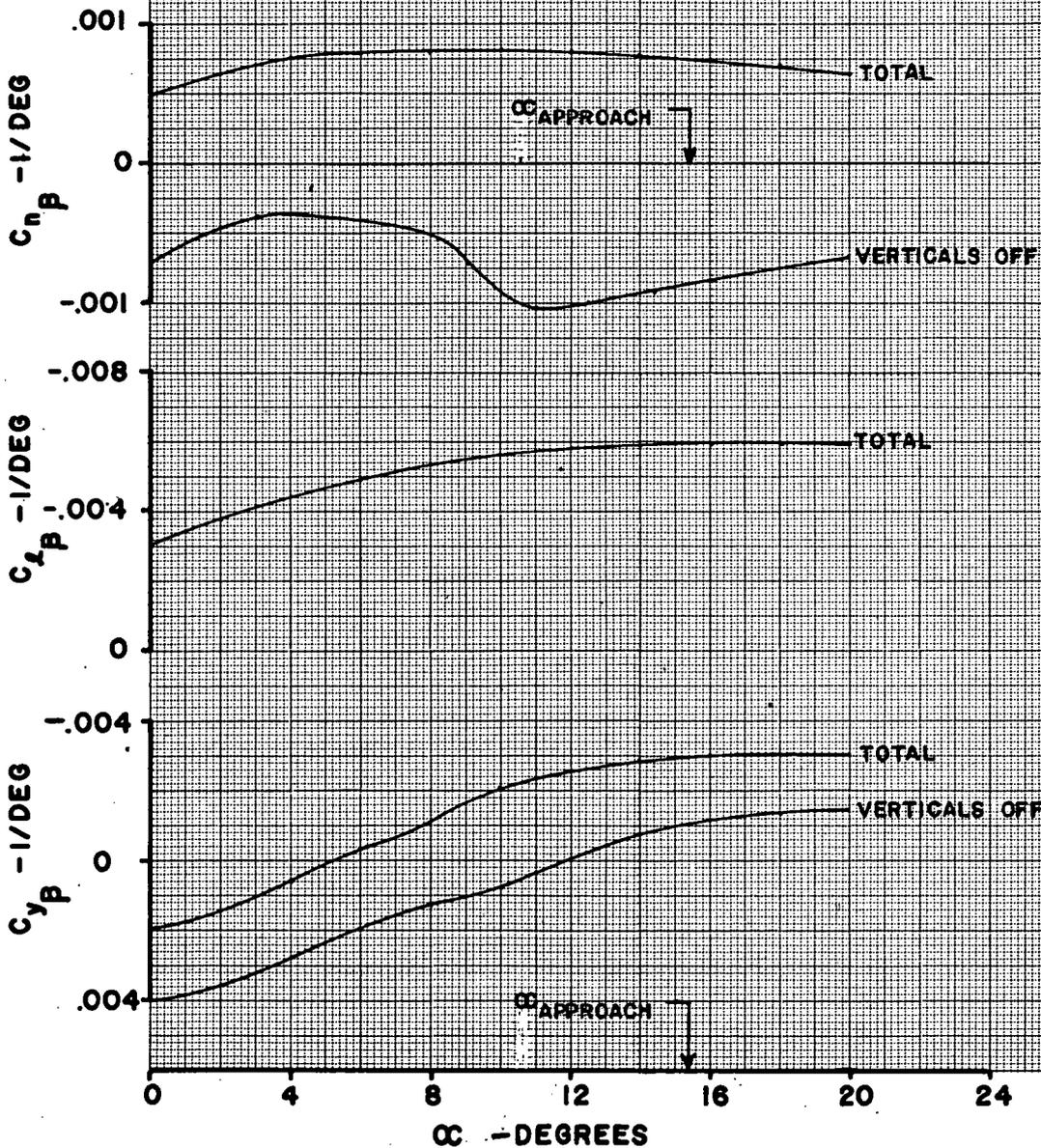
FIG. 18   LOW SPEED LATERAL DIRECTION CHARACTERISTICS -
HIGH SPEED DESIGN

84
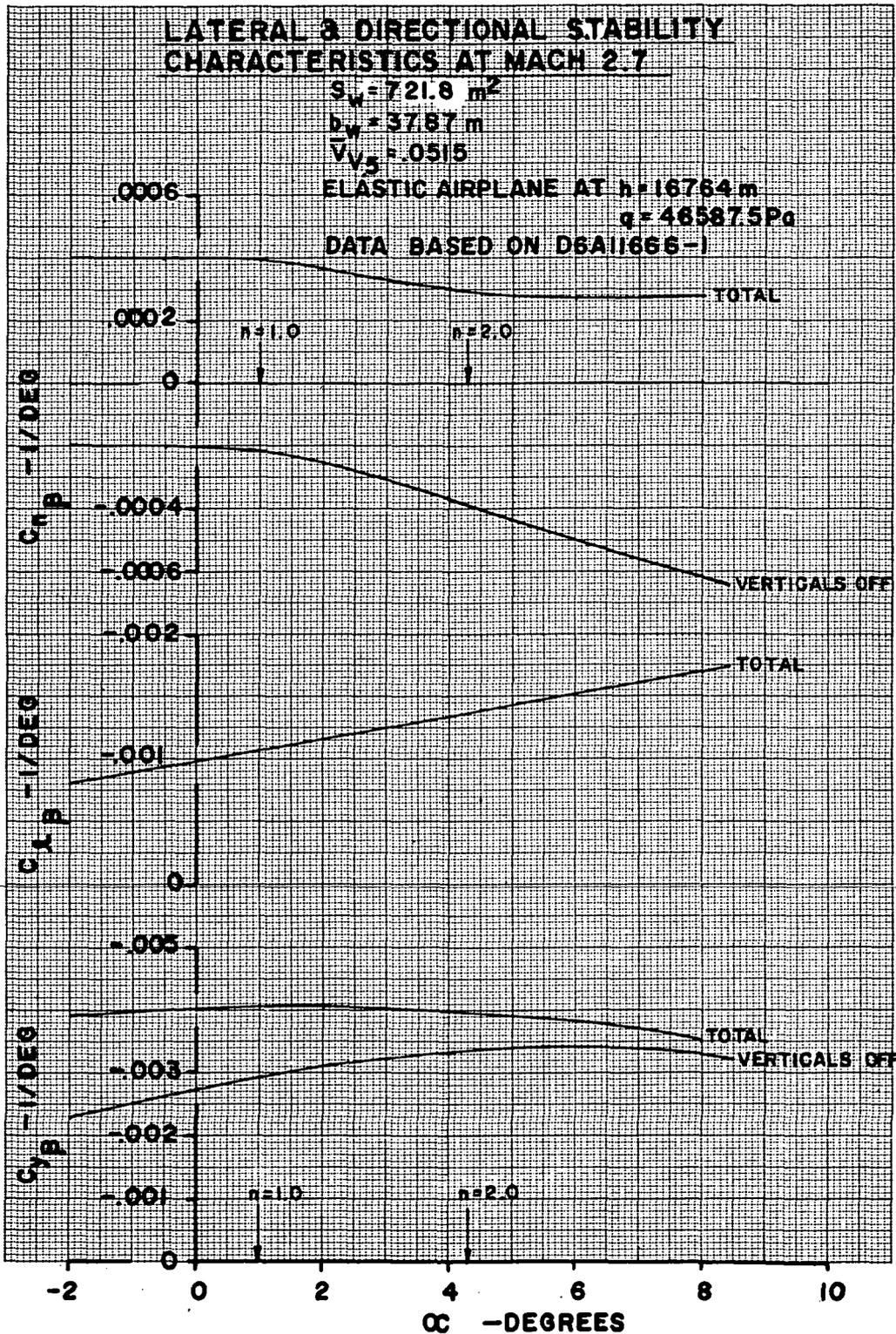
FIG. 19 CRUISE LATERAL-DIRECTIONAL CHARACTERISTICS -
HIGH SPEED DESIGN

85
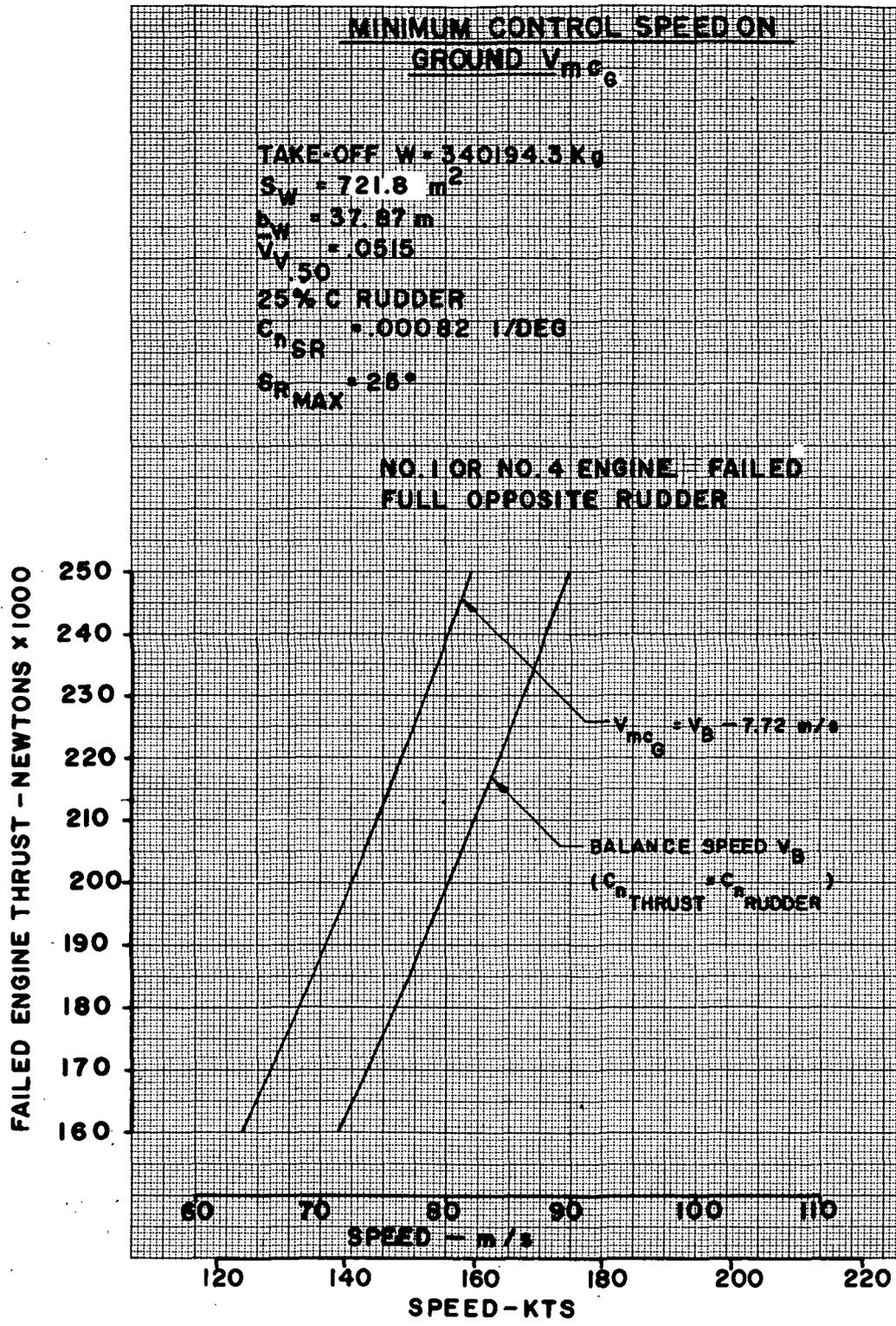
FIG. 20   MINIMUM CONTROL SPEED - HIGH SPEED DESIGN
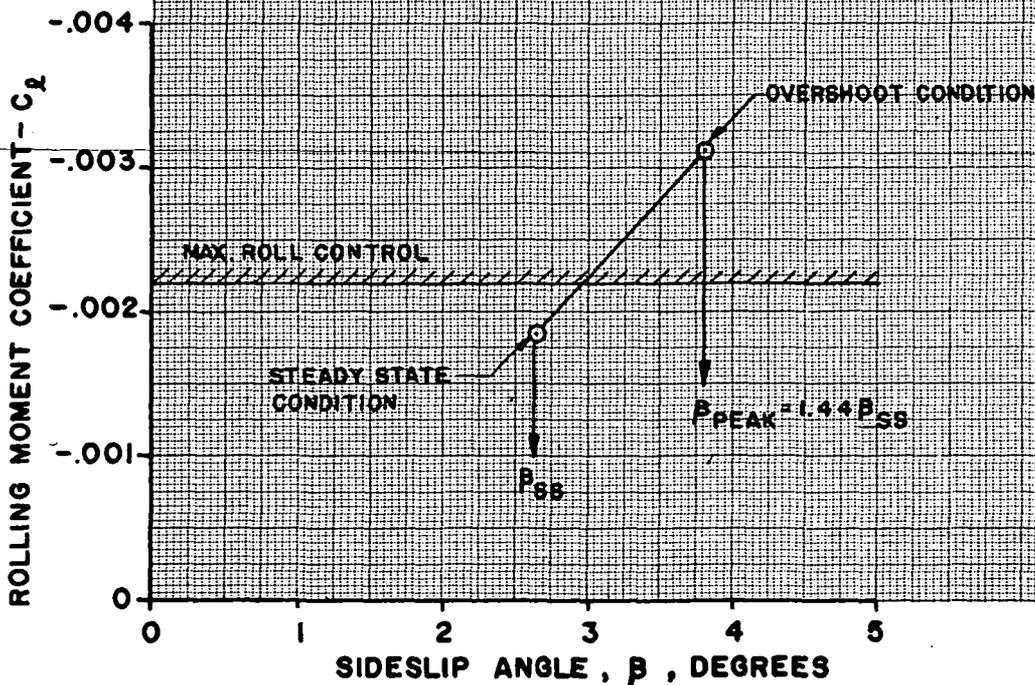
FIG. 21 EFFECT OF ENGINE FAILURE DURING CRUISE,
n = 1 - HIGH SPEED DESIGN

FIG. 22 EFFECT OF ENGINE FAILURE DURING CRUISE,
n = 2 - HIGH SPEED DESIGN
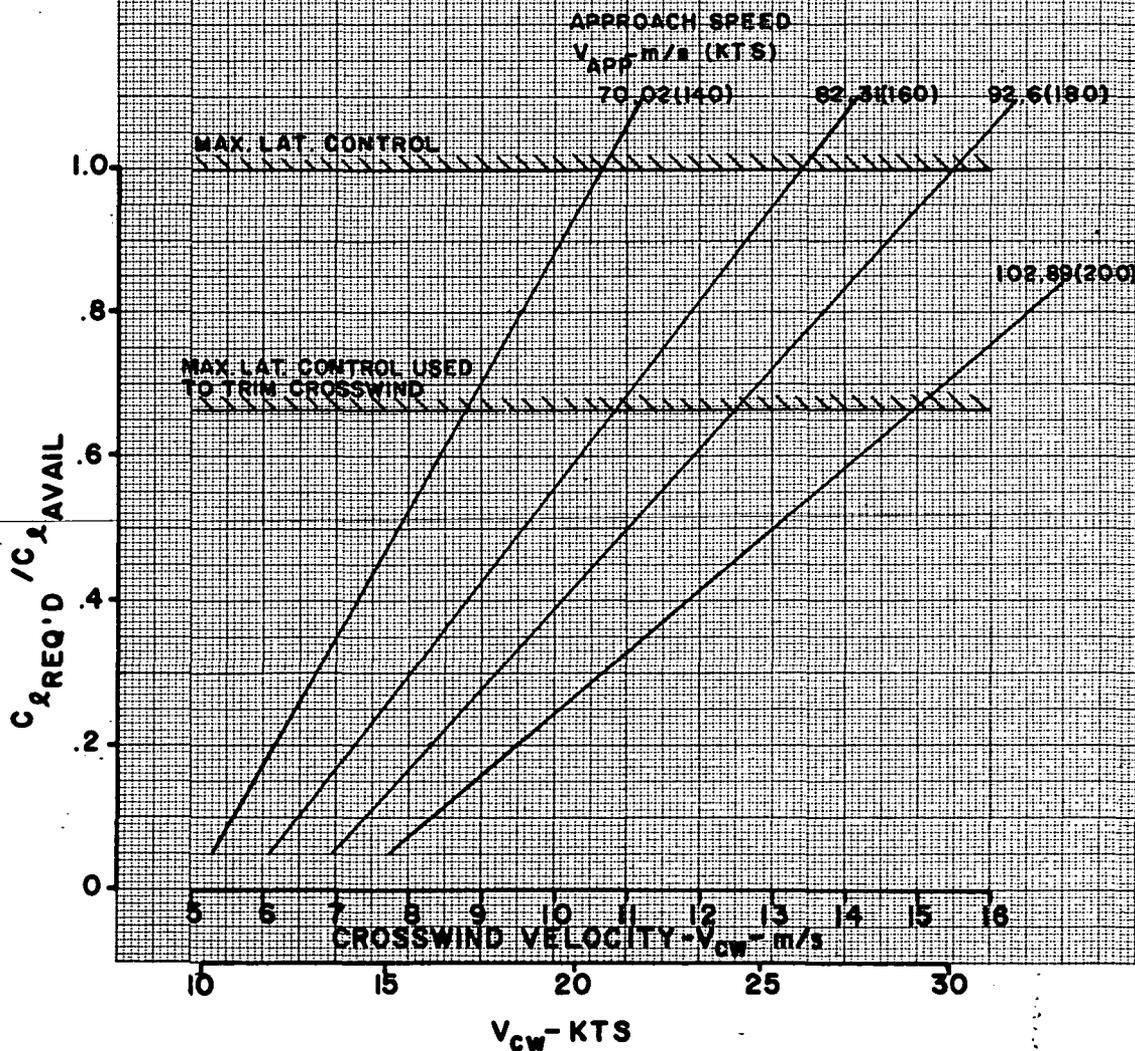
FIG. 23 LATERAL CONTROL REQUIREMENT FOR CROSSWIND
LANDING - HIGH SPEED DESIGN
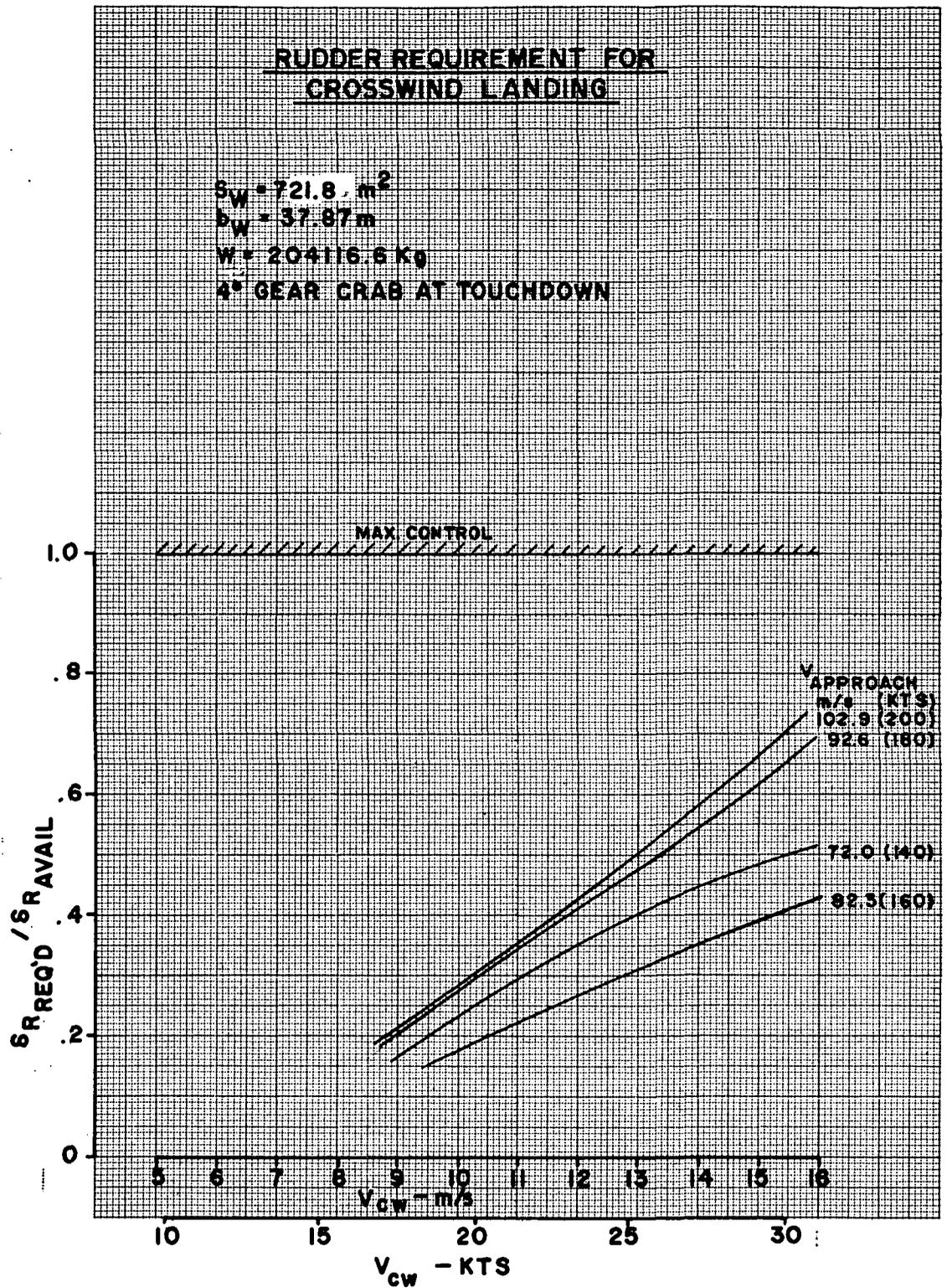
FIG. 24 RUDDER REQUIREMENT FOR CROSSWIND LANDING-
HIGH SPEED DESIGN

90

FIG. 25 APPROACH AND LANDING CONTROL POWER REQUIREMENT
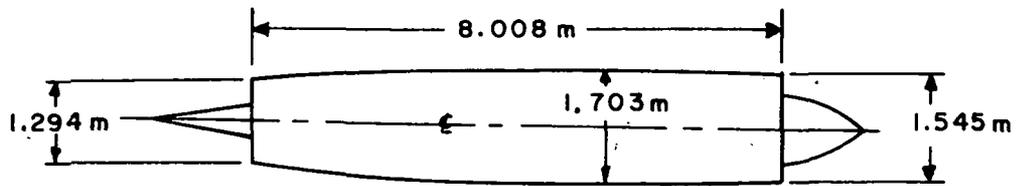
FIG. 26   ENGINE POD DEFINITION FOR HIGH SPEED DESIGN
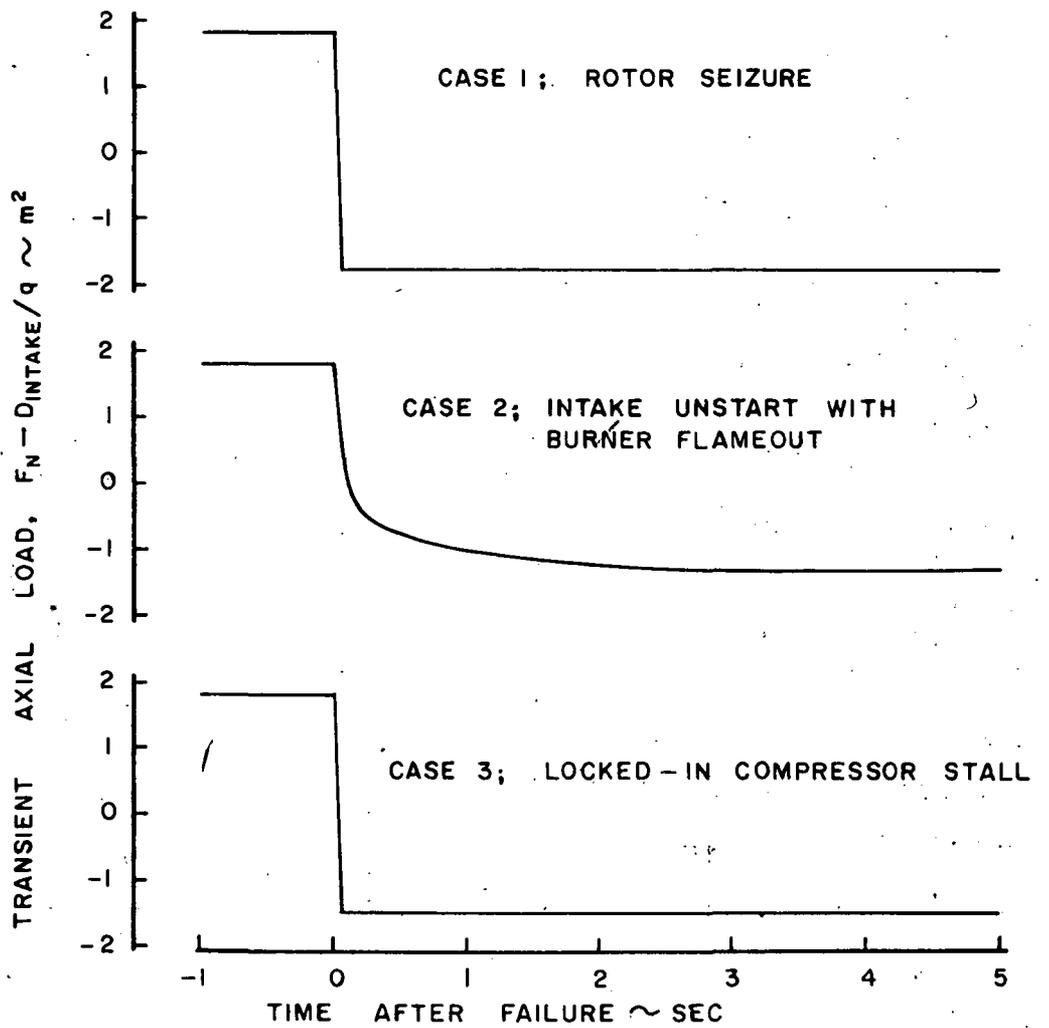
FIG. 27   TRANSIENT AXIAL LOAD DUE TO ENGINE FAILURE –
HIGH SPEED DESIGN
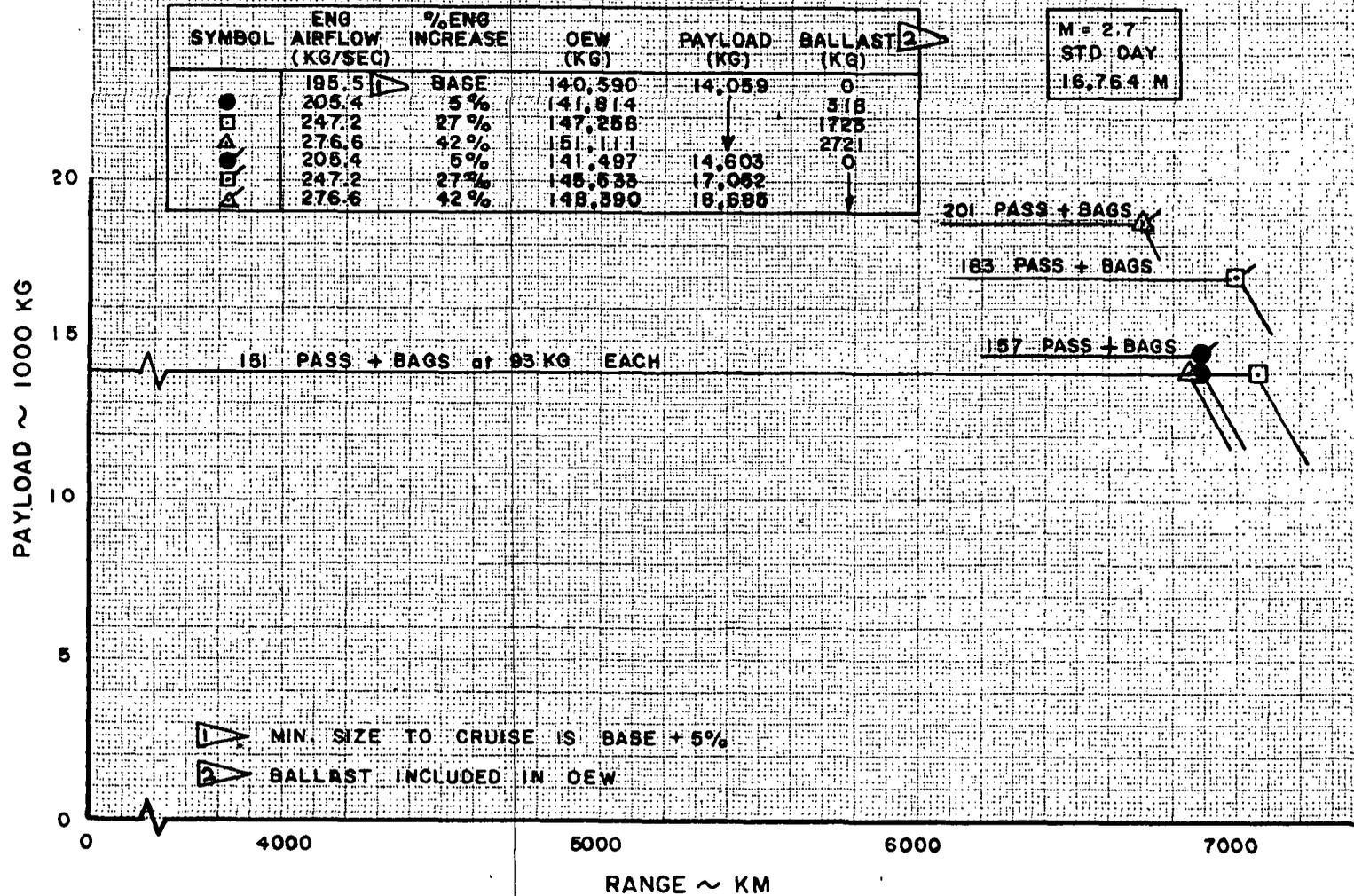
FIG. 28 PAYLOAD - RANGE SUMMARY - HIGH SPEED DESIGN
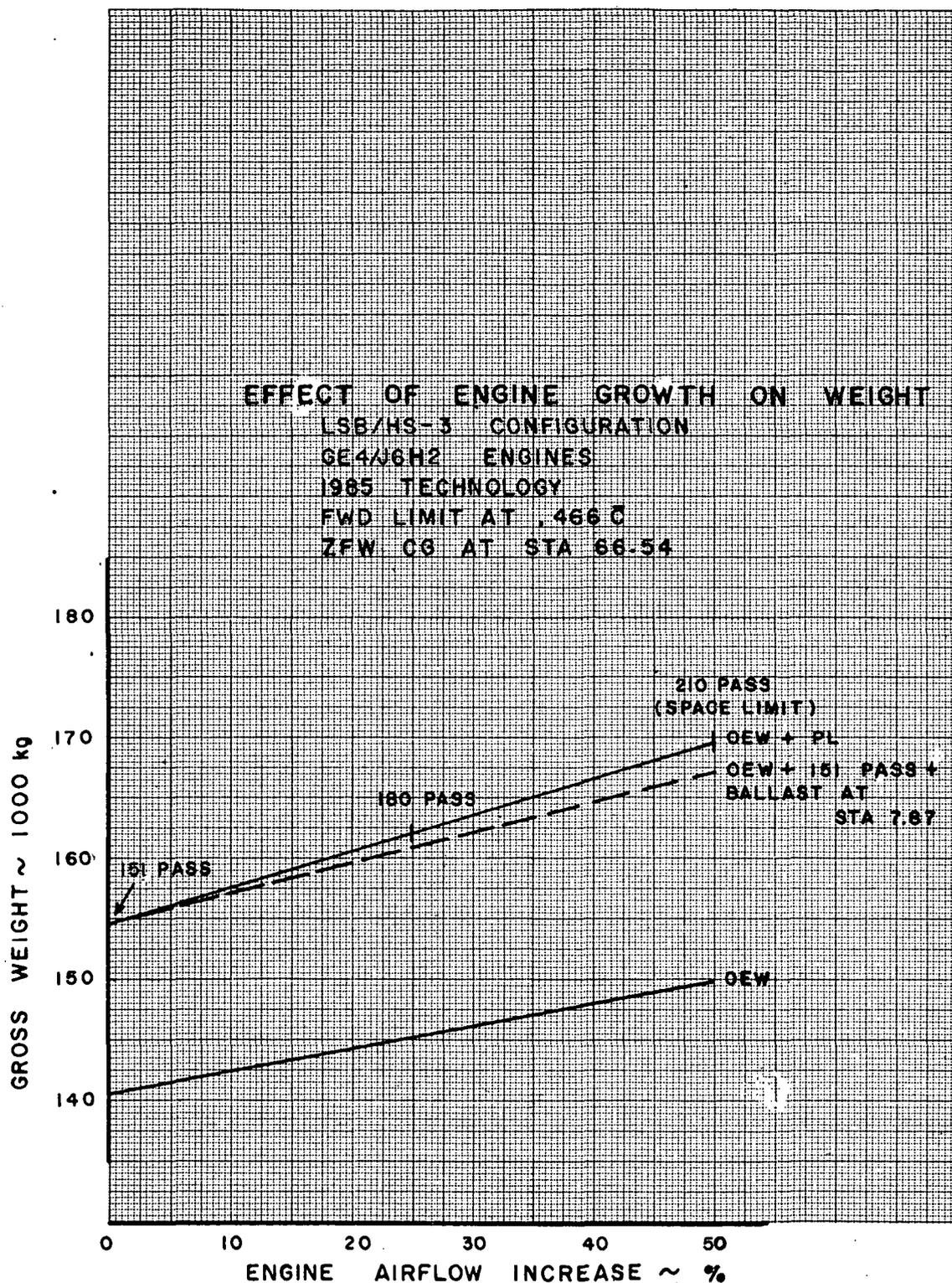
FIG. 29 EFFECT OF ENGINE SIZE ON AIRPLANE WEIGHT -
HIGH SPEED DESIGN
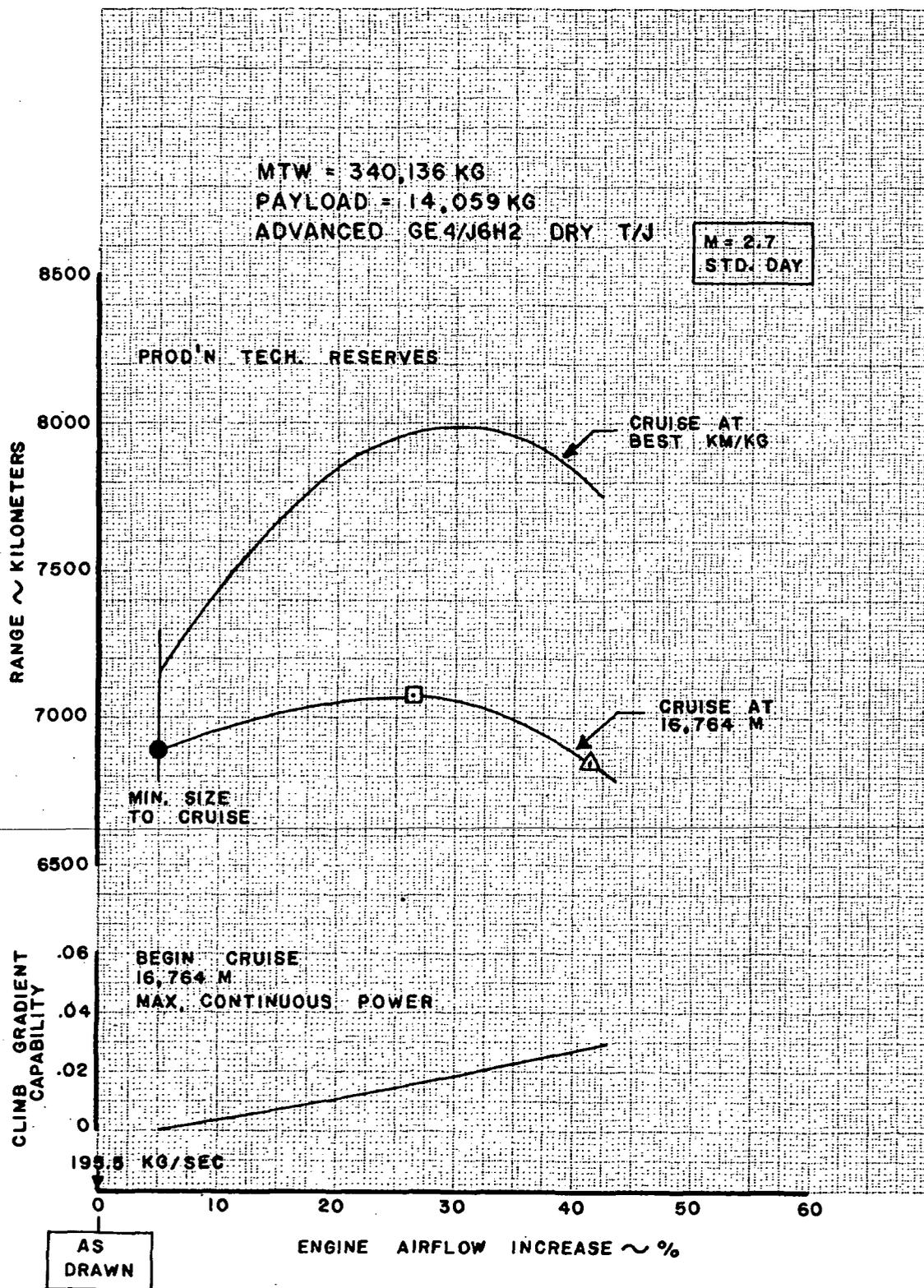
FIG. 30 EFFECT OF ENGINE SIZE ON AIRPLANE PERFORMANCE - HIGH SPEED DESIGN
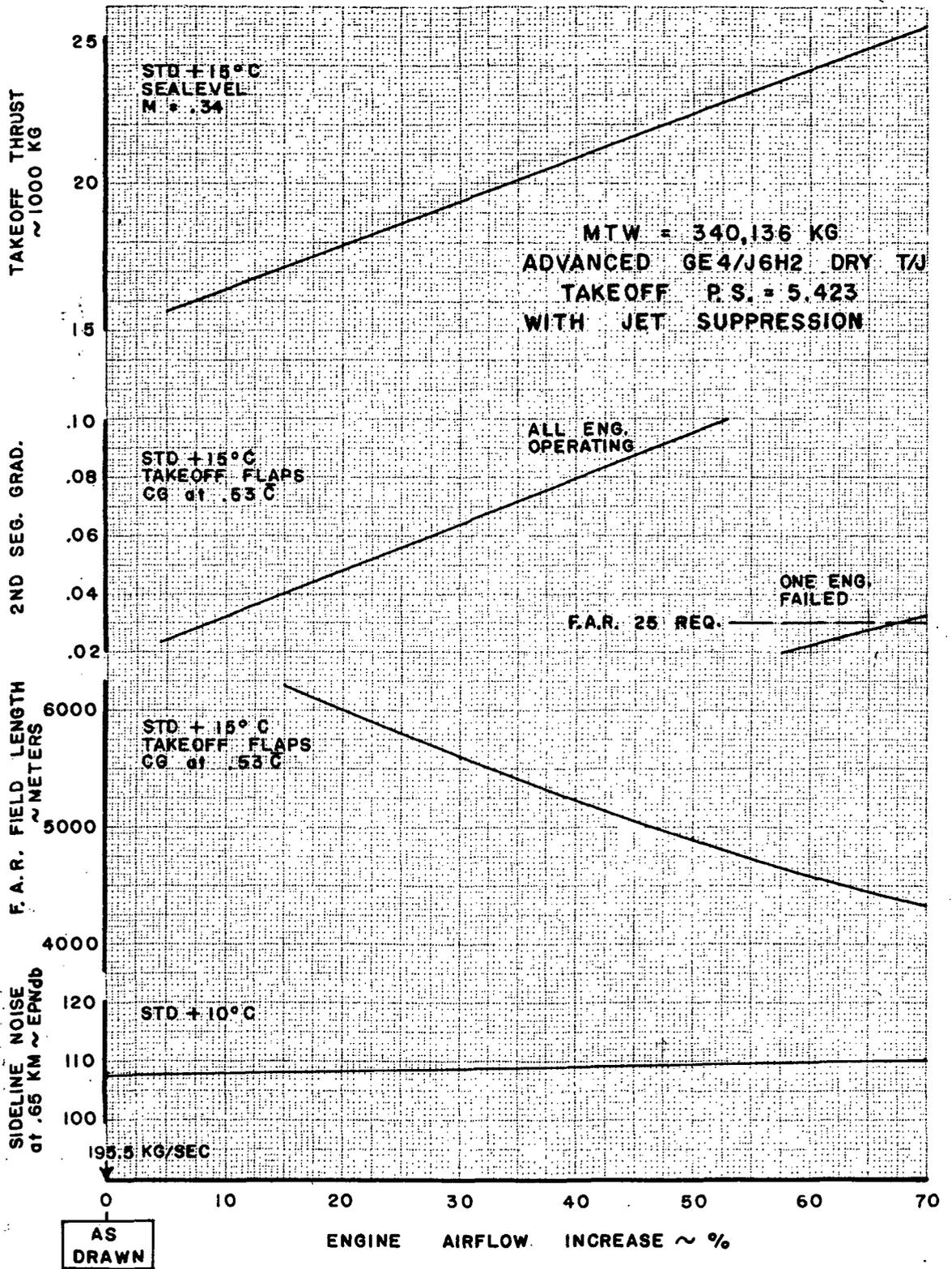
FIG. 31 TAKEOFF PERFORMANCE SUMMARY - HIGH SPEED DESIGN

SUMMARY OF SONIC BOOM SIGNATURES
BASELINE AIRPLANE (LSB/HS-3) + 5% ENGINE AIRFLOW INCREASE
151 PASSENGERS   MTW = 340,136 kg
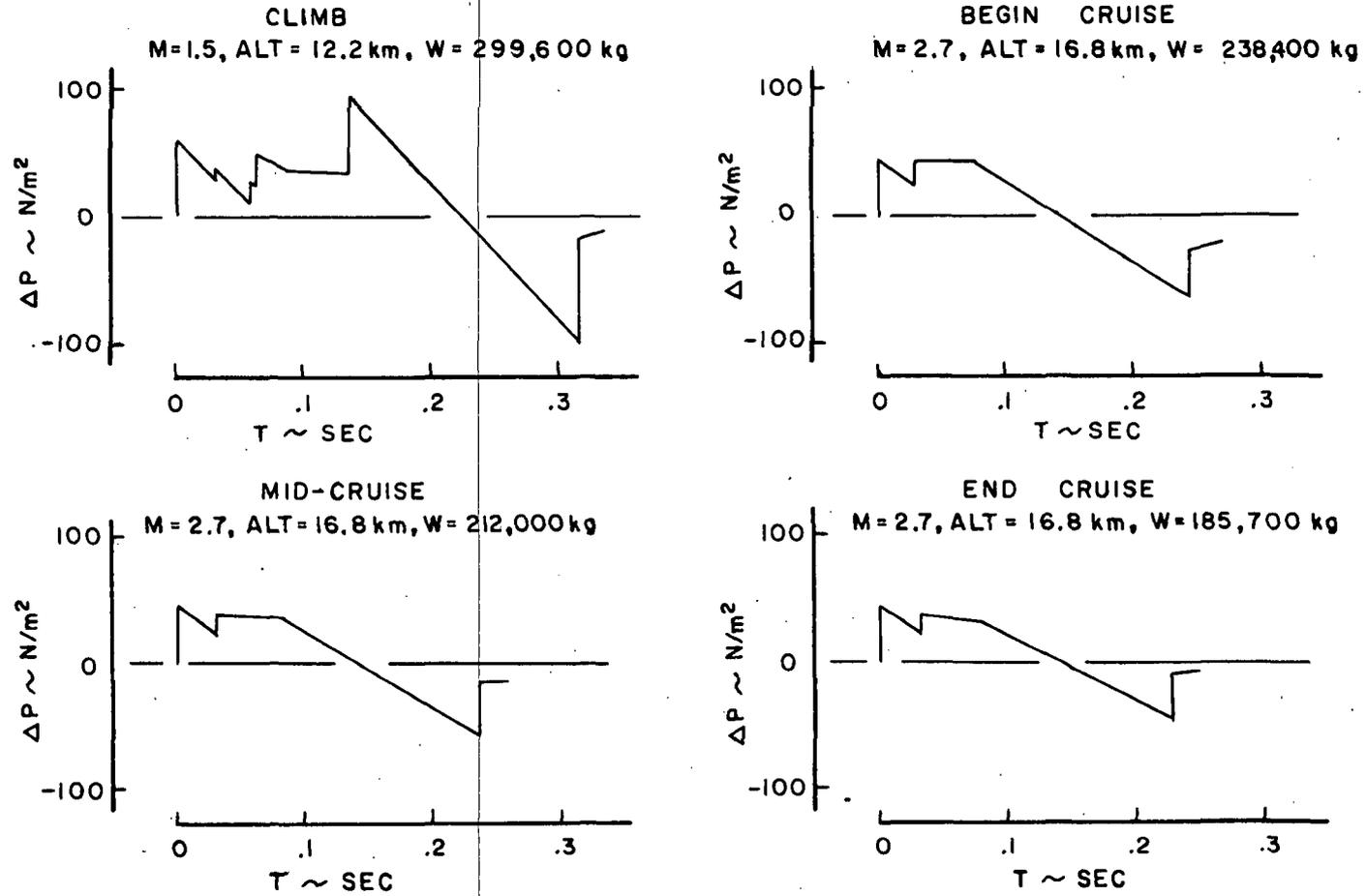
FIG. 32   SONIC BOOM SIGNATURES FOR BASELINE HIGH SPEED DESIGN

FIG. 33 SONIC BOOM SIGNATURES FOR 27% INCREASED AIRFLOW - HIGH SPEED DESIGN

SUMMARY OF SONIC BOOM SIGNATURES
BASELINE AIRPLANE (LSB/HS-3) + 27% AIRFLOW INCREASE
183 PASSENGERS   MTW = 340,136 kg

CLIMB
M = 1.5, ALT = 12.2 km, W = 313,300 kg

BEGIN CRUISE
M. = 2.7, ALT = 17.7 km, W = 277,400 kg

MID CRUISE
M = 2.7, ALT = 18.6 km, W = 234,700 kg

END CRUISE
M = 2.7, ALT = 19.7 km, W = 192,000 kg
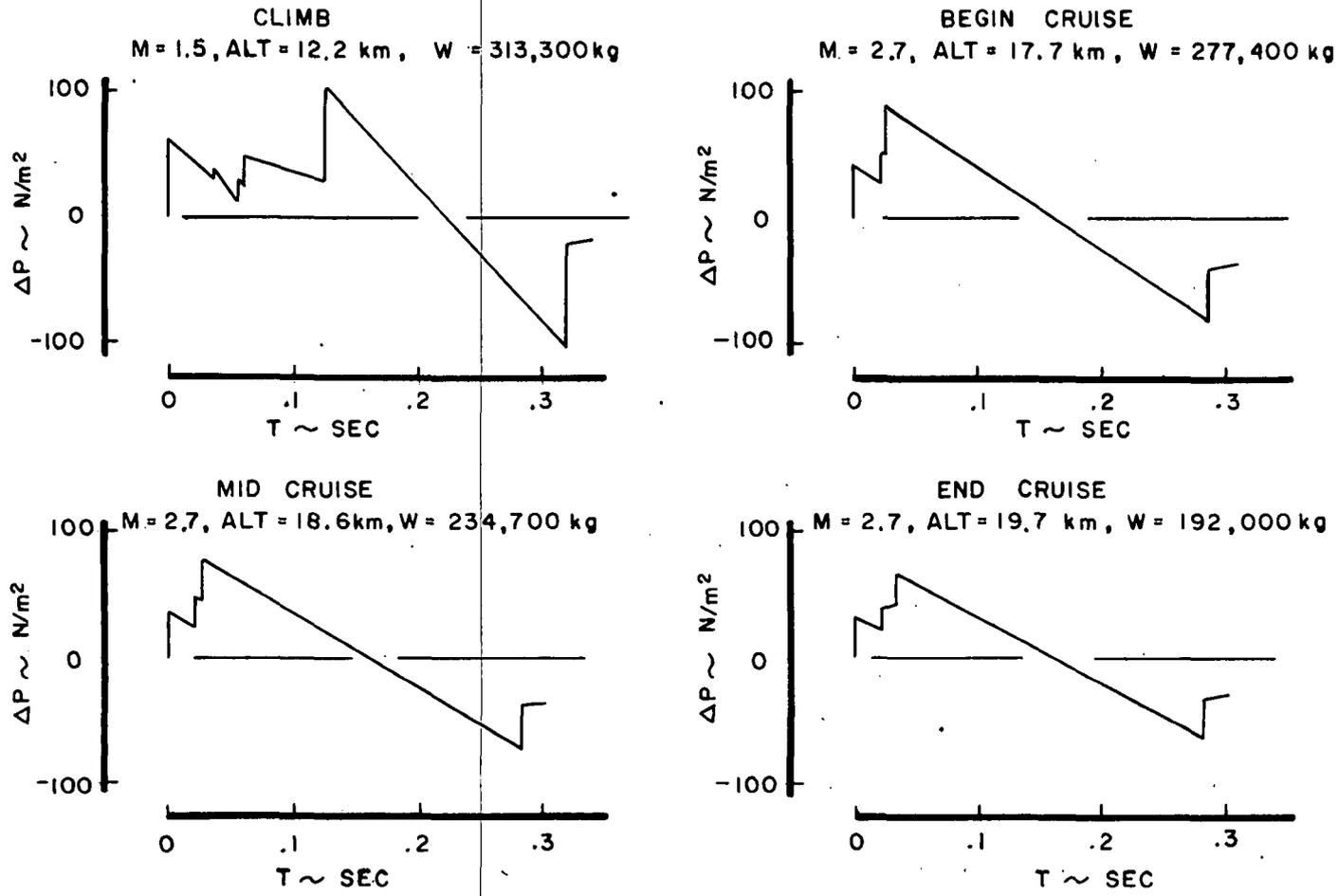
FIG. 34   SONIC BOOM SIGNATURES FOR MAXIMUM RANGE (CLIMBING) CRUISE -
HIGH SPEED DESIGN
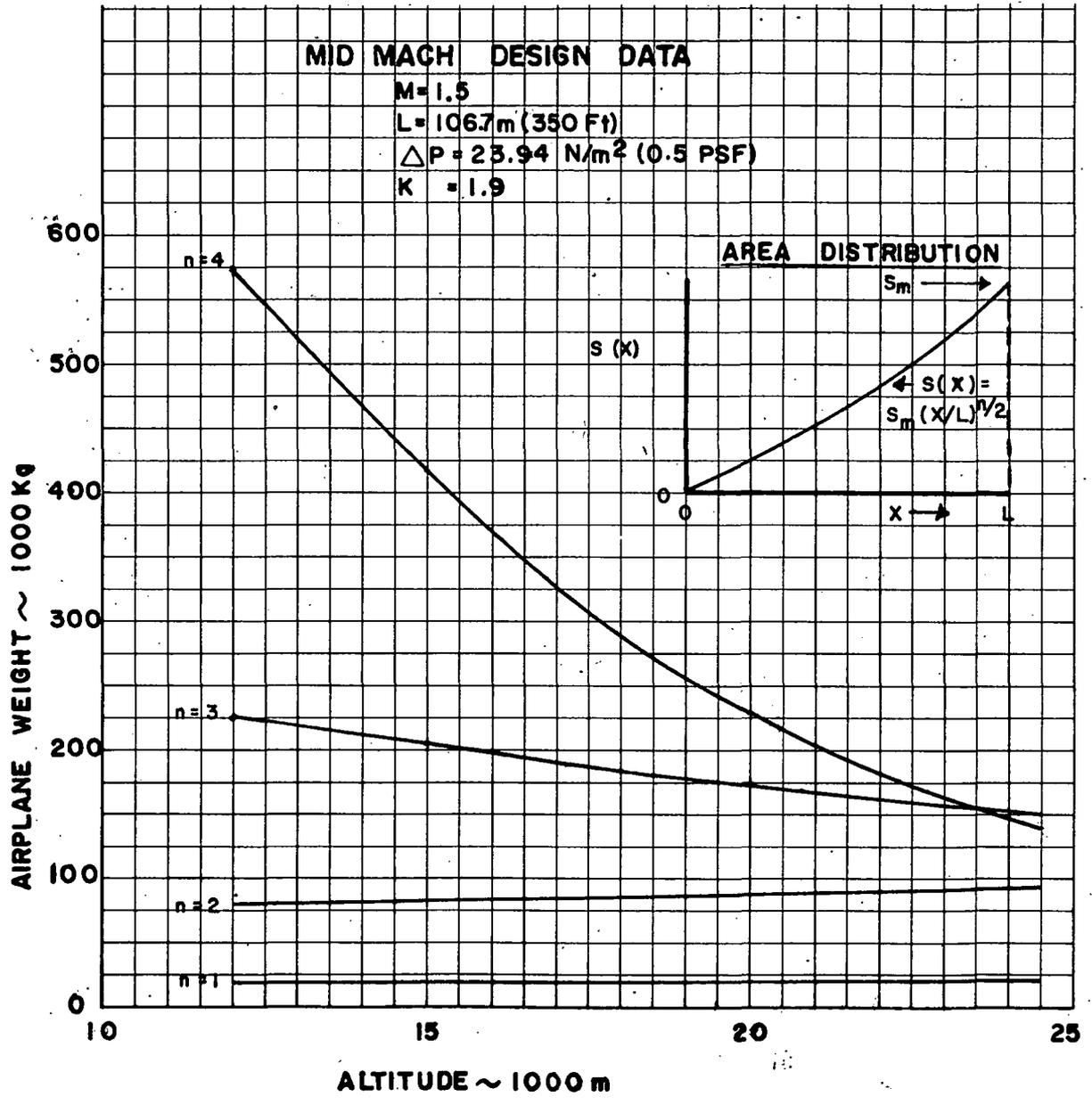
FIG. 35   MID-MACH DESIGN DATA

100

MID-MACH DESIGN
LSB/MM-3   M=1.5
ΔP = 23.94 N/m^2 (0.5psf)
ALT = 13,715m (45,000ft)
Sref = 751.2m^2 (8086 ft^2)
GW = 283,500kg (625,000lb) MID CRUISE

PLANFORM DEFINITION

POINT	X ~ m	Y ~ m	CHORD	t/c ~ %
A	32.13	0	52.12	—
SOB	41.09	1.91	43.16	3.5
B	60.17	5.96	24.08	3.0
C	92.99	19.81	6.10	2.5

WING & TAIL LIFT WITH PODS

DESIGN ENVELOPE

FUSELAGE

NACELLES

HORIZONTAL TAIL

VERTICAL TAIL

WING

S(X) ~ meters^2

X ~ meters
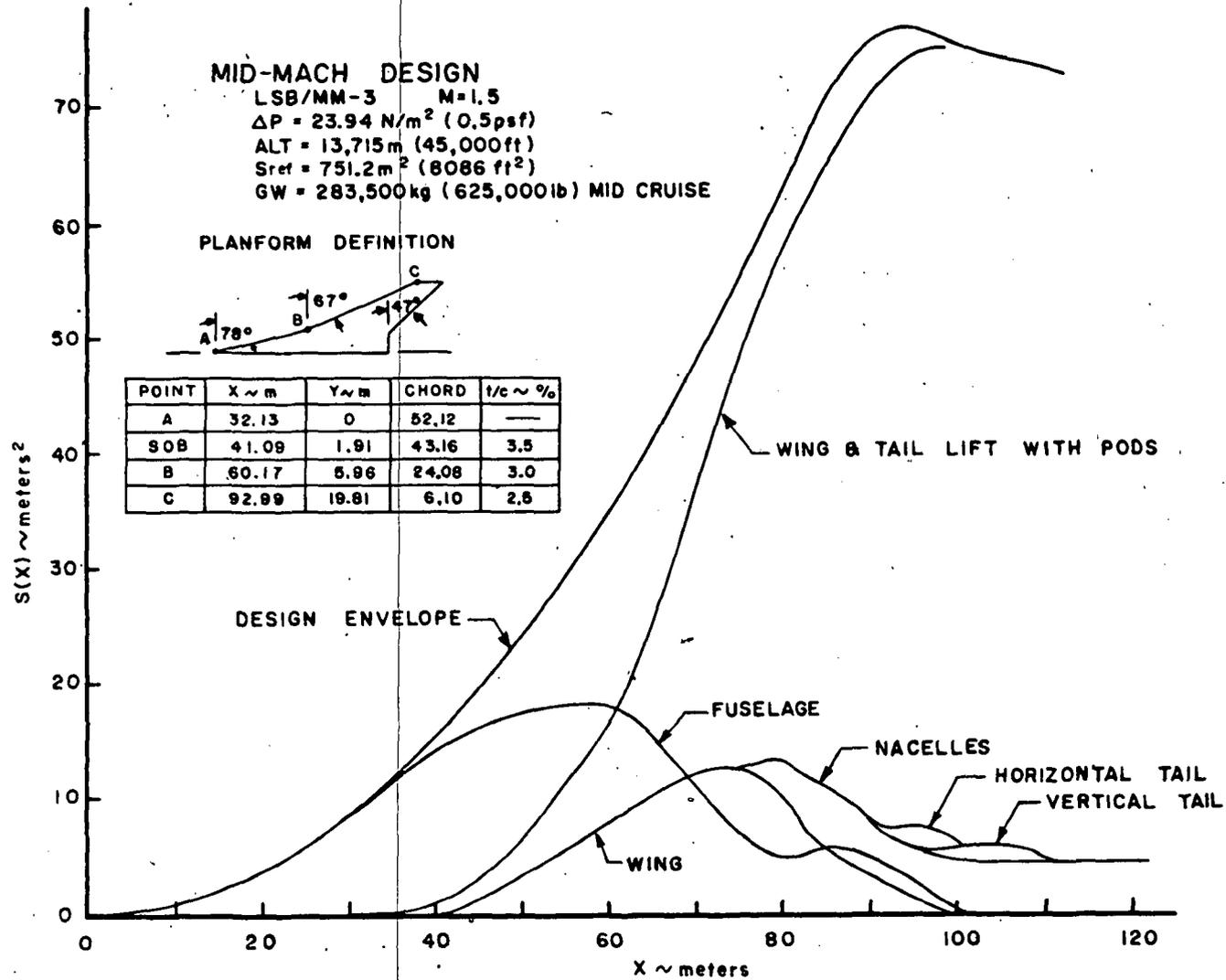
FIG. 36   DESIGN POINT AREA DISTRIBUTION - MID-MACH DESIGN

FIG. 37   MID-MACH DESIGN CONFIGURATION - LSB/MM-3
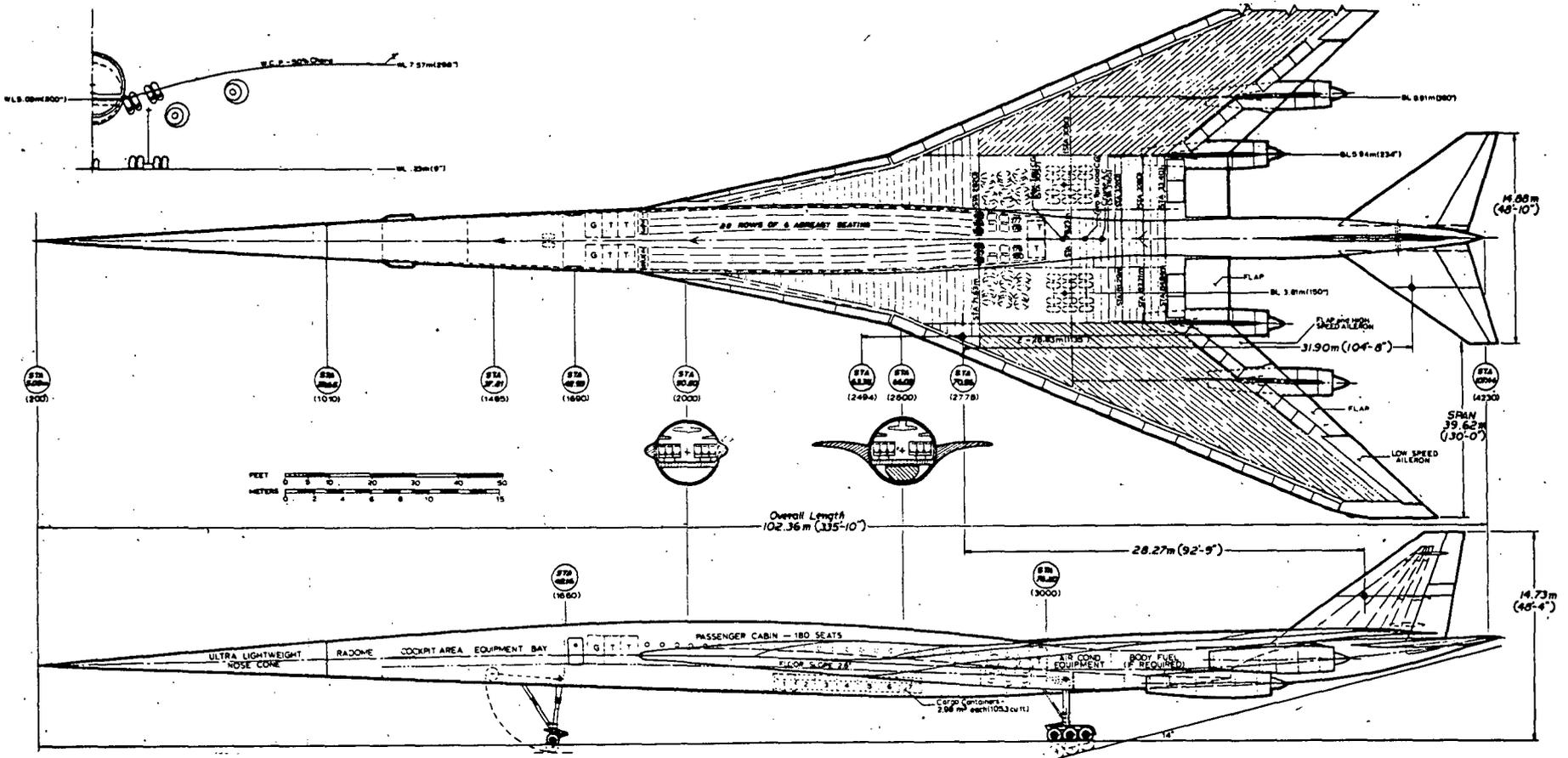
LSB/MM-3   Mach = 1.5 CONFIGURATION DATA

GROSS WEIGHT	NOMINAL PAYLOAD			O. E. W.
351,534 kg. (775,000 lbs.)	16,748 kg. (36,900 lbs.)			155,133 kg. (342,100 lbs.)
SURFACES	WING	HORIZONTAL	VERTICAL	CANARD
Area m^2 (ft^2)	751.2 * (8086)	75.4 (812)	54.6 (588)	———
Aspect Ratio	2.09	2.25	1.0	———
Taper Ratio	.117	.25	.235	———
Thick. Ratio	3.5%/2.5%	3.0%	3.0%	———
Dihedral	15°/ -2°	5°	———	———
Incidence	3°	———	———	———
L.E. Sweep	78°/ 67°	55°	55°	———
BODY	Length	Max. Dia.	Seating	Baggage
	102.4m (335.8 ft.)	4.85m (131 in.)	180	3,266 kg. (7200 lbs.)
POWERPLANT	No. Eng.	Type	Airflow **	Inlet Dia.
	4	Adv. Tech. GE4/J6H2	229.5 kg./sec. (506 lbs./sec.)	1.09 m (43.1 in.)
LANDING GEAR	Nose	Main	Main Loc.	Pressure
	.86 x .36 m (34" x 14")	1.0 m x .36 m (40" x 14")	50.2% MAC	1.24 x10^6 N/m^2 (180 psi)
FUEL CAPACITY	Wing	Body	Total	C. G.
kg. (lbs.)	168,283 (371,000)	83,915 (185,000)	252,198 (556,000)	STA 77.04 m (STA 3033 in.)
C.G. LIMITS	Takeoff & Landing		Mid-Cruise	
	STA 75.82 —78.46 m (STA 2985"—3089 ")		STA 76.50 —79.78 m (STA 3012" — 3141 ")	
MATERIAL	ALUMINUM			

* REFERENCE AREA; ACTUAL AREA-872m^2 (9,389 ft^2).
** ENGINE PERFORMANCE SHOULD BE CALCULATED FOR A 270.0KG/SEC (595.3 LB/SEC) SIZE GE4/J6H2 ENGINE AND ENGINE WEIGHT AND DIMENSIONS TO BE BASED ON 229.5 KG/SEC (506 LB/SEC).

(All dimensions are in International Standard Units [S I]with U. S. units shown in parenthesis.)

FIG. 37 (CONT.) MID-MACH DESIGN CONFIGURATION-
LSB/MM-3
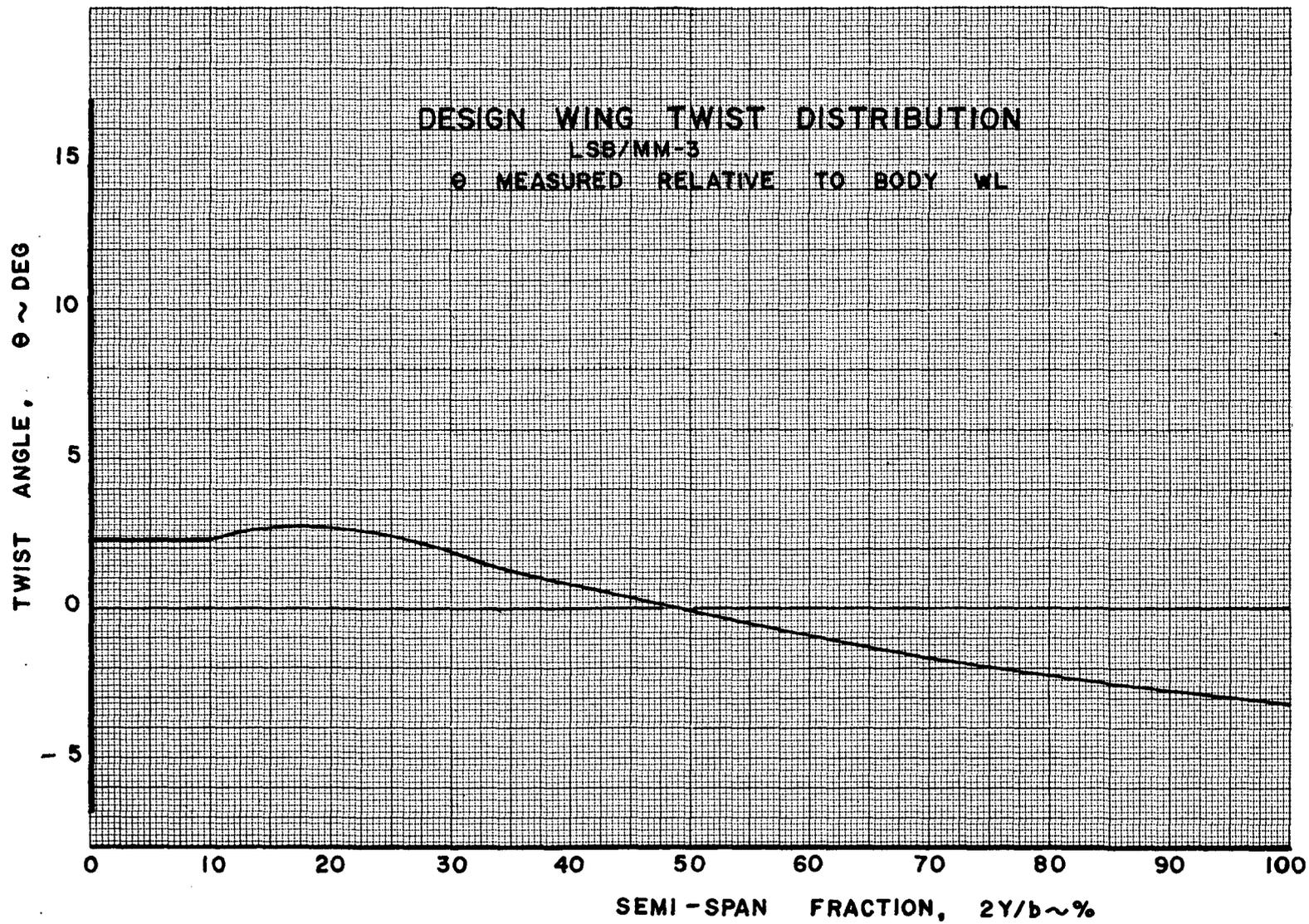
FIG. 38 WING TWIST DISTRIBUTION - MID-MACH DESIGN

FIG. 39 CRUISE LIFT-DRAG CHARACTERISTICS - MID-MACH DESIGN

FIG. 40 ZERO LIFT DRAG AND POLAR SHAPE - HIGH SPEED DESIGN
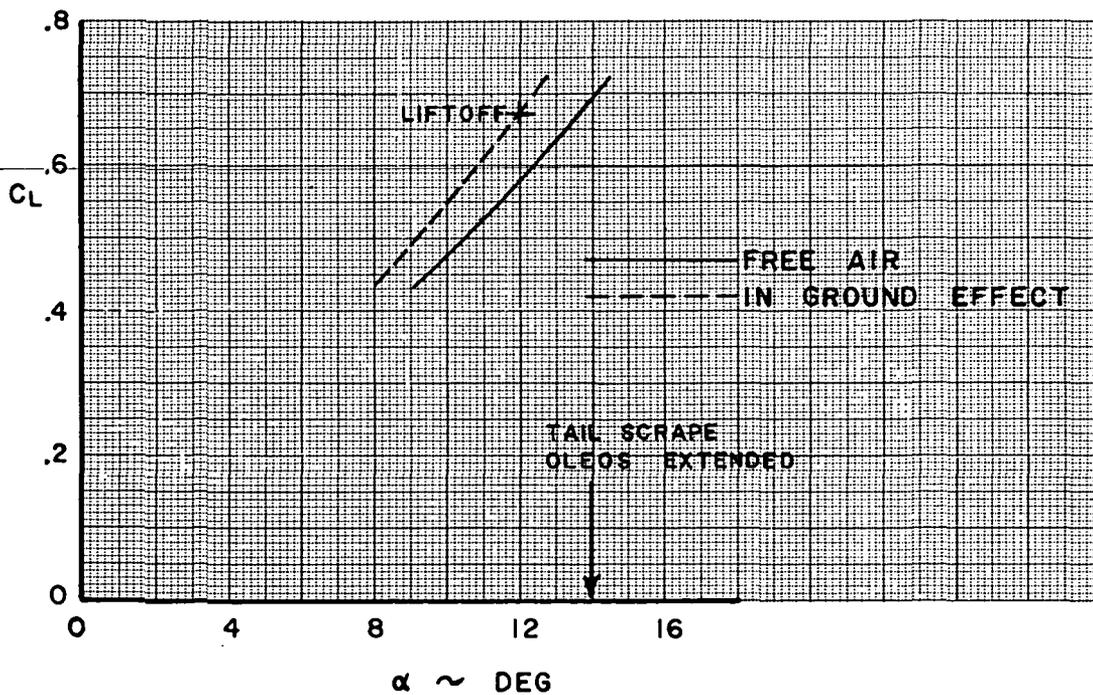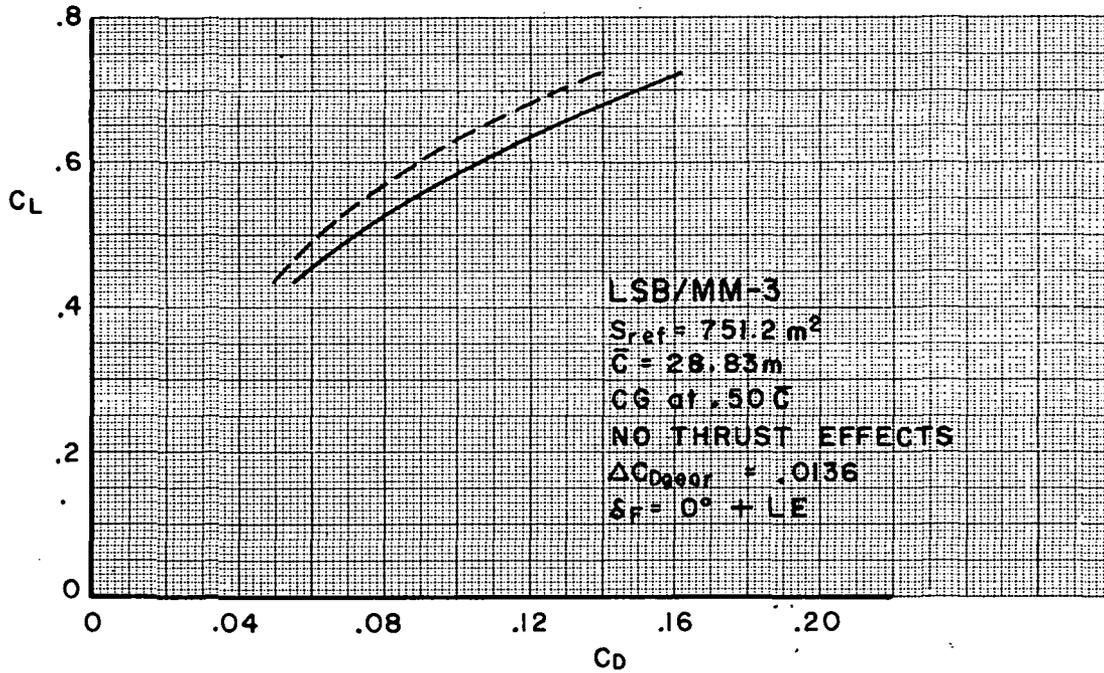
FIG. 41 TAKEOFF CHARACTERISTICS, $\delta_F = 0^\circ$ + LE -
MID-MACH DESIGN

107
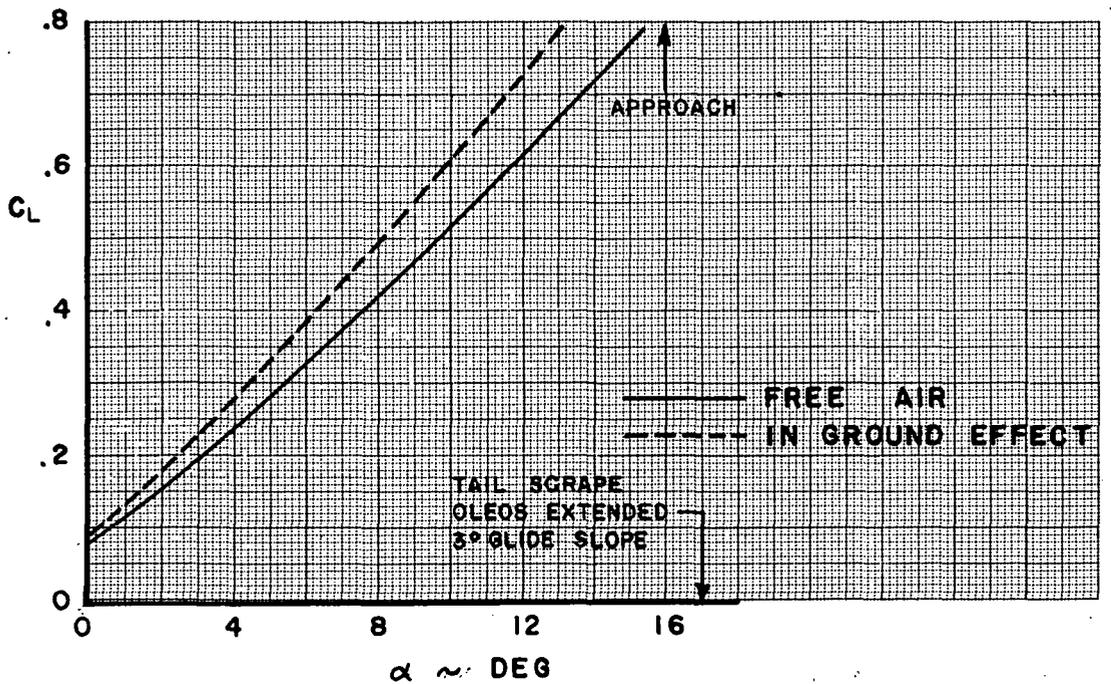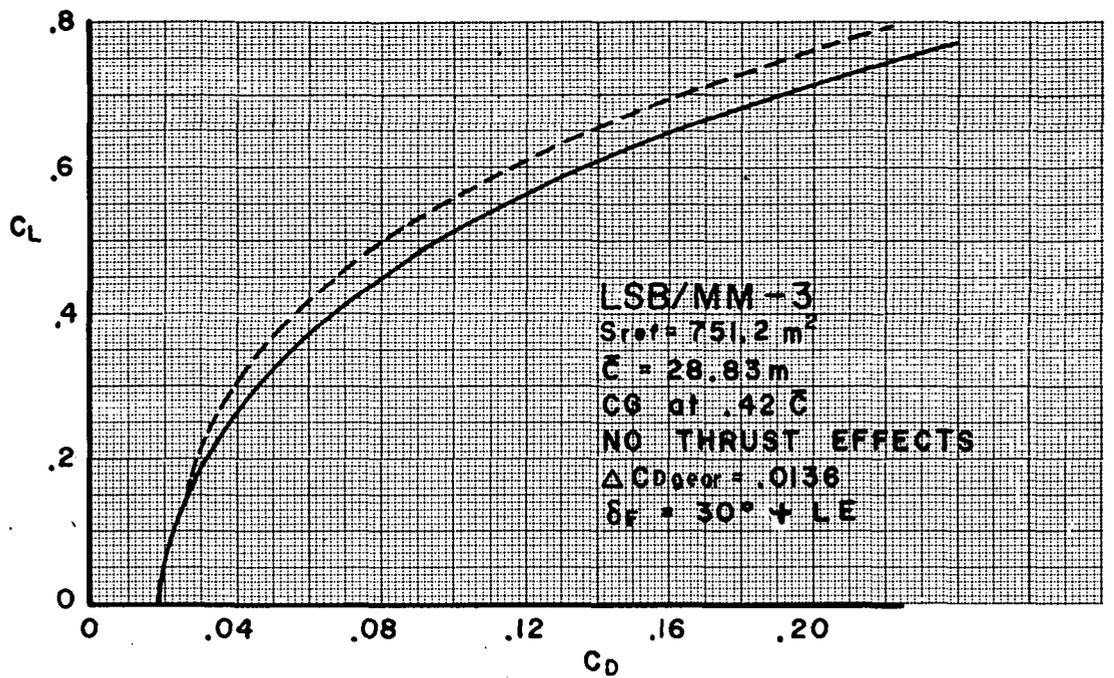
FIG. 42   LANDING CHARACTERISTICS, $\delta_F = 30^0$ + LE -
MID-MACH DESIGN

GROSS WEIGHT - THOUSANDS OF KILOGRAMS (POUNDS)
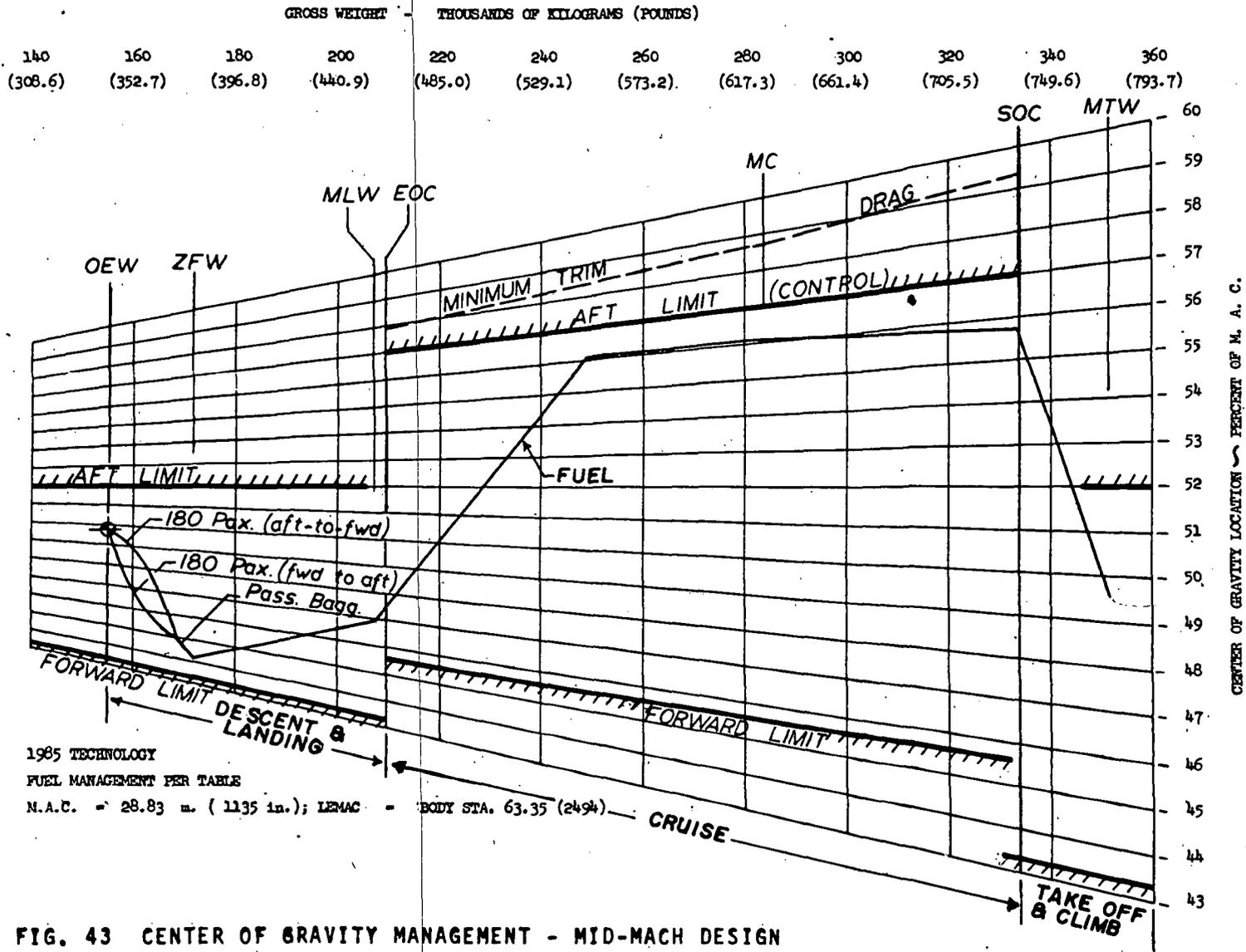
FIG. 43 CENTER OF GRAVITY MANAGEMENT - MID-MACH DESIGN

109
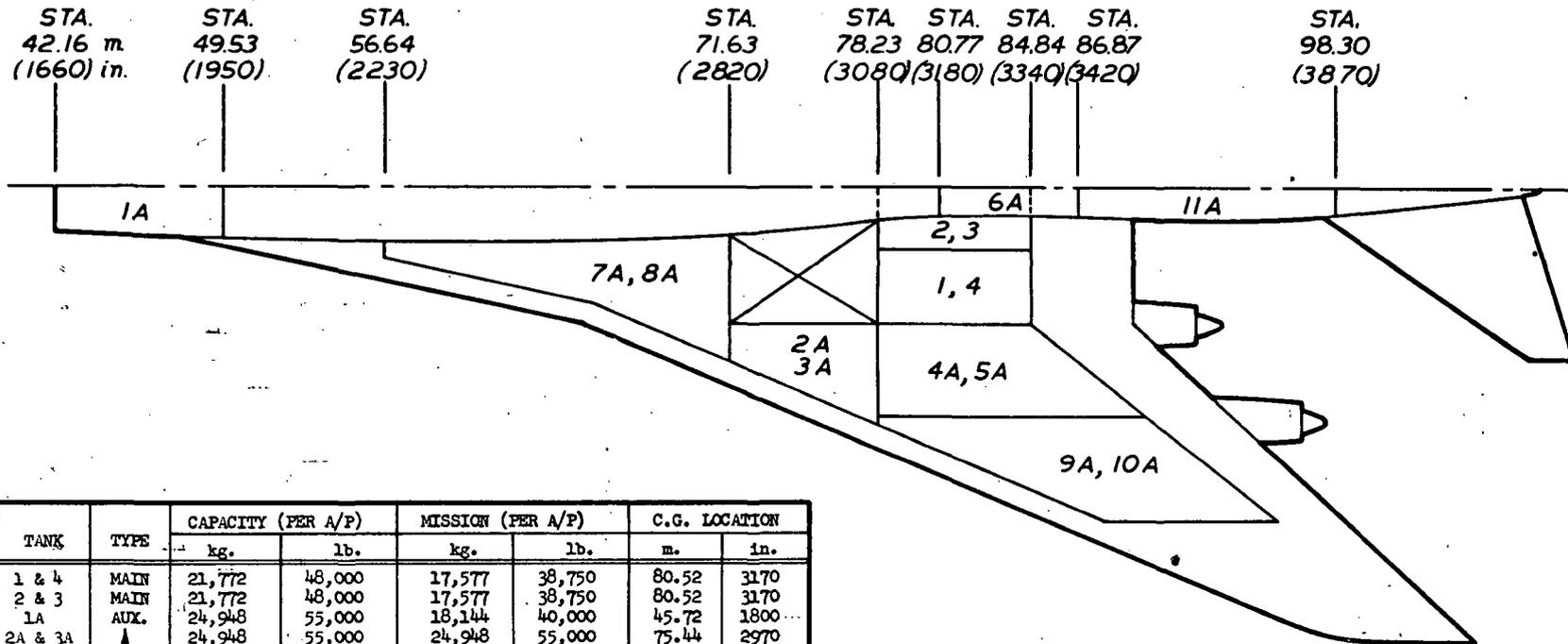
TANK	TYPE	CAPACITY (PER A/P)		MISSION (PER A/P)		C.G. LOCATION	
		kg.	lb.	kg.	lb.	m.	in.
1 & 4	MAIN	21,772	48,000	17,577	38,750	80.52	3170
2 & 3	MAIN	21,772	48,000	17,577	38,750	80.52	3170
1A	AUX.	24,948	55,000	18,144	40,000	45.72	1800
2A & 3A	↑	24,948	55,000	24,948	55,000	75.44	2970
4A & 5A		25,401	56,000	24,948	55,000	82.04	3230
6A		13,608	30,000	0	0	83.82	3300
7A & 8A		50,802	112,000	12,837	28,300	67.31	2650
9A & 10A	↓	23,587	52,000	21,319	47,000	86.87	3420
11A	AUX.	45,359	100,000	42,275	93,200	92.71	3650
TOTAL		(252,197)	(556,000)	(179,622)	(396,000)		(3033)

▷1▷ Based on Capacity

FIG. 44   FUEL TANK DEFINITION - MID-MACH DESIGN
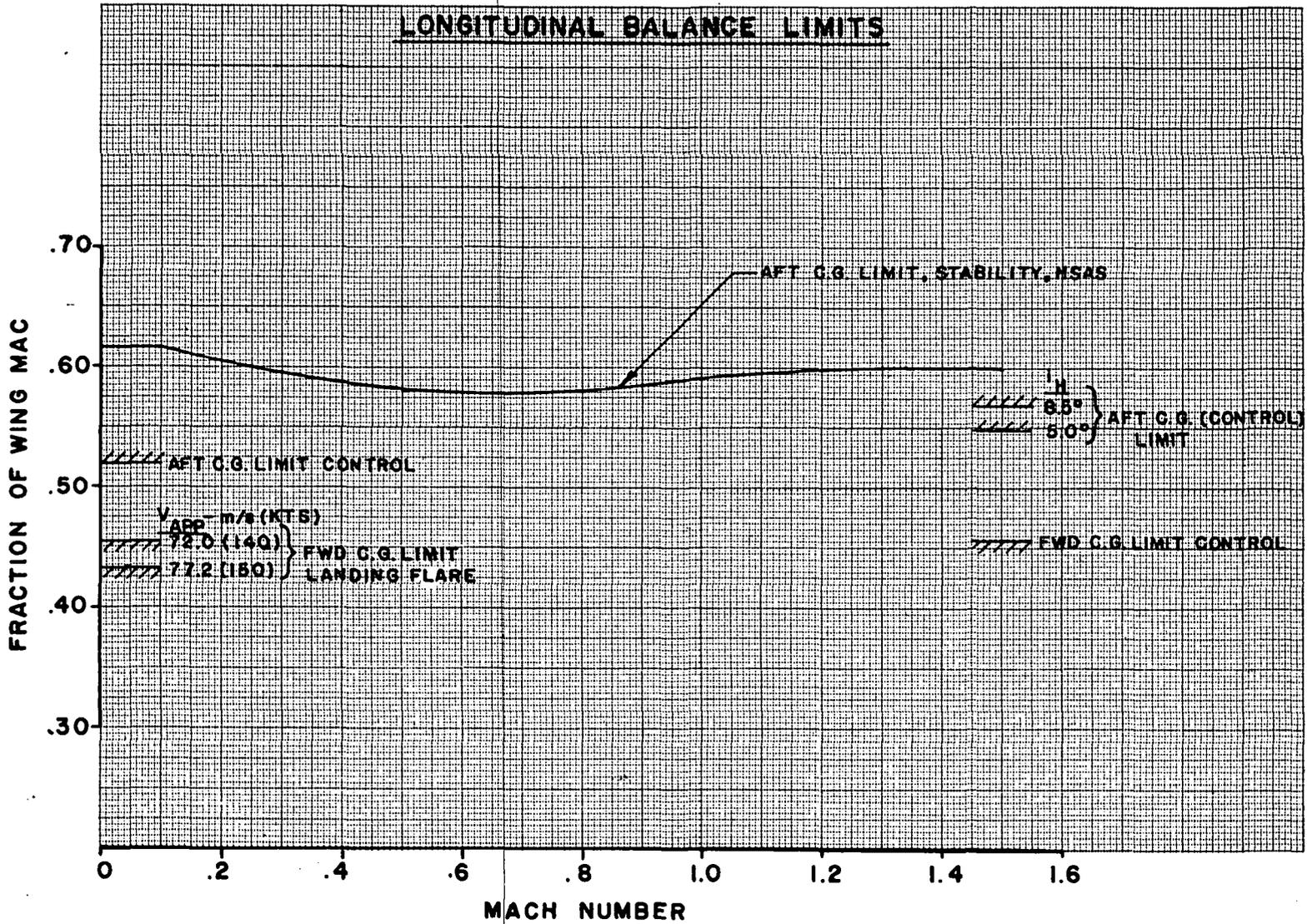
FIG. 45 LONGITUDINAL AERODYNAMIC LIMITS - MID-MACH DESIGN
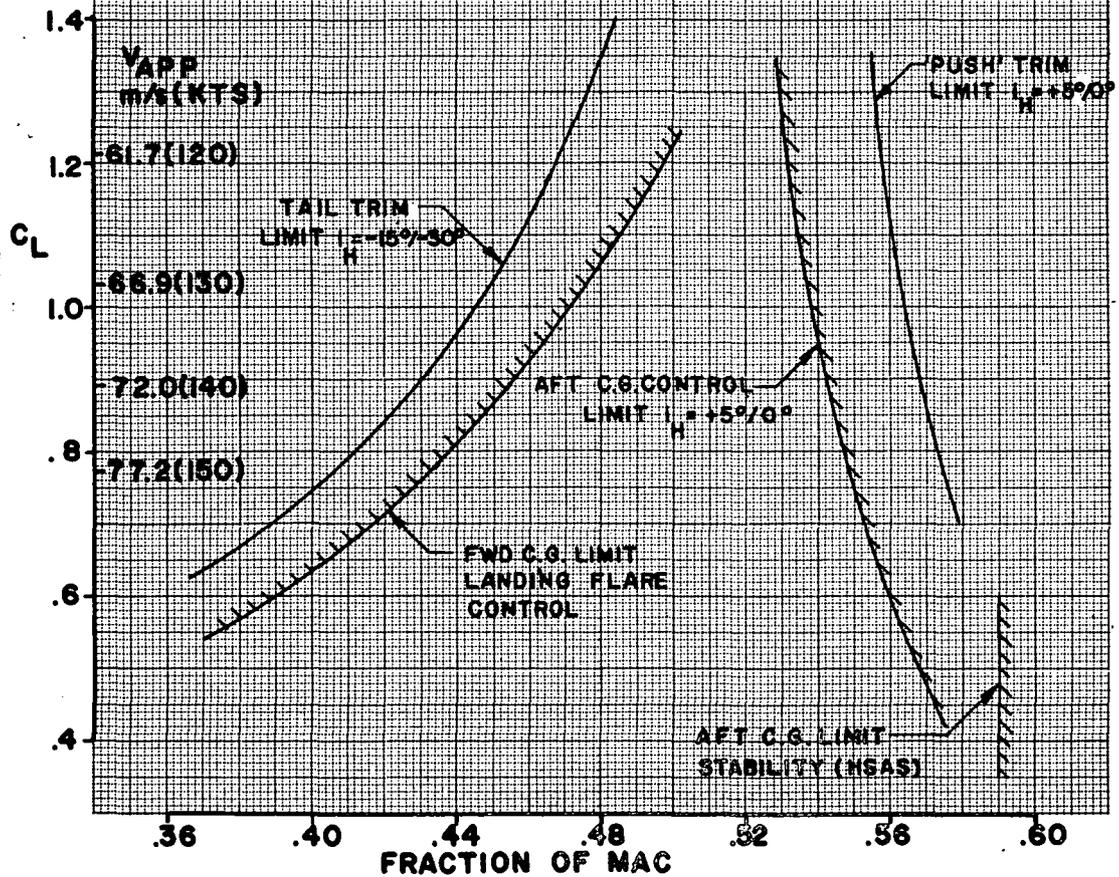
FIG. 46   LOW SPEED AERODYNAMIC LIMITS - MID-MACH DESIGN
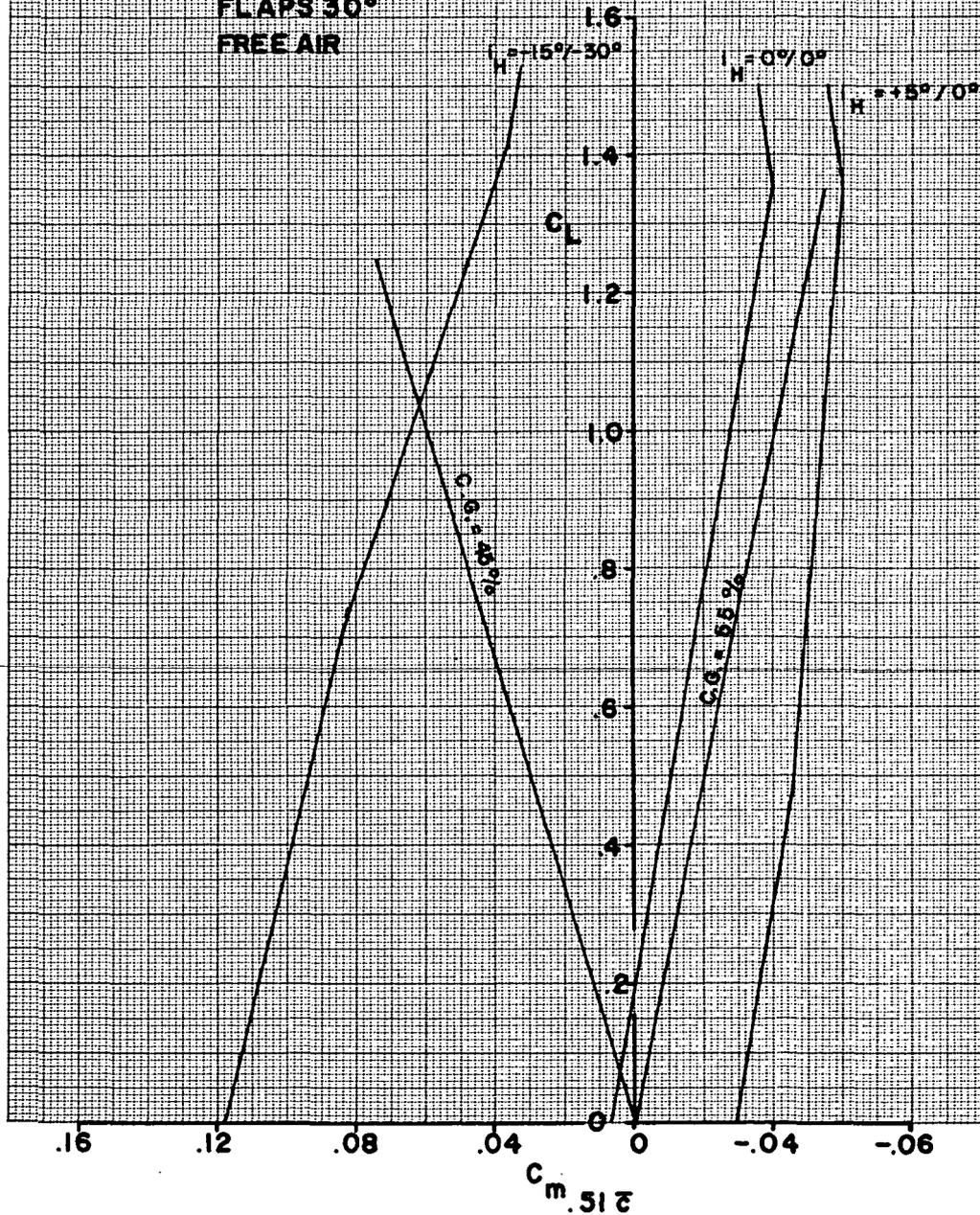
FIG. 47 LOW SPEED PITCHING MOMENT CURVES -
MID MACH DESIGN
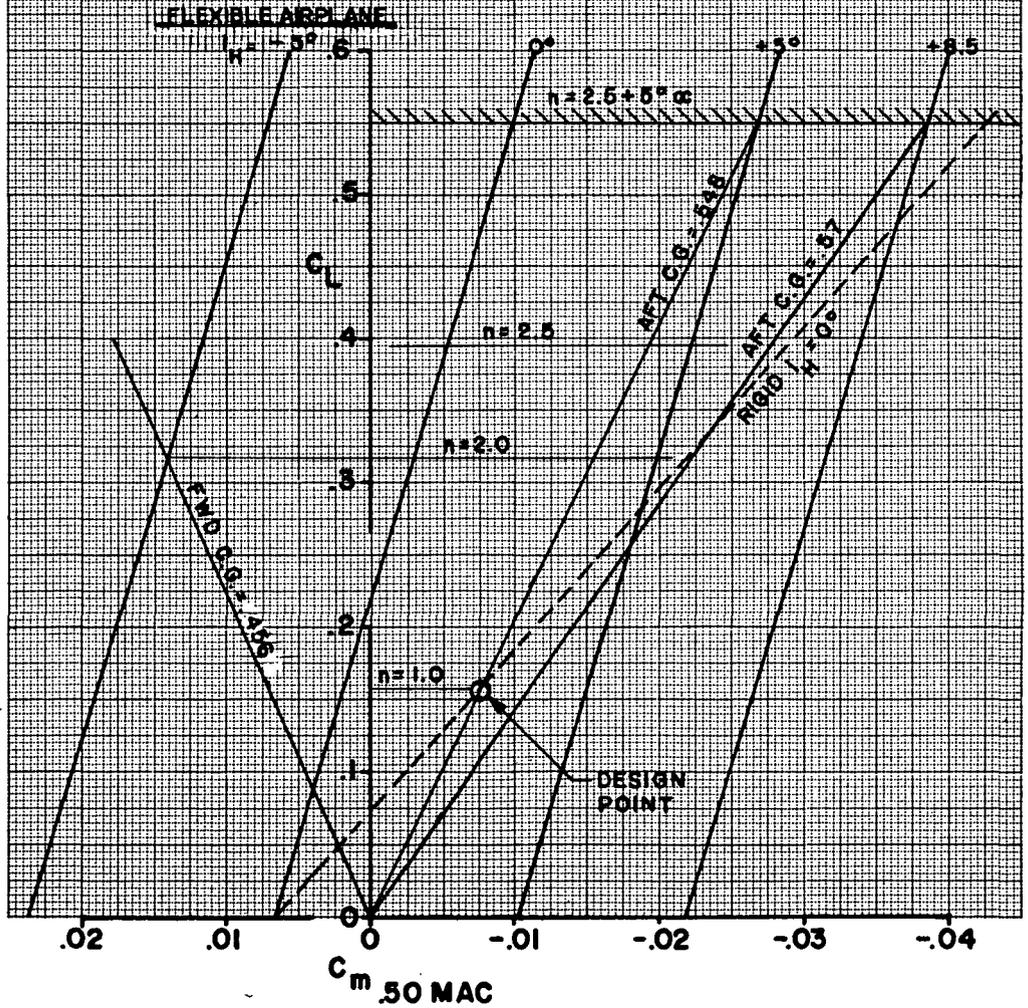
FIG. 48 CRUISE PITCHING MOMENT - MID-MACH DESIGN
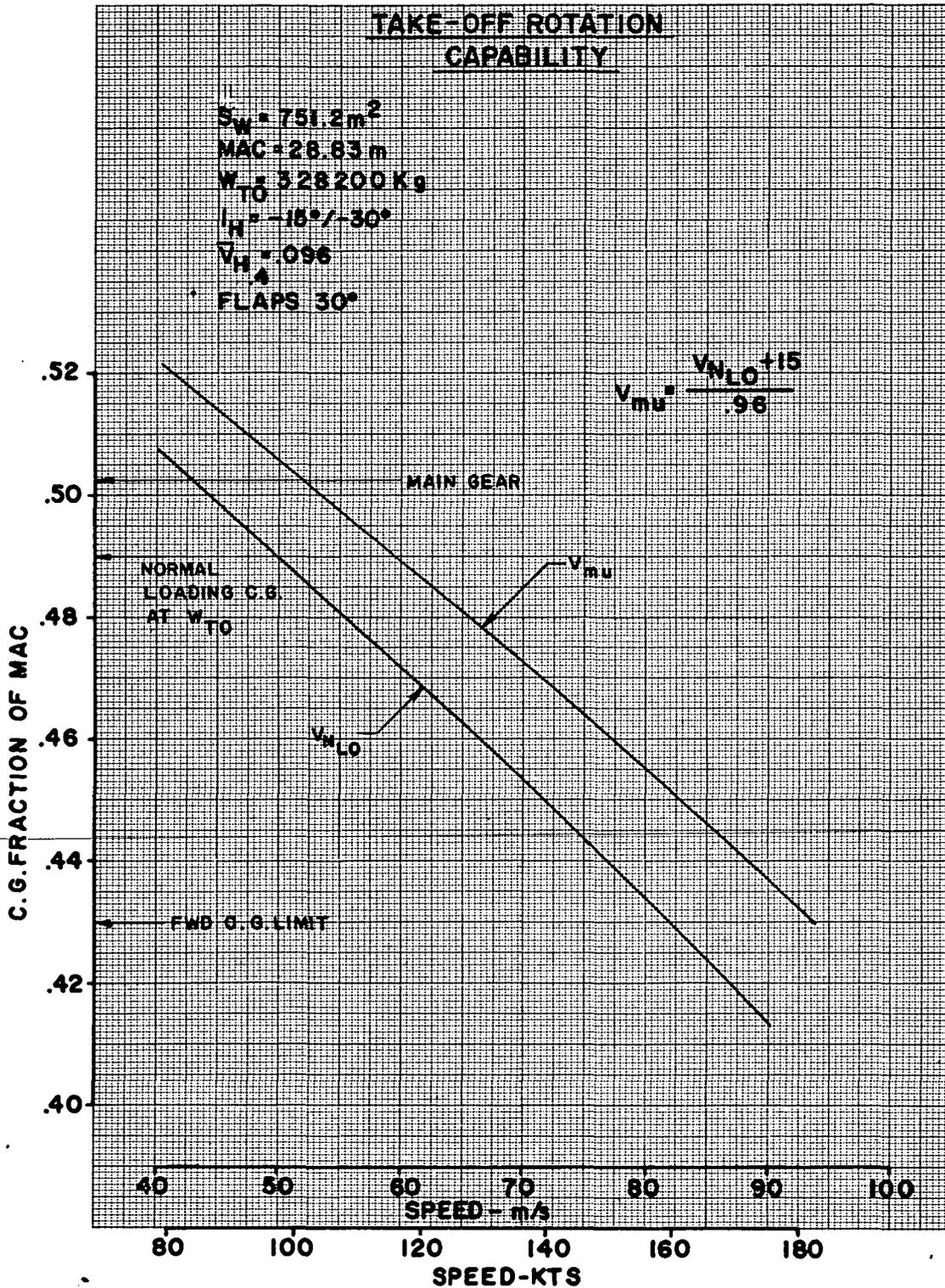
FIG. 49   TAKEOFF ROTATION CAPABILITY - MID-MACH DESIGN
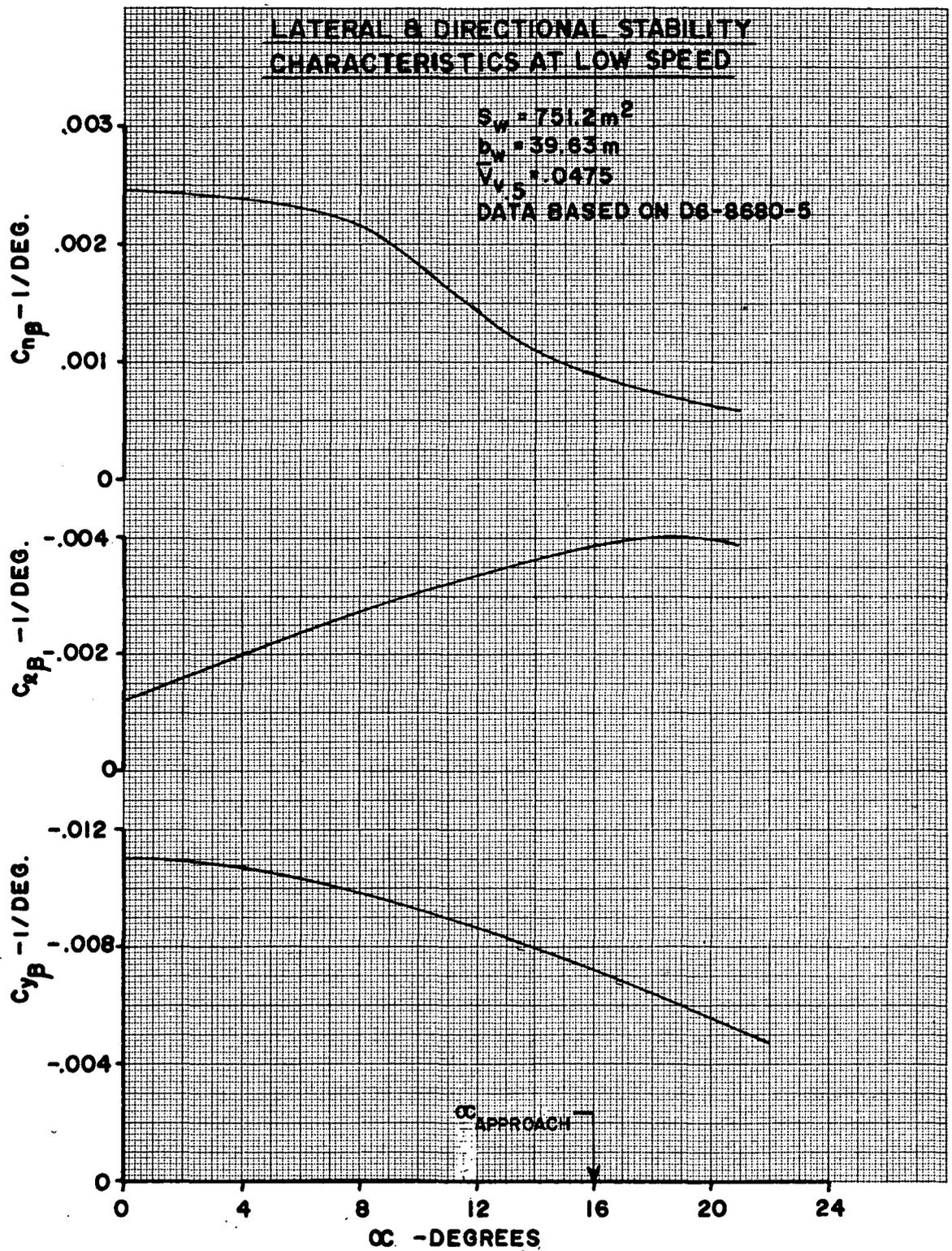
115

FIG. 50 LOW SPEED LATERAL-DIRECTIONAL CHARACTERISTICS - MID-MACH DESIGN

116
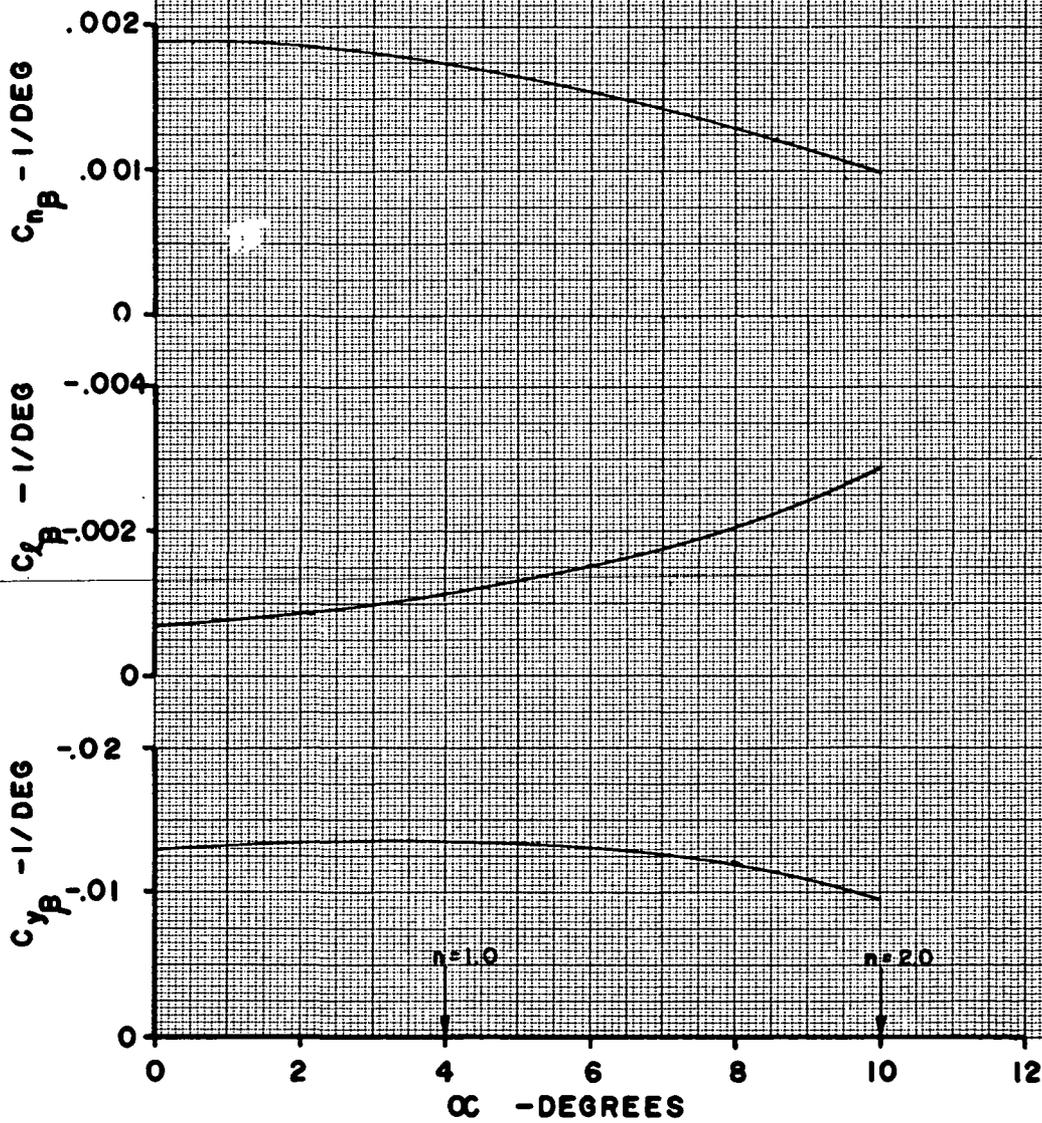
FIG. 51   CRUISE LATERAL-DIRECTIONAL CHARACTERISTICS -
MID-MACH DESIGN
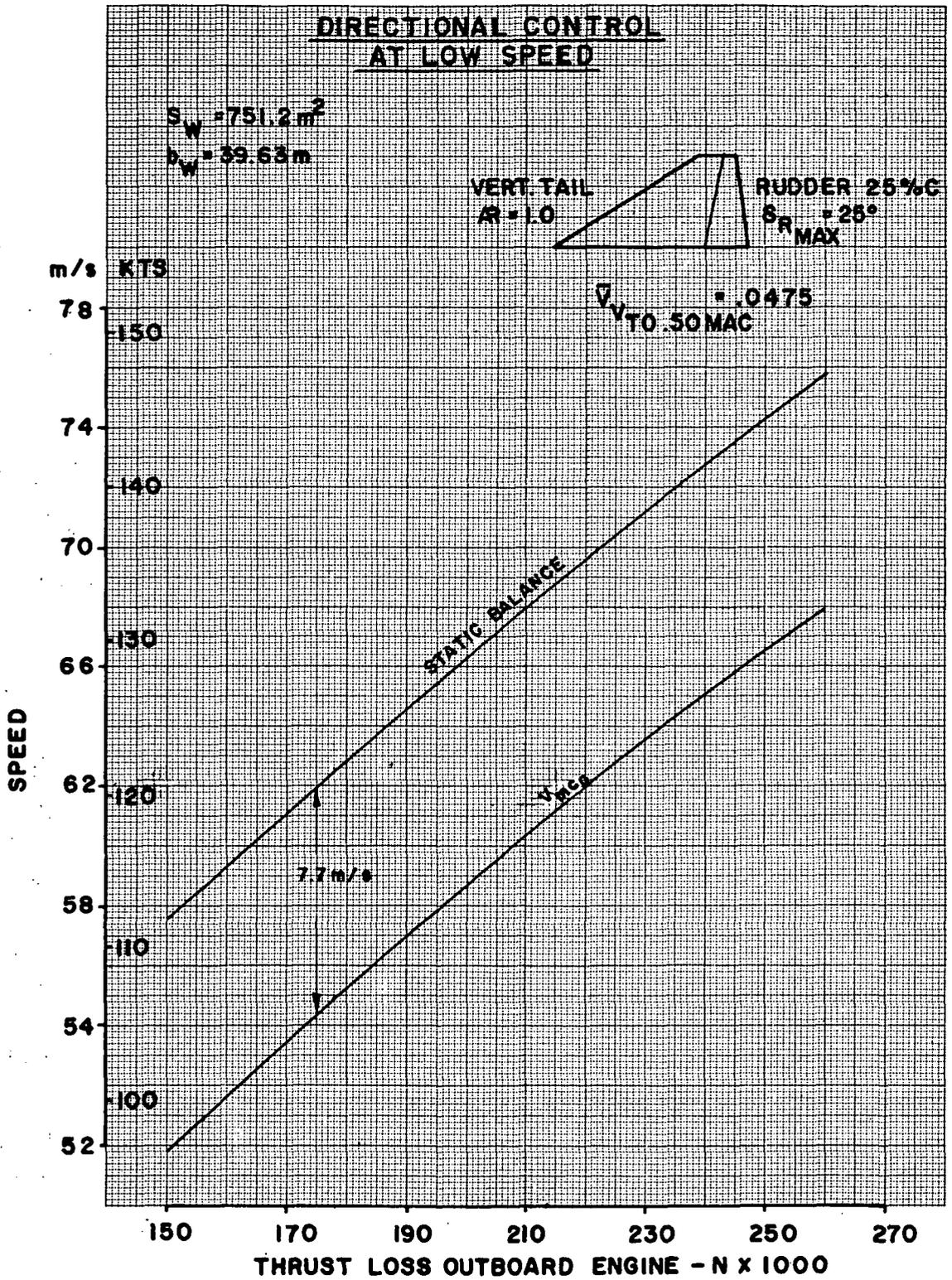
FIG. 52 LOW SPEED DIRECTIONAL CONTROL - MID-MACH DESIGN
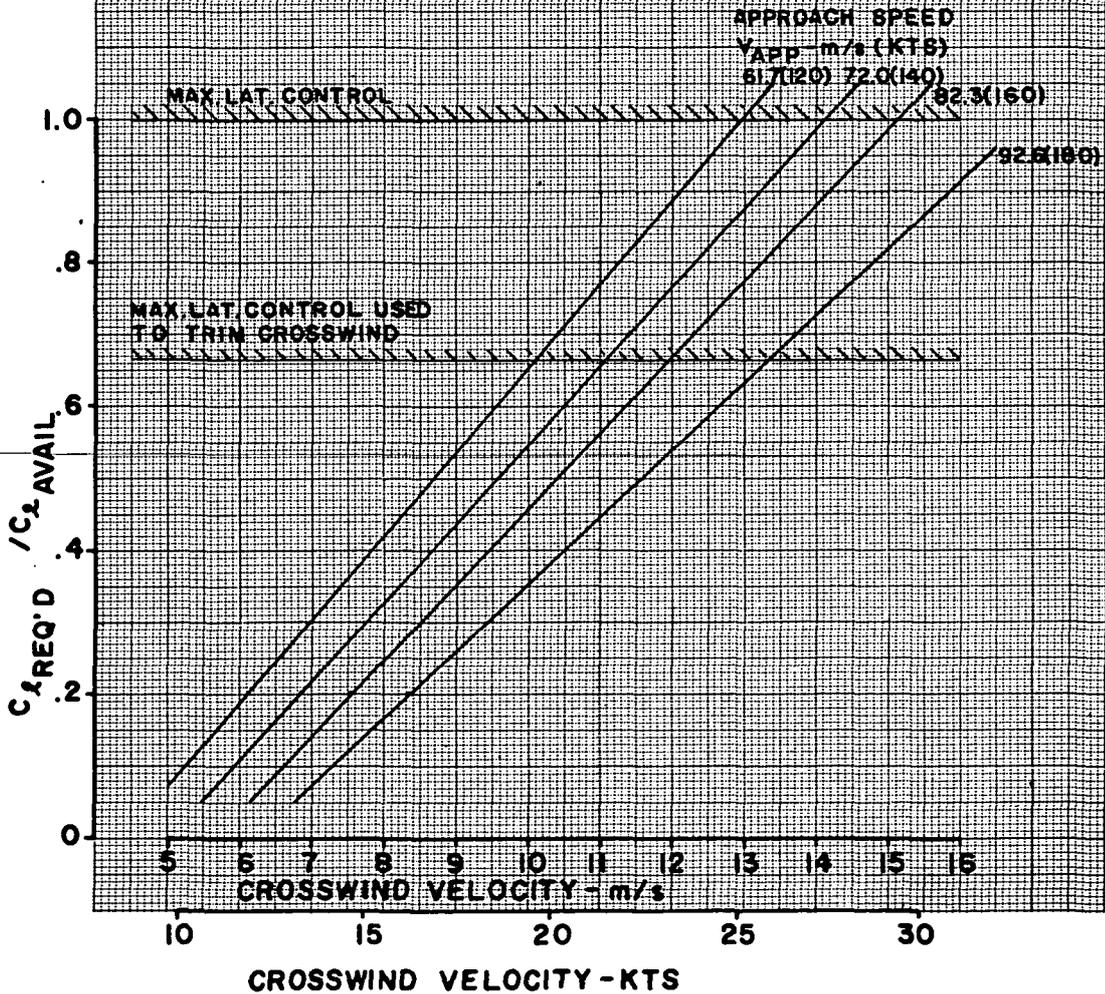
FIG. 53 LATERAL CONTROL REQUIREMENT FOR CROSSWIND
LANDING - MID-MACH DESIGN

119
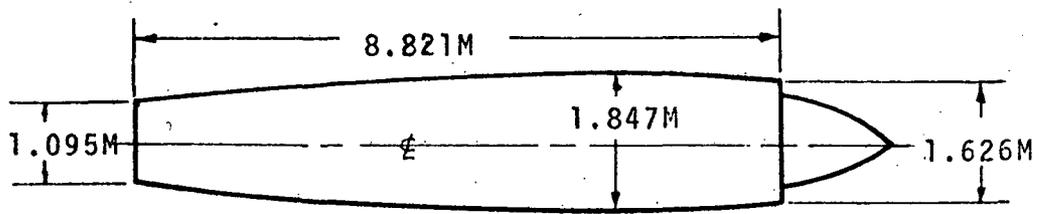
FIGURE 54   ENGINE POD DEFINITION FOR MACH 1.5 LSB/MM-3
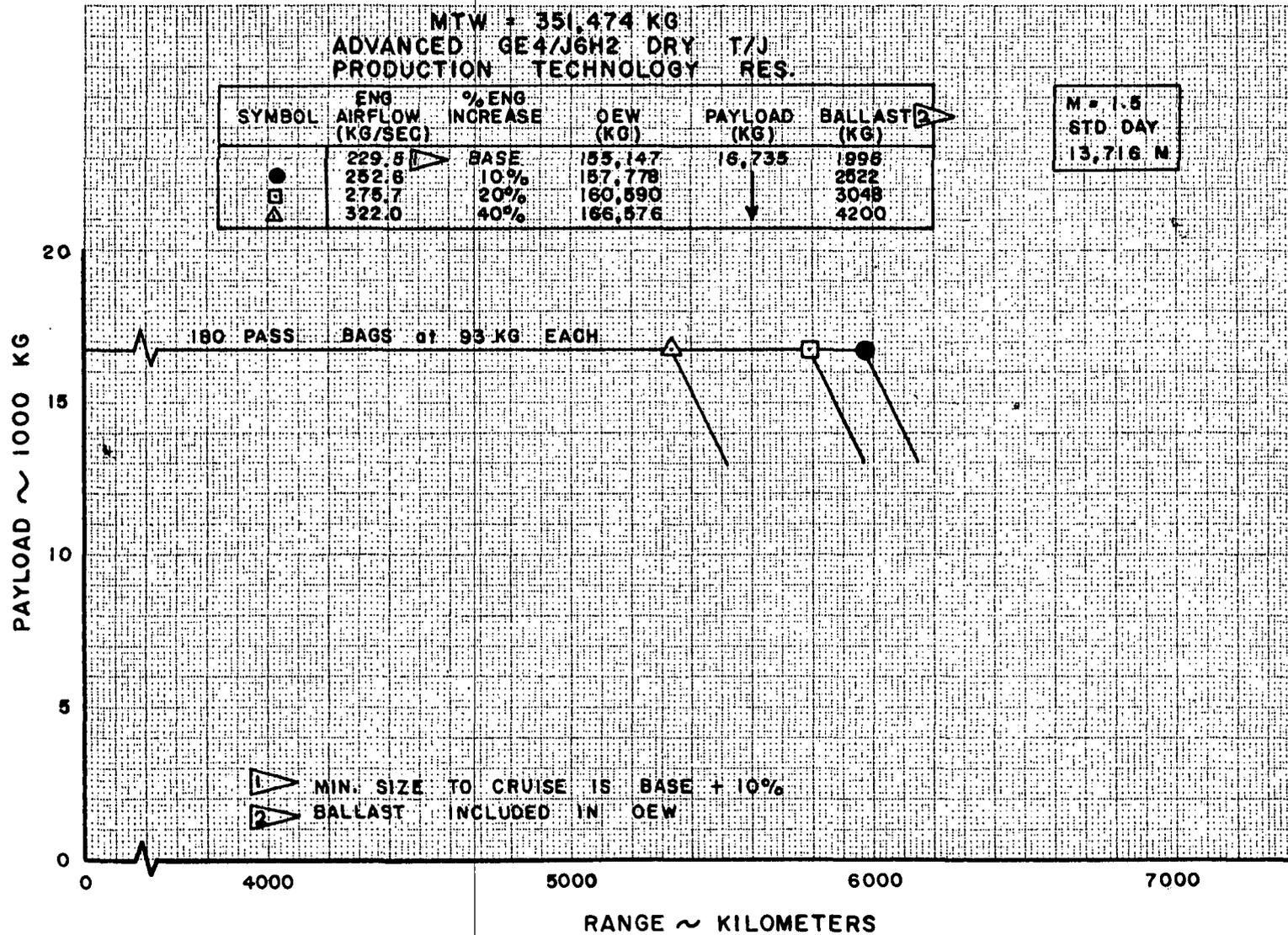
FIG. 55   PAYLOAD - RANGE SUMMARY - MID-MACH DESIGN

EFFECT OF ENGINE GROWTH ON WEIGHT
   LSB/MM-3 CONFIGURATION
   GE4/J6H2 ENGINES
   1985 TECHNOLOGY
   FWD LIMIT AT .433C
   OEW CG AT STA 77.69
   BALLAST AT STA 25.65
   180 PASSENGERS
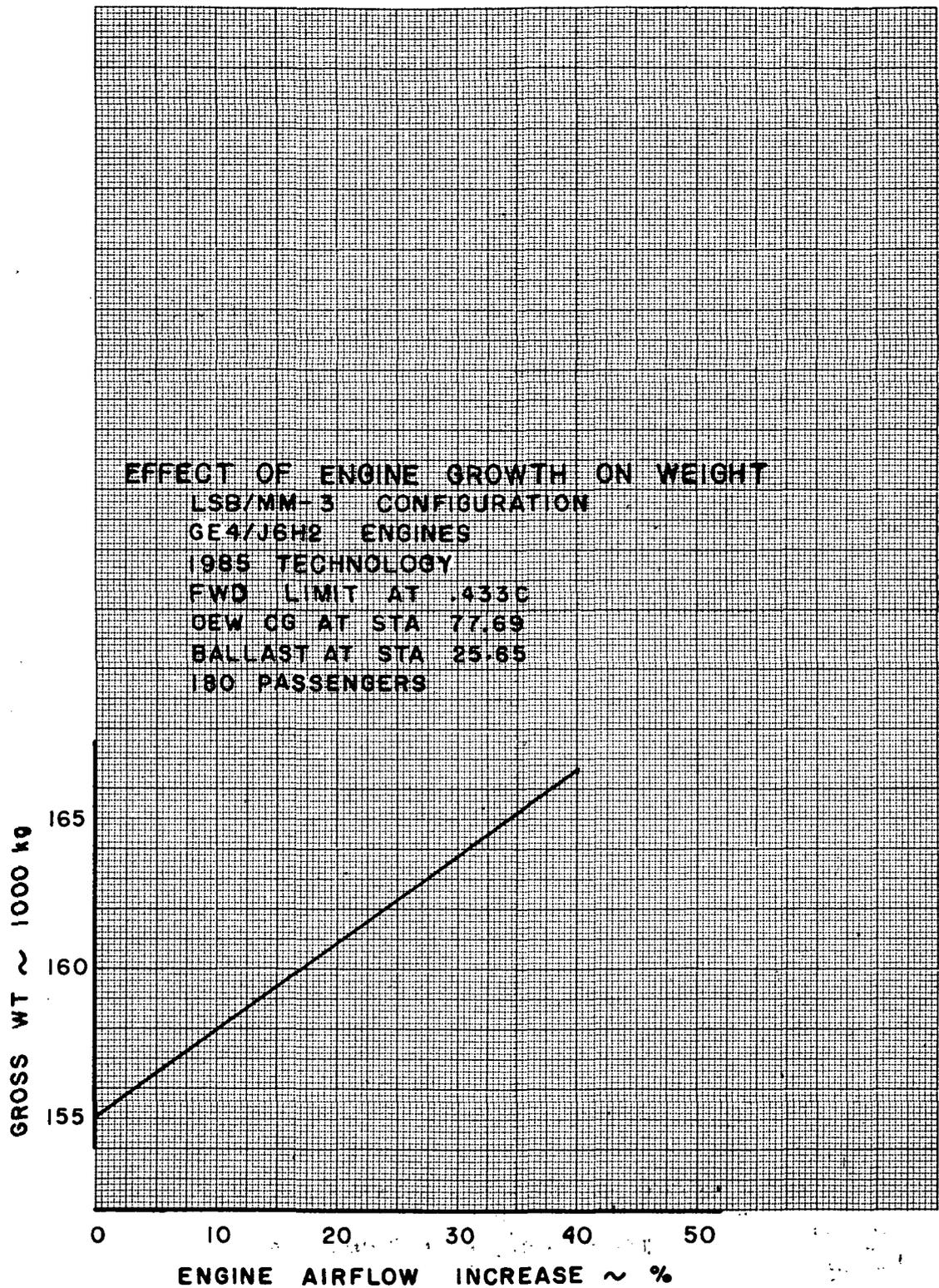
FIG. 56   EFFECT OF ENGINE SIZE ON AIRPLANE WEIGHT -
          MID-MACH DESIGN

MTW = 351,474 KG
PAYLOAD = 16,735 KG
ADVANCED GE4/J6H2 DRY T/J | M = 1.5 STD. DAY |

RANGE ~ KILOMETERS

6500 — PROD'N TECH RESERVES

6000

MIN. SIZE
TO CRUISE

CRUISE AT
BEST KM/KG

5500

CRUISE AT
13,716 M

5000

CLIMB GRADIENT CAPABILITY

.06 — BEGIN CRUISE
13,716 M
.04 — MAX. CONTINUOUS POWER

.02

0

229.9 KG/SEC

0   10   20   30   40   50   60

AS DRAWN

ENGINE AIRFLOW INCREASE ~ %
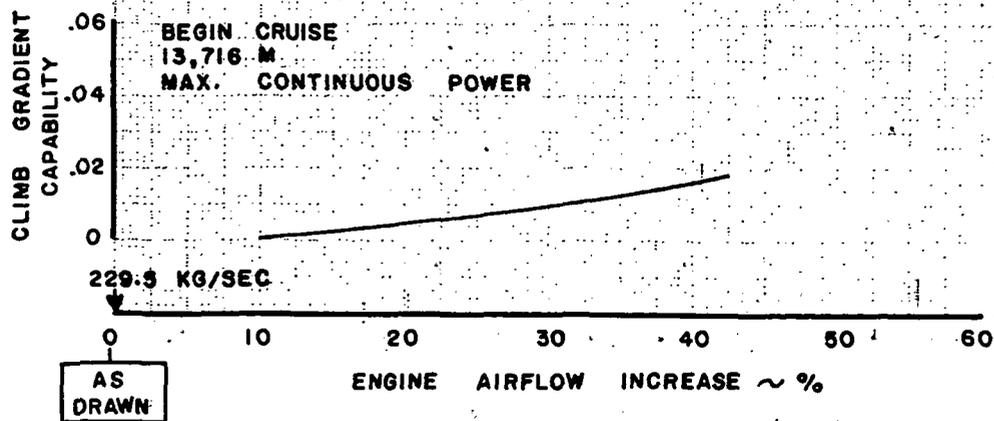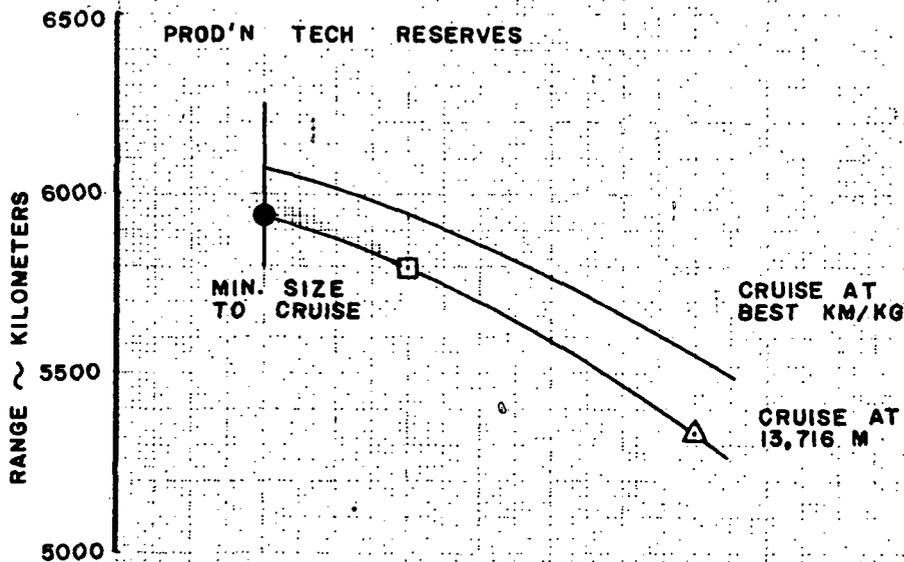
FIG. 57   EFFECT OF ENGINE SIZE ON AIRPLANE PERFORMANCE -
MID-MACH DESIGN
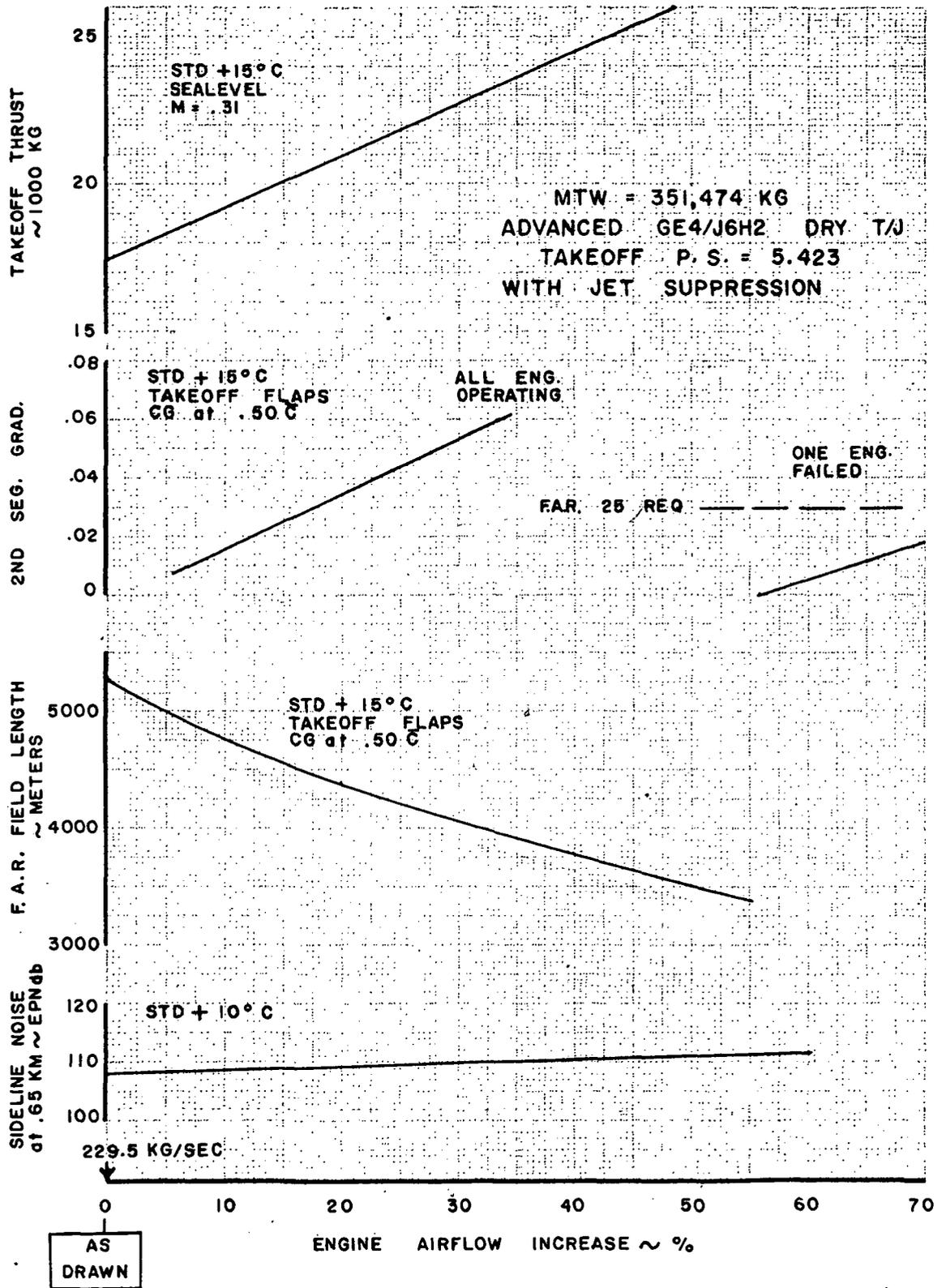
FIG. 58 TAKEOFF PERFORMANCE SUMMARY - MID-MACH DESIGN

124

SUMMARY OF SONIC BOOM SIGNATURES
BASELINE AIRPLANE (LSB/MM-3)
ENGINE AIRFLOW INCREASED BY 10%
180 PASSENGERS, MTW = 352,000 kg

BEGIN CRUISE
M = 1.5, ALT = 13.7 km, GW = 315,000 kg
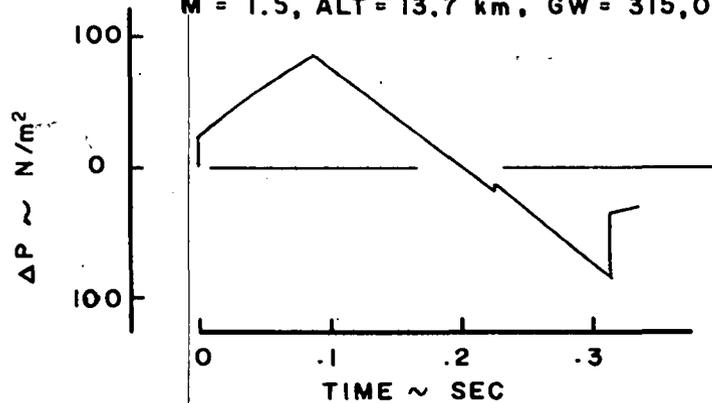
MID CRUISE
M = 1.5, ALT = 13.7 km, GW = 261,000 kg
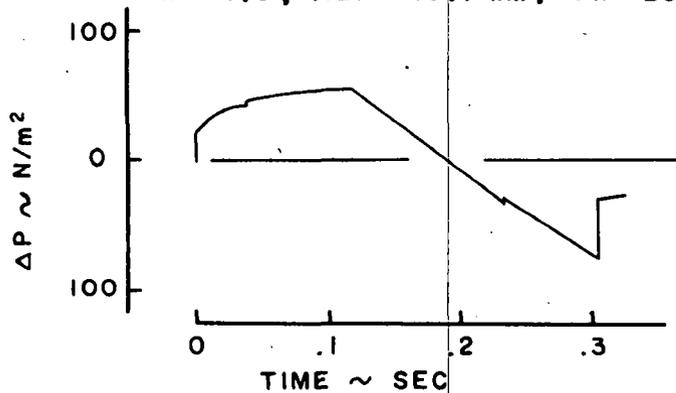
END CRUISE
M = 1.5, ALT = 13.7 km, GW = 204,000 kg
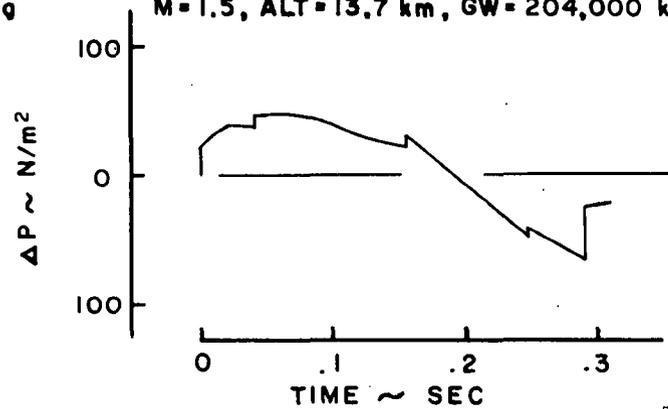
FIG. 59 SONIC BOOM SIGNATURES FOR BASELINE MID-MACH AIRPLANE, CONSTANT ALTITUDE CRUISE

125

SUMMARY OF SONIC BOOM SIGNATURES
BASELINE AIRPLANE (LSB/MM-3) + 10% AIRFLOW INCREASE
180 PASSENGERS MTW = 352,000 kg

BEGIN CRUISE
M = 1.5, ALT = 13.7 km, W = 315,000 kg

MID CRUISE
M = 1.5, ALT = 13.9 km, W = 261,000 kg

END CRUISE
M = 1.5, ALT = 15.8 km, W = 204,000 kg
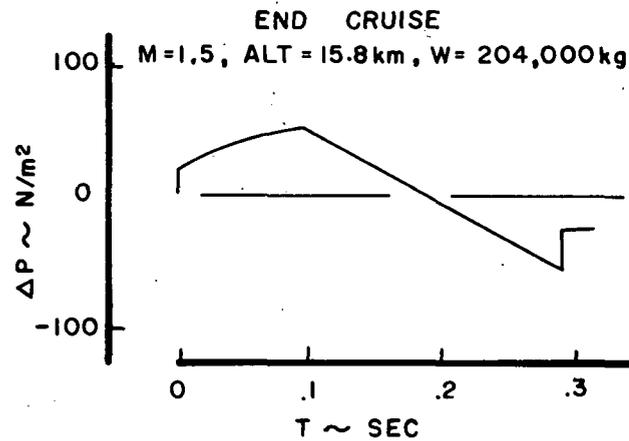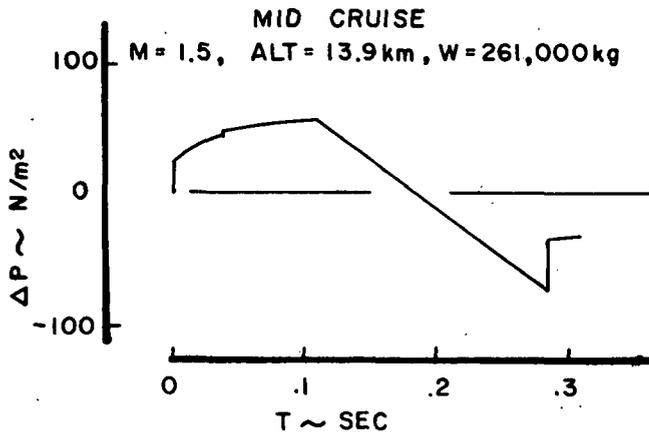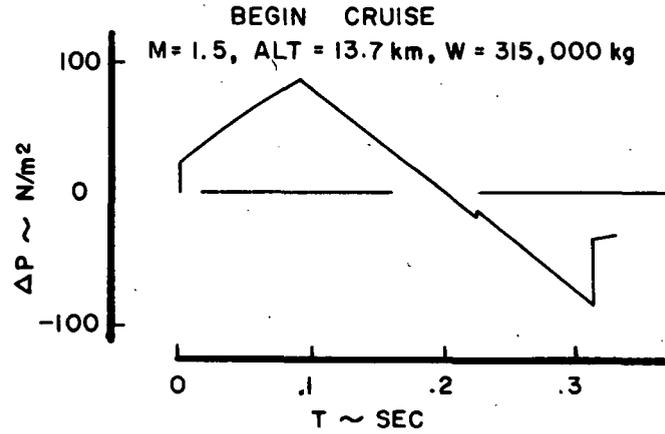
FIG. 60 SONIC BOOM SIGNATURES FOR MAXIMUM RANGE (CLIMBING) CRUISE - MID-MACH DESIGN